Investigation of β-arrestin 2 recruitment, downstream signal transduction and lateral mobility of adenosine A_1 receptor after treatment with valerian extract Ze 911

Dissertation

zur

Erlangung des Doktorgrades (Dr. rer. nat.)

der

Mathematisch-Naturwissenschaftlichen Fakultät

der

Rheinischen Friedrich-Wilhelms-Universität Bonn

vorgelegt von

Luisa Katharina Säcker

aus

Esslingen am Neckar

Bonn 2025

Angefertigt mit Genehmigung der Mathematisch-Naturwissenschaftlichen Fakultät der Rheinischen Friedrich-Wilhelms-Universität Bonn.

Gutachter / Betreuer: Prof. Dr. Hanns Häberlein

Gutachterin: Prof. Dr. Evi Kostenis

Tag der Promotion: 05.05.2025

Erscheinungsjahr: 2025

Die vorliegende Arbeit wurde in der Zeit von März 2020 bis Januar 2025 am Institut für Biochemie und Molekularbiologie der Rheinischen Friedrich-Wilhelms-Universität Bonn unter der Leitung von Herrn Prof. Dr. Hanns Häberlein angefertigt.

Für meine Familie

Abstract

Sleep is a complex physiological process with a variety of molecules involved. Even though a lot of research and progress has been made until today, the exact underlying mechanism still eludes us. Many people must deal with sleep disorders that have a great influence on their daily lives. It is known that the endogenous molecule adenosine plays a superior role in the sleep-wake cycle mediating effects at corresponding adenosine A_1 receptor (A_1AR). A_1AR is highly expressed in the central nervous system and regulator of pathological as well as physiological processes like sleep. Stimulation of A_1AR with agonists results in receptor activation and binding of G proteins, particularly G_i or G_o proteins. This causes inhibition of adenylate cyclase and consequently decrease of cyclic adenosine monophosphate (cAMP) concentration. Activation of A_1AR additionally leads to G protein-coupled receptor kinase (GRK)-mediated receptor phosphorylation at the C-terminus and consequently to the recruitment of adaptor proteins like β-arrestins. Four different isoforms of arrestins are described – 1 and 4 are visual arrestins and exclusively expressed in the visual system. The two non-visual isoforms 2 and 3, also known as β-arrestin 1 and 2 play a key role in the regulation of G protein-coupled receptor (GPCRs). Once recruited to A_1AR, binding of β-arrestin 2 can lead to desensitization and/or internalization of the receptor. Besides, β-arrestin 2-mediated downstream signal transduction of A_1AR has been reported. Signal transduction of A_1AR via G protein activation is well studied compared to signalling after recruitment of β-arrestins. However, β-arrestins have gained interest since they are multifunctional proteins that regulate several functions of GPCRs. The preference of activating either G proteins or β-arrestins is called ligand bias – this complex phenomenon can improve safety and efficacy of certain drugs. The mild sleep-inducing agent valerian extract improves sleep quality and is widely used as phytopharmaceutical in several countries. Even though the effect is proven in clinical studies, the exact mechanism of action including potential targets is not fully understood. This present study addresses the influence of valerian extract Ze 911 on A_1AR in detail. One focus was the investigation of β-arrestin 2 recruitment after A_1AR stimulation with valerian extract or synthetic ligands. For that reason, a cell-based β-arrestin 2 recruitment assay was developed. This so-called NanoBiT® assay worked A_1AR-specific with highly reproducible results. Agonistic effects were measured for endogenous agonist adenosine as well as synthetic agonists like N6-cyclopentyladenosine (CPA) and capadenoson. Moreover, valerian extract Ze 911 showed a robust agonistic effect, which was later attributed to the adenosine detected in the extract. Dicaffeoylquinic acids (DQAs), a substance class present in Ze 911, showed a modulatory effect on A_1AR combined with the endogenous ligand adenosine. Additionally, CPA and Ze 911 treatment decreased cAMP concentration in A_1AR overexpressing HEK 293 GloSensor™ cells. In a calcium mobilization assay, CPA, Ze 911 and DQAs showed no significant calcium mobilization after single

treatment. Interestingly, they modulated the calcium mobilization of the positive control methacholine. Single-particle tracking (SPT) experiments were conducted to investigate lateral mobility of A_1AR after agonist treatment on A_1AR-overexpressing HEK 293 cells. SPT measurements were started 15 minutes after cells were treated with either CPA or Ze 911. No differences in any of the investigated parameters have been detected compared to control cells. Since time played an important part in the response curves of the other assays, a time-dependent approach was conducted next. Five time intervals were investigated from 1 up to 30 minutes after treatment with CPA. Confined fractions and state occupancies of A_1AR were influenced in certain time intervals. Longer incubation times significantly increased those parameters compared to shorter incubation times. Diffusion coefficients and receptor homo-oligomerization were not altered over time. These findings demonstrate that Ze 911 contains agonistic as well as modulatory substances that influence A_1AR in various ways.

Table of Contents

Table Index

Figure Index

List of abbreviations

AC	adenylate cyclase
ACN	acetonitrile
ADA	adenosine deaminase
Ado	adenosine
ADP	adenosine diphosphate
ATP	adenosine triphosphate
AR	adenosine receptor
A_1AR	adenosine A_1 receptor
A_{2A}AR	adenosine A_{2A} receptor
A_{2B}AR	adenosine A_{2B} receptor
A_3AR	adenosine A_3 receptor
β_1AR	β_1-adrenergic receptor
β_2AR	β_2-adrenergic receptor
BAY 60-6583	2-[[6-Amino-3,5-dicyano-4-[4-(cyclopropylmethoxy)phenyl]-2-pyridinyl]thio]-acetamide (A_{2B}AR agonist)
cAMP	cyclic adenosine monophosphate
CGS 21680	3-[4-(2-{[6-Amino-9-(N-ethyl-β-D-ribofuranosyluronamide)-9H-purin-2-yl]amino}ethyl)phenyl]propanoic acid (A_{2A}AR agonist)
CHO cells	Chinese hamster ovary cells
CNS	central nervous system
CPA	N6-cyclopentyladenosine (A_1AR agonist)
CREB	cAMP response element binding protein
DMSO	dimethyl sulfoxide
DMEM	Dulbecco's Modified Eagle Medium
DPCPX	8-cyclopentyl-1,3-dipropylxanthine (A_1AR antagonist)
DQA	dicaffeoylquinic acid
DSMZ	Deutsch Sammlung von Mikroorganismen und Zellkulturen (Leibniz-Institut)
EC_{50}	half maximal effective concentration
EMCCD	Electron-Multiplying Charge-Coupled Device
ER	endoplasmic reticulum
ERK1/2	extracellular signal-regulated kinases 1 and 2
FA	formic acid
FBS	fetal bovine serum
FD	fast digest

FSK	forskolin
GABA	gamma-aminobutyric acid
GPCR	G protein-coupled receptor
GRK	G protein-coupled receptor kinase
h	hour
HBSS	Hanks' balanced salt solution
HEK 293 cells	human embryonic kidney cells
HEPES	2-[4-(2-Hydroxyethyl)piperazin-1-yl]ethane-1-sulfonic acid
HPLC	high-performance liquid chromatography
IC_{50}	half maximal inhibitory concentration
IP_3	inositol 1,4,5-triphosphate
Iso	isoprenaline
LC-MS/MS	liquid chromatography tandem-mass spectrometry
log	logarithm to the base 10
MAPK	mitogen-activated protein kinase
NanoLuc	nanoluciferase
min	minutes
NaCl	sodium chloride
NECA	(2S,3S,4R,5R)-5-(6-amino-9H-purin-9-yl)-N-ethyl-3,4-dihydroxy-tetrahydrofuran-2-carboxamide (5′-N-Ethylcarboxamidoadenosine, non-specific AR agonist)
NREM	non-rapid eye movement
PBS	phosphate buffered saline
PCA	protocatechuic acid
PEI	polyethylenimine
Pen/Strep	penicillin-streptomycin
PIP_2	phosphatidylinositol 4,5-bisphosphate
PIP_3	phosphatidylinositol (3,4,5)-trisphosphate
PKA	protein kinase A
PLC	phospholipase C
REM	rapid eye movement
RLU	relative light unit
RT	room temperature
SD	standard deviation
SEM	standard error of the mean
SPT	single-particle tracking
s	seconds

TAE	TRIS/Acetate/EDTA
VCP 171	[2-Amino-4-[3-(trifluoromethyl)phenyl]-3-thienyl]phenyl-methanone (positive allosteric modulator at A_1AR)
VLPO	ventrolateral preoptic area
Ze 911	valerian extract by Max Zeller Söhne AG Switzerland
2-Chloro-IB-MECA (MECA)	1-[2-chloro-6-[[(3-iodophenyl)methyl]amino]-9H-purin-9-yl]-1-deoxy-N-methyl-β-D-ribofuranuronamide (A_3AR agonist)

1 Introduction

Human beings must sleep – in general one-third of their lives. An uninterrupted and restful night sleep is tremendously pleasing while sleep deprivation or disorders cause a lot of stress to the human body[1]. Many researchers have focused on the question: why do we have to sleep and what is the function behind it? Even though a lot of progress has been made in the past decades, the exact purpose and function of sleep still eludes us. It is a complex, heterogeneous process including an impact of several different brain regions and neurochemicals[2]. In general, two different states of sleep are distinguished: rapid eye movement (REM) and non-rapid eye movement (NREM) sleep. REM and NREM sleep underly a specific neuronal circuit and are controlled by neurons in the hypothalamus and brainstem[3]. REM sleep is triggered by activation of cholinergic neurons, while serotonergic and noradrenergic neurons are non-active. There is a switch mechanism in the brainstem that can either activate REM promoting or NREM promoting neurons leading to the characteristic cycle between both types during sleep period[2]. Sleep and wakefulness are controlled by a large network of neuronal structures and pathways. Wakefulness is promoted by the so-called “ascending arousal system”, that includes the neurochemicals serotonin from the midline raphe nuclei, norepinephrine from the locus coeruleus, dopamine from the ventral periaqueductal grey matter, histamine from the tuberomammillary nucleus, acetylcholine from the pedunculopontine tegmentum and orexin from the perifornical area. In reverse, initiation and preservation of sleep depends on the suppression of the ascending arousal system[1,2]. Neurons of the ventrolateral preoptic area (VLPO) are responsible for the suppression of the ascending arousal system[4]. Even though it is still not fully understood how VLPO is activated, adenosine seems to play a key role in this complex process. There is a hypothesis that VLPO neurons are indirectly activated and supported by adenosine via the reduction of GABAergic inhibition. These “disinhibited” neurons are now able to supress the ascending arousal system and consequently promote sleep[5].

The market nowadays is well-equipped with several synthetic sleep-inducing pharmaceuticals. Even though these substances are usually very effective most of them come with great disadvantages and risks. One of the biggest risks of regularly prescribed hypnotics like Z-drugs and benzodiazepines is addiction[6]. Moreover, overdosing hypnotics can lead to respiratory arrest[7,8]. Consequently, the prescription and intake of synthetic sleep-inducing agents should be well considered. Sleep-promoting phytopharmaceuticals containing extracts from valerian, hop or balm for example are a lot safer. Their reliability has been proven over several decades all over the world[9]. Valerian extract is a well-established sleep-inducing agent that is frequently used for sleep disorders. However, the existing data is not strong enough to include valerian extract within the medical guidelines for the treatment of sleep disorders[10]. The data situation

must be improved including clinical and preclinical studies. Since plant extracts are highly complex mixtures containing different substances, it is not trivial to investigate the active constituents. In fact, it is quite the opposite - investigating and identifying substances of interest involved in signalling pathways is rather challenging for plant extracts. The identification of the active substances is difficult and time-consuming. It has been described that one target of valerian extract is the gamma aminobutyric acid ($GABA_A$) receptor that causes sedation[11]. The expression of the gene *GABRB3*, which encodes the β subunit of $GABA_A$ receptor, was increased by valerian extract inducing a sedative and anxiolytic effect[12,13]. Another promising target of valerian is the adenosine A_1 receptor (A_1AR) that plays a major role in sleep-wake-cycle[14,15]. Müller et al. 2002[16] showed that valerian extract acts as partial A_1AR agonist explaining its sleep-inducing effect. However, there is still a lot of potential in understanding the exact mechanism, including the identification of certain substances or substance classes that may be responsible for the sedative effect.

1.1 Adenosine A_1 receptor and its role in sleep regulation

Adenosine is a ubiquitous endogenous nucleoside that is found in practically all tissues of the human body[17]. It is involved in dozens of cellular processes including key pathways like purinergic nucleic acid base synthesis. Consequently, it is a very well-studied molecule[18,19]. Adenosine is generated by hydrolysis of adenosine diphosphate (ADP) and adenosine triphosphate (ATP) intracellularly as well as extracellularly and is one of the major metabolites in living organisms[20]. The release of adenosine is transmitted by adenosine transporters, which are classified into concentrative nucleoside transporters (CNTs) and equilibrative nucleoside transporters (ENTs)[21]. It acts as neuromodulator and controls several brain functions by binding to adenosine receptors (ARs)[22]. ARs belong to G protein-coupled receptors (GPCRs), and they are differentiated into four subtypes named A_1AR, $A_{2A}AR$, $A_{2B}AR$ and A_3AR. The affinity towards adenosine is different for the receptors, the affinities of A_1AR and $A_{2A}AR$ are considered high whereas they are considered low for $A_{2B}AR$ and A_3AR[22]. ARs are commonly differentiated by coupling either to stimulatory or inhibitory G proteins. Binding of an agonist to the receptor results in conformational changes leading to downstream signalling via G proteins consisting of α, β and γ subunits[23] (Figure 1). $A_{2A}AR$ and $A_{2B}AR$ are binding to $G_{s/olf}$ proteins and consequently activate adenylate cyclase (AC) while A_1AR and A_3AR bind to $G_{i/o}$ proteins leading to inhibition of AC activity. In conclusion, activation of A_1AR and A_3AR results in inhibition of cyclic adenosine monophosphate (cAMP) formation and consequently a decreased protein kinase A (PKA) activity and phosphorylation of cAMP response element binding protein (CREB). Activation of $A_{2A}AR$ and $A_{2B}AR$ vice versa increase the formation of cAMP resulting in activation of PKA and phosphorylation of CREB[20]. Additionally, phospholipase C (PLC) is activated by

A_1AR leading to an increase of inositol 1,4,5-triphosphate (IP_3) and in turn to a release of calcium from the endoplasmic reticulum (ER) into the cytosol[24] (Figure 1). ARs are expressed in all kinds of different cells, body tissues and major organs including brain, liver, kidney, lungs and heart[20,25,26]. A_1AR is widely distributed in the central nervous system (CNS) including the brain, predominantly in the hippocampus, cerebellum, cortex and spinal cord[26–30]. A_1ARs have gained interest as potential pharmaceutical target for several diseases since they are involved in many different physiological and pathophysiological processes[20,31,32]. Changes of adenosine levels have been linked to disease-related conditions such as cancer, neurodegenerative disorders, asthma or inflammatory diseases[26].

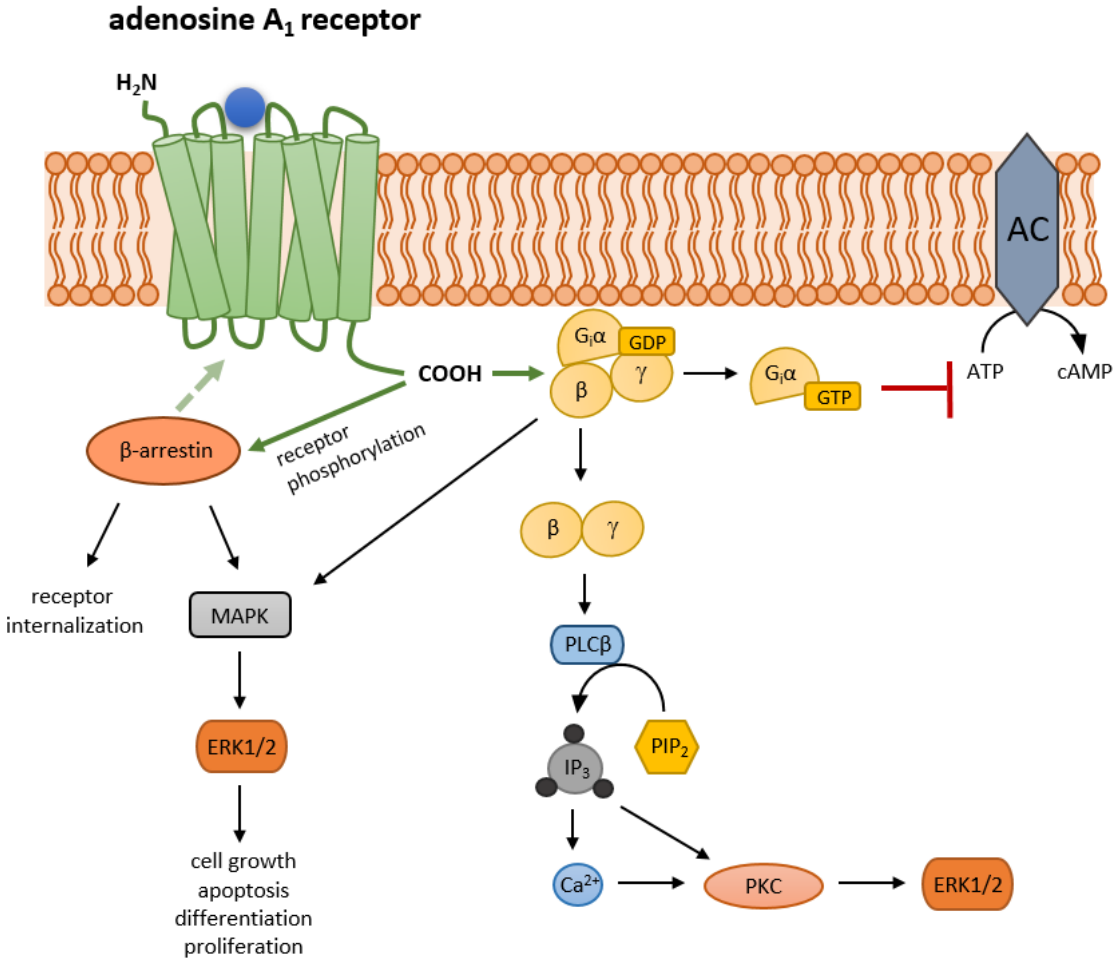

Figure 1. Adenosine A_1 receptor signalling. Stimulation of A_1AR results in activation of $G_{i}\alpha$ which decreases AC activity and consequently cAMP production. PLCβ is activated by βγ subunit that catalyses PIP_2 to IP_3 leading to Ca^{2+} mobilization. Receptor phosphorylation at C-terminus provokes recruitment of β-arrestins. This either leads to receptor internalization or promotes downstream signalling processes. Figure was created in PowerPoint and adapted from Zhong et al. 2022[33].

A_1AR agonists are usually modification products of the endogenous AR agonist adenosine (Figure 2A). N6-cyclopentyladenosine (CPA) for example is modified at N^6-position that ensures high selectivity at A_1AR[34] (Figure 2C). The potent non-selective AR agonist 5′-N-Ethylcarboxamidoadenosine (NECA) arises from a 5′-N alkyluronamide modification[35] (Figure 2B). Antagonists of A_1AR are usually differentiated in xanthine derivatives and non-xanthine antagonists. Commonly used antagonist 8-cyclopentyl-1,3-dipropylxanthine (DPCPX) belongs to xanthine derivatives with a highly selective effect at A_1AR[35] (Figure 2D). Investigations of the crystal structure of A_1AR revealed a second extracellular loop with an open-binding cavity containing a secondary binding pocket allowing the receptor to interact with allosteric as well as orthosteric ligands[36].

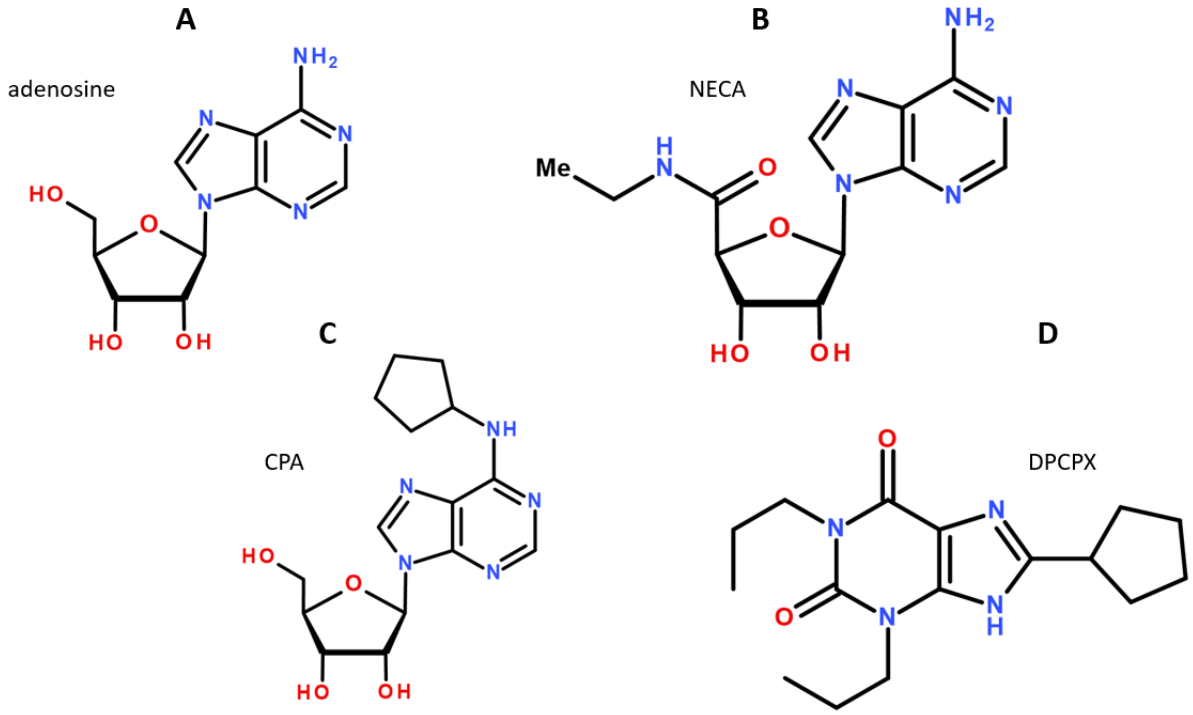

Figure 2. A_1AR agonists and antagonist. Non-selective endogenous AR agonist adenosine (A), non-selective AR agonist NECA (B), selective A_1AR agonist CPA (C) and A_1AR antagonist DPCPX (D). Chemical structures were created using BIOVIA Draw 2017 version R2.

The role of adenosine in the sleep-wake cycle has been studied in vitro as well as in vivo in the last decades. Extracellular adenosine concentrations in the brain increase during prolonged wakefulness and decrease during sleep recovery[37,38]. The sedative effect of adenosine has been demonstrated frequently[39–41]. Sleep-promoting properties are forwarded by two of the four adenosine receptors, A_1AR and $A_{2A}AR$. Several cells and brain regions that could play a role were investigated. Prolonged wakefulness or sleep deprivation resulted in upregulation of A_1AR in cortical and subcortical brain regions[42]. It has been shown that adenosine induces

sleep via A_1AR by inhibiting arousal cell groups (wake-promoting) in the basal forebrain[43]. In addition, the sleep-promoting effect of adenosine via A_1AR can be explained by the suppression of hypocretin/orexin neurons in the lateral hypothalamus[44]. Furthermore, it has been demonstrated that injection of A_1AR agonist CPA into rat brain (tuberomammillary nucleus) increased NREM sleep[45]. Additionally, injections of adenosine deaminase (ADA) inhibitor or adenosine into rat brain also increased NREM sleep. This effect was completely reversed by A_1AR antagonist[45]. Furthermore, infusion of an A_{2A}AR receptor agonist into rat basal forebrain increased NREM and REM sleep profoundly[46]. It is suggested that stimulated A_{2A}AR activates sleep promoting neurons in the VLPO area. The probably most famous opponent of adenosine is caffeine, a trimethylxanthine present in coffee or tea for example[47]. Caffeine antagonizes A_1AR and A_{2A}AR in the brain and promotes wakefulness.

1.1.1 Potential of β-arrestins

Activation of A_1AR induces G protein dependent signalling. Additionally, A_1AR activation can also provoke recruitment of multifunctional adapter proteins called β-arrestins. The recruitment and binding of β-arrestins and subsequent signal transduction is initiated by receptor phosphorylation through G protein-coupled receptor kinases (GRKs) (Figure 1). Four different isoforms of arrestins have been identified, isoform 1 and 4 are so-called visual arrestins while isoform 2 and 3 are considered non-visual[48]. The two non-visual arrestins together with ubiquitously expressed GRKs are key players in the regulation of GPCR signal transduction and are better known as β-arrestin 1 and 2[49,50]. Once β-arrestins are activated, they can either promote downstream signalling processes or direct receptor desensitization[50–52]. In case they function as G protein independent adaptor proteins, they e.g. activate mitogen-activated protein kinases (MAPKs) like extracellular signal-regulated kinases 1 and 2 (ERK1/2) or c-Jun N-terminal protein kinases[53]. Hence, β-arrestins can perform as both negative and positive regulators: as positive modulators, they signal to specific targets[54,55] while they inhibit G protein signal transduction as negative modulators[56]. Selective coupling of β-arrestins might be more useful and crucial to some GPCRs than to others - in fact, in some cases, signalling via β-arrestins could be even more important than G protein signalling. In the last decades, the great potential of substances favouring and activating only one pathway by stabilizing a subset of receptor conformations has been studied extensively. This phenomenon called biased signalling or ligand bias has been investigated for several GPCRs[57]. A very prominent example is the β-arrestin-biased β_1-adrenergic receptor (β_1AR) antagonist carvedilol that promotes cardioprotection by β-arrestin mediated EGFR transactivation[58]. LUF5589, an A_1AR agonist that showed functional selectivity for G protein dependent signalling over β-arrestin signalling has

been identified[59]. Even though it has been shown that stimulated A_1AR recruits β-arrestins[53,60,61], the data situation is narrow. There is evidence that β-arrestins play a part in sleep regulation. Kim et al. 2018[62] developed a β-arrestin-biased serotonin receptor (5-HT_7R) agonist that decreased REM sleep time and increased NREM sleep time. Although, little has been published about β-arrestins and possible influences on sleep wake-cycle, there is evidence that sleep-affecting orexin 1 and 2 receptors are regulated by β-arrestins[63].

1.2 Medicinal properties of Valeriana officinalis

The herbal medicinal product valerian (Valeriana officinalis) is commonly used as a mild sleep-inducing agent since decades. Back in 1982, a study with 128 volunteers already showed a significant improve in sleep quality after using valerian preparations[64]. Valerian belongs to the Caprifoliaceae family and the name is derived from “valere”, which means well-being or health in Latin[65]. Herbal medicinal products have advantages over synthetic medicinal products, particularly fewer severe side effects and risks of intoxication[66]. The root extract is applied medically in many countries all over the world because of its sedative and anxiolytic properties. Furthermore, it is also known to act antimicrobial, anti-inflammatory, neuroprotective and antioxidative[67–69]. The plant appears up to 1.5 m in height with small pink flower clusters[66] (Figure 3A). The pharmaceutically active root extract comes as brownish powder and has a very characteristic smell (Figure 3C), which is further processed to tablets, capsules or liquids. Valerian is either used as a monopreparation or combined with other herbal drugs like hop or lavender. Even though the sedative effect of valerian is known for a long time, there are still controversies about the responsible components. It is already known that components of valerian are binding to and interacting with A_1AR. A partial agonistic effect of the extract has been shown[14,16]. Lignans, especially 4‘-O-β-d-glucosyl-9-O-(6“-deoxysaccharosyl)olivil (olivil) seemed to be a promising component[15]. However, Sendker et al. 2020[70] investigated the occurrence of several lignans in valerian root extract and lack finding olivil. They hypothesised that olivil might not occur in valerian root regularly in the expected amounts. There is a lot of potential to improve the current data situation about valerian extract concerning both, the mechanisms of action and the responsible active substances.

Figure 3. Valeriana officinalis. (A) Blooming Valeriana officinalis with clusters of pink or white flowers. (B) Brown roots that are typically used for medicinal purposes. Valerian extract is prepared by maceration of dried roots. The resulting dry extract (C) is further processed e.g. into capsules or liquids[1].

1.2.1 Chemical composition

About 150-200 chemical components are found in Valeriana officinalis[65,71]. Variations in the composition can occur due to different growing-, storing- or processing conditions. Even the composition of standardized valerian extracts can differ slightly with a consistent quality[65]. The roots and rhizomes are composed of two main constituent groups: Valepotriates including valtrate and sesquiterpenes of the volatile oil including valerenic acids and its derivates. In addition, other components like triterpenes, flavonoids, lignans, alkaloids and free amino acids are found in the plant extract[72–74]. Alkaloids make up around 0.01 – 0.05 % of the overall extract composition. One of the main alkaloids in the essential volatile oil of valerian is actinidine, that is a pheromone for insects and known to attract cats. As a psychoactive alkaloid, actinidine interferes with the GABAergic metabolism[75]. Other alkaloids present in the extract are valerianine, valerene, chatinine, naphthyridine and methyl ketone[76,77]. Other components in the volatile essential oil are organic acids and terpenes, which represent 0.2 – 2.8 % of the root extract. Terpenes are chemically divided and characterized as sesquiterpenes and monoterpenes. Most substantial are valerenic, isovalerenic, valeric, isovaleric, acetoxyvalerenic acid and hydroxyvalerenic acid. In addition, considerable amounts of valeranone, cryptofauronol, 1-pinene, 1-comphene, 1-borneol, terpineol, bornyl acetate and bornyl isovalerenate are found in Valeriana officinalis[75].

[1](A): https://www.samendirekt.de/echter-baldrian-valeriana-officinalis.html (accessed November 5th, 2024)
(B): https://www.etsy.com/de/listing/477903143/baldrianwurzel-geschnitten-valeriana (accessed November 5th, 2024)
(C): https://www.herbathek.com/heilkraeuter-fuer-tiere/kraeuter-geschnitten-und-gemahlen/baldrianwurzel-gemahlen-bio (accessed November 5th, 2024)

2 Aim and Approach

The herbal medicinal product Valeriana officinalis is used as a mild sleep-inducing agent all over the world since decades. It has already been proven in 1982 that valerian significantly improves sleep quality in humans[64]. It unfolds its potential either as single medicinal preparation or in combination with other medicinal plants like hop, balm or lavender. One of the biggest advantages of phytopharmaceuticals over chemical sleeping-inducing agents is the safety – they have less side effects that are usually not severe. The brownish root of valerian contains around 200 substances and is therefore a complex mixture with a lot of potential[75].

Even though there has been progress about the active components and potential targets of valerian extract in the last two decades, there still is a lot of capacity in identifying the active substances and understanding their effects. Until today, valerian preparations are not included in medicinal guidelines for the treatment of sleeping disorders. However, it has been shown that valerian extract acts as partial A_1AR agonist[14,16,78]. The agonistic effect was demonstrated by the inhibition of adenylate cyclase and in conclusion decrease of cAMP accumulation in isolated membranes of A_1AR overexpressing Chinese hamster ovary (CHO) cells that were treated with valerian extract[16]. Other signalling pathways and mechanisms that could be influenced by valerian are rarely studied by now. It is still controversial, which components are mainly responsible for the sleep-inducing effect. Therefore, this work aimed to improve the current limited data situation about valerian extract and its components responsible for the sleep-inducing effect.

Considering that A_1AR is a key player in the sleep-wake cycle and one of the most promising targets, it was the focus of this study. Since β-arrestin dependent signalling is becoming more and more important for drug research and it has not been addressed for valerian extract, a β-arrestin 2 recruitment assay has been established. A_1AR-mediated β-arrestin 2 recruitment was investigated after stimulation with valerian extract Ze 911 and other A_1AR ligands. Besides investigating potential agonistic effects of Ze 911, this work aimed to identify effective components and detect possible A_1AR-modulating properties of valerian extract. To get a comprehensive picture of valerian interacting with A_1AR, cAMP assay and calcium mobilization assay were conducted as well. Additionally, lateral diffusion behaviour and corresponding receptor characteristics were investigated after A_1AR stimulation using single-particle tracking. Improving the data situation including verifying the efficacy as well as ensuring the safety for patients using valerian extracts for mild sleep disorders was the overriding aim of this work. The confidence of using and prescribing phytopharmaceuticals before choosing chemical alternatives would be desirable – this however is dependent on solid clinical and preclinical data.

3 Materials and Methods

3.1 Materials

Table 1. Cell lines

Cell line	Cell type	Culture medium	Supplier
HEK 293	Human embryonic kidney cells	DMEM Low Glucose (Gibco, 31885-023) + 10% FBS + 1 % Pen/Strep	DSMZ, ACC 305
SH-SY5Y	Human neuroblastoma cells	DMEM High Glucose (Gibco, 41965-039) + 15% FBS + 1 % Pen/Strep	DSMZ, ACC 209

Table 2. Stably transfected cell lines

Name	Expressed genetic information	Transfection method	Culture medium
HEK 293-GloSensor™-HiBiT-A_1AR	cAMP dependent firefly luciferase (pGloSensor™-22F cAMP), HiBiT-tagged human A_1AR	PEI	DMEM Low Glucose (Gibco, 31885-023) + 10 % FBS + 1 % Pen/Strep
HEK 293-GloSensor™-HiBiT-A_1AR **single clone**	cAMP dependent firefly luciferase (pGloSensor™-22F cAMP), HiBiT-tagged human A_1AR	PEI	DMEM Low Glucose, no phenol red (Gibco, 11054-020) + 10 % FBS + 1 % Pen/Strep + 1X Glutamax
HEK 293-A_1AR-LgBiT-SmBiT-β-arrestin 2	LgBiT-tagged human A_1AR, SmBiT-tagged β-arrestin 2	PEI	DMEM Low Glucose (Gibco, 31885-023) + 10% FBS + 1 % Pen/Strep

Table 3. Enzymes

Enzyme	Supplier	Reference number
Adenosine Deaminase from bovine spleen (ADA)	Sigma-Aldrich, Darmstadt, Germany	A5043-250UN
FastDigest NheI	Thermo Fisher Scientific™ Waltham, MA, USA	FD0974
FastDigest XhoI	Thermo Fisher Scientific™ Waltham, MA, USA	FD0694
FastDigest PvuII	Thermo Fisher Scientific™ Waltham, MA, USA	FD0634
FastDigest Eco32I	Thermo Fisher Scientific™	FD0304

	Waltham, MA, USA	
FastDigest BcuI	Thermo Fisher Scientific™ Waltham, MA, USA	FD1253
FastDigest NotI	Thermo Fisher Scientific™ Waltham, MA, USA	FD0593
FastDigest NcoI	Thermo Fisher Scientific™ Waltham, MA, USA	FD0574
FastDigest HindIII	Thermo Fisher Scientific™ Waltham, MA, USA	FD0504
FastDigest BamHI	Thermo Fisher Scientific™ Waltham, MA, USA	FD0054
Q5® High-Fidelity DNA Polymerase	New England Biolabs®, Ipswich, MA, USA	M0491S
T4 DNA Ligase (5 U/µl)	Thermo Fisher Scientific™ Waltham, MA, USA	EL0011

Table 4. Purchased solutions and chemicals

Solution / Chemical	**Supplier**	**Reference number**
Fetal Bovine Serum (FBS)	Thermo Fisher (Gibco™), Waltham, MA, USA	10270106
Dulbecco's Modified Eagle Medium (DMEM)	Thermo Fisher (Gibco™), Waltham, MA, USA	31885049
Dulbecco's Modified Eagle Medium High Glucose	Thermo Fisher (Gibco™), Waltham, MA, USA	11574486
Dulbecco's Modified Eagle Medium Low Glucose, no phenol red, no glutamine	Thermo Fisher (Gibco™), Waltham, MA, USA	11054020
Glutamax™ Supplement 100X	Thermo Fisher (Gibco™), Waltham, MA, USA	35050061
Hank's Balanced Salt Solution (HBSS)	Thermo Fisher (Gibco™), Waltham, MA, USA	14025050
Hygromycin B Gold™	InvivoGen, Toulouse, France	31282-04-9, ant-hg-1
Zeocin™ Selection Reagent	Thermo Fisher (Gibco™), Waltham, MA, USA	R25001
Geneticin™ Selective Antibiotic (G418)	Thermo Fisher (Gibco™), Waltham, MA, USA	10131035
Penicillin-Streptomycin 10,000 U/ml (Pen/Strep)	Thermo Fisher (Gibco™), Waltham, MA, USA	15140122
Trypsin EDTA 0.05%, phenol red (T/E)	Thermo Fisher (Gibco™), Waltham, MA, USA	25300104
Poly-D-Lysine (PDL)	Thermo Fisher (Gibco™), Waltham, MA, USA	A3890401
Dimethyl sulfoxide, HPLC grade, > 99.9 % (DMSO)	Thermo Fisher Scientific™, Waltham, MA, USA	022914-K2

GloSensor™ cAMP Reagent	Promega GmbH, Walldorf, Germany	E129A
Q5® High-Fidelity 2X Master Mix	New England Biolabs®, Ipswich, MA, USA	M0492S
GeneRuler 1 kb DNA ladder	Thermo Fisher Scientific™ Waltham, MA, USA	11823963
T4 DNA Ligase buffer (10x)	Thermo Fisher Scientific™ Waltham, MA, USA	B69
XL1-Blue competent cells	VWR International GmbH, Darmstadt, Germany	AGLS200249
Cal-520®, AM	AAT Bioquest®, Pleasanton, CA, USA	ABD-21130
Janelia Fluor® HaloTag® Ligand 646	Promega GmbH, Walldorf, Germany	GA1120
Polyethylenimine (PEI)	Sigma-Aldrich, Darmstadt, Germany	408727
Pluronic® F-127	Sigma-Aldrich, Darmstadt, Germany	P2443-250G
HEPES	AppliChem, Darmstadt, Deutschland	A1069
Sodium chloride (NaCl)	AppliChem, Darmstadt, Deutschland	146994
Potassium chloride (KCl)	AppliChem, Darmstadt, Deutschland	191494
D(+)-Glucose	Sigma-Aldrich, Darmstadt, Germany	G8270
Forskolin	Sigma-Aldrich, Darmstadt, Germany	F3917
Bacto™ Tryptone	Thermo Fisher (Gibco™), Waltham, MA, USA	211705
Bacto™ Yeast extract	Thermo Fisher (GibcoTM), Waltham, MA, USA	212750
Isoprenaline hydrochloride	Sigma-Aldrich, Darmstadt, Germany	I5627
Methacholine hydrochloride	Sigma-Aldrich, Darmstadt, Germany	A2251
Coelenterazine h	Biomol GmbH, Hamburg, Germany	Cay16894-500
Agarose	Sigma-Aldrich, Darmstadt, Germany	A4718
Ampicillin	Sigma-Aldrich, Darmstadt, Germany	A9518
Ethidium Bromide	Thermo Fisher Scientific™ Waltham, MA, USA	15585011
Acetonitrile	VWR International GmbH, Darmstadt, Germany	20060.320

Valerenic acid	Sigma-Aldrich, Darmstadt, Germany	02010595-10MG
Acetoxyvalerenic acid	PhytoLab GmbH, Vesten-bergsgreuth, Germany	89151
Hydroxyvalerenic acid	PhytoLab GmbH, Vesten-bergsgreuth, Germany	89224
(+)-Pinoresinol	PhytoLab GmbH, Vesten-bergsgreuth, Germany	89525
Pinoresinol diglucoside	PhytoLab GmbH, Vesten-bergsgreuth, Germany	89850
(-)-Olivil	PhytoLab GmbH, Vesten-bergsgreuth, Germany	83883
Protocatechuic acid	Biomol GmbH, Hamburg, Germany	Cay14916-25

Table 5. Self-generated solutions

Solution	Composition
Lysogeny broth-medium (LB medium), pH 7.0	1% (w/v) Bacto™ Tryptone 0.5% (w/v) Bacto™ Yeast extract 1% (w/v) NaCl
HBSS/HEPES 20 mM, pH 7.4	20 mM HEPES in 500 ml HBSS
Sodium chloride solution (150 mM)	150 mM NaCl in 50 ml H_2O
Locke's solution (Locke), pH 7.4	150 mM NaCl 5.6 mM KCl 2.3 mM $CaCl_2$ 1.0 mM $MgCl_2$ 3.6 mM NaHCO3 5.0 mM HEPES 20 mM Glucose

Table 6. Test compounds / ligands

Compound	Supplier	Solvent	Reference number
CPA	Cayman Chemicals, Ann Arbor, MI, USA	DMSO	21448
NECA	Sigma-Aldrich, St. Louis, MO, USA	DMSO	119140
DPCPX	Tocris, Bristol, UK	DMSO	0439
CGS 21680	Cayman Chemicals, Ann Arbor, MI, USA	DMSO	17126
BAY 60-6583	Tocris, Bristol, UK	DMSO	4472
Adenosine	Sigma-Aldrich, St. Louis, MO, USA	H_2O	A9251
2-Chloro-IB-MECA	Cayman Chemicals, Ann Arbor, MI, USA	DMSO	27336
VCP 171	Tocris, Bristol, UK	DMSO	6261

Capadenoson	Cayman Chemicals, Ann Arbor, MI, USA	DMSO	28422
Ze 911 valerian extract	Max Zeller Söhne AG, Romanshorn, Switzerland	DMSO	-
1,5-Dicaffeoylquinic acid	PhytoLab GmbH, Vestenbergsgreuth, Germany	DMSO	82221
3,4-Dicaffeoylquinic acid	PhytoLab GmbH, Vestenbergsgreuth, Germany	DMSO	80425
3,5-Dicaffeoylquinic acid	PhytoLab GmbH, Vestenbergsgreuth, Germany	DMSO	80426
4,5-Dicaffeoylquinic acid	PhytoLab GmbH, Vestenbergsgreuth, Germany	DMSO	80427

Table 7. Kits

Kit	Supplier	Reference number
NucleoSpin® Gel and PCR Clean-up	Macherey-Nagel, Düren, Germany	740609
NucleoSpin® Plasmid (NoLid), Mini Kit for plasmid DNA isolation	Macherey-Nagel, Düren, Germany	740499
NucleoBond® Xtra Midi Kit for plasmid DNA	Macherey-Nagel, Düren, Germany	740410
Nano-Glo® HiBiT Extracellular Detection System	Promega GmbH, Walldorf, Germany	N2420

Table 8. Software

Software	Supplier	Version
Agilent ChemStation	Agilent Technologies Inc., Santa Clara, CA, USA	Rev. B04.01
GraphPad® Prism	GraphPad Software Inc., San Diego, CA, USA	6.01 / 8.3.0
MATLAB®	The MathWorks, Inc. Natick, MA, USA	R2016b
Tecan® Spark Control	Tecan Group AG, Maennedorf, Switzerland	3.1
Clone Manager	Sci Ed Software LCC, Westminster, CO, USA	9

3.2 Methods

3.2.1 Cell culture

The two cell lines HEK 293 and SH-SY5Y were obtained from the German Collection of Microorganisms and Cell Cultures GmbH (DSMZ, Braunschweig, Germany; ACC 305 and ACC 209 respectively). HEK 293 cells were cultivated in Dulbecco's Modified Eagle Medium (DMEM) Low Glucose supplemented with 100 units/ml penicillin, 100 µg/ml streptomycin and 10 % FBS. SH-SY5Y cells were cultivated in DMEM High Glucose supplemented with 100 units/ml penicillin, 100 µg/ml streptomycin and 15 % FBS. Cells were passaged at 80-90 % confluency twice a week in a ratio of either 1:5 (SH-SY5Y) or 1:10 (HEK 293) in 10 cm dishes (10 cm dish, TC-treated, VWR International GmbH, 430165). They were maintained at 37°C and 5 % CO_2. Transfected HEK 293 cell lines were cultivated in the same manner.

3.2.2 Generation of expression plasmids and stably expressing cell lines

3.2.2.1 A_1AR-overexpressing HEK GloSensor™ cells

Cloning of pCDNA3.1Zeo_HiBiT-ADORA1

The plasmid ADORA1-Tango was a gift from Bryan Roth (Addgene plasmid #66209; http://n2t.net/addgene:66209; PRID: Addgene 66209). ADORA1-Tango containing the coding region for ADORA1 was amplified by addition of a NheI site and XhoI site to the 5'- and 3'-end using a PCR (forward primer: 5'-GATCGCTAGCATCCGATATGCCTCCCAGTATATCC-3'; reverse primer: 5'-GATCCTCGAGTTAGTCGTCAGGCCGTTCCTCTG-3'). The PCR was performed with a Q5 High-Fidelity DNA Polymerase using the conditions described in Table 9.

Table 9. PCR cycling conditions

PCR condition		
Step	**Temperature (°C)**	**Time (s)**
Initial denaturation	98 °C	120
Denaturation	98 °C	15 (25 cycles)
Annealing	63 °C	15 (25 cycles)
Extension	72 °C	30 (25 cycles)
Final extension	72 °C	120
End	4 °C	Infinite

The conditions remained the same for all PCRs following except for annealing and extension temperature and time. The excised PCR product containing the ADORA1 coding region was exchanged with the coding region for ADRB2 from the HiBiT-containing plasmid pCDNA3.1Zeo_HiBiT-ADRB2 using the same restriction sites.

Gel electrophoresis, ligation, transformation and transfection described below were performed in the same way for all plasmids following if not stated otherwise. Plasmid cards are attached in the supplementary material and data (see 8.1. plasmids).

Agarose gel electrophoresis and gel extraction

Digested samples were separated on a 1 % agarose gel. Agarose was dissolved in 1 x Tris-acetate-EDTA (TAE) buffer by heating up the mixture in a microwave until the solution was clear and free from solid agarose particles. Solution was cooled down to approximately 55 °C before adding ethidium bromide (1 µg/ml). Solution was carefully homogenized and slowly poured into a casting tray with comb. After the gel completely polymerized, comb was removed, and gel was placed into an electrophoresis chamber filled with 1 x TAE buffer. DNA samples and 1 kb DNA ladder were loaded onto the gel and electric current was applied (120 V / 45 min). UV detector was used to detect DNA fragments. Insert and corresponding vector DNA were cut out of the agarose gel using a scalpel and purified via NucleoSpin® Gel and PCR Clean up Kit.

Ligation and Transformation

Vector-DNA (20 ng) plus fivefold amount of Insert-DNA were mixed with 1 Unit T4 DNA Ligase and corresponding T4 DNA ligase reaction buffer and ligation took place at RT for one hour. Ten microliter ligation product was added to 100 µl competent XL-1 blue bacteria cells and the mixture was stored on ice for 30 min. Afterwards heat shock was performed at 42 °C for 1 min. Bacteria were stored on ice for another minute before adding 900 µl lysogeny broth (LB) medium. After incubation at 37 °C and vigorous shaking suspension was centrifuged at 3,000x g for 5 minutes supernatant was discarded. Cell pellet was resuspended in 50 µl fresh LB medium and spread onto an agar-LB-plate containing 50 µg/ml ampicillin. Single clones were picked from plates after incubation overnight at 37 °C. Clones were transferred into 5 ml LB medium containing 50 µg/ml ampicillin and incubated on a shaker overnight at 37 °C before purification using a NucleoSpin® Plasmid (NoLid) Mini kit for plasmid DNA isolation. Control digest was performed using the restriction enzyme FD-PvuII. Integrity of the construct was verified by agarose gel electrophoresis and confirmed by DNA sanger sequencing (Eurofins Genomics, Ebersberg, Germany) using two primers (forward primer: 5'-CGCAAATGGGCGG-TAGGCGTG-3'; reverse primer: 5'-TAGAAGGCACAGTCGAGG-3').

Transfection

100,000 HEK 293 cells per well were seeded into a 12-well plate (12-well tissue culture plate, surface treated, sterile, VWR International GmbH, Darmstadt, Deutschland) and co-transfected on the following day with the two plasmids pCDNA3.1Zeo_HiBiT-ADORA1 and

pGloSensor™-22F cAMP (Promega GmbH, GU174434) using 1 mg/ml polyethylenimine (PEI) in 150 mM sodium chloride (NaCl) solution. Therefore, 1 µg DNA was mixed with 2.5 µl PEI solution in 100 µl NaCl 150 mM. DNA-PEI-mixture was added dropwise to the cells containing 900 µl fresh growth medium. Cells were incubated 24 hours at 37 °C and 5 % CO_2. Medium was changed to fresh growth medium und cells were incubated for another 24 hours at 37 °C and 5 % CO_2. Afterwards, cells were seeded and tested for expression using Nano-Glo® HiBiT Extracellular Detection system (Promega GmbH, Walldorf, Germany). Simultaneously transient transfected cells were selected using Hygromycin B Gold (100 µg/ml, selection GloSensor™ system) and Zeocin™ (100 µg/ml). Once cells showed resistance, growth medium without antibiotics was used.

3.2.2.2 A_1AR-NanoBit®-β arr2 HEK 293 cells

Cloning of pCDNA3.1Zeo_SmBiT-ARRB2

Two cloning steps were necessary to generate the above-mentioned plasmid. The two plasmids pCerulean-N-ARRB2 and pCDNA3_SmBiT-ADRB2 were digested with the two restriction enzymes FD-NheI and FD-XhoI for 1 hour at 37 °C. Vector and insert DNA were obtained by 1% agarose gel extraction and purified via NucleoSpin® Gel and PCR Clean up Kit as described above. Ligation was carried out 30 min at RT with T4 DNA Ligase (5 U/µl) using the protocol described earlier. Transformation took place in XL1-Blue competent cells. Clones were picked from ampicillin-resistant agar plates after incubation overnight at 37 °C. Clones grew in LB medium containing 50 µg/ml ampicillin overnight before purification using a NucleoSpin® Plasmid (NoLid) Mini kit for plasmid DNA isolation. Control digest was performed using the restriction enzyme FD-Eco32I. To remove the signal peptide form the newly generated plasmid pCDNA3_SigPep-SmBiT-ARRB2, the coding region for SmBiT-ARRB2 was amplified by addition of a BcuI site and NotI site to the 5'- and 3'-end using a PCR (forward primer: 5'-GATCACTAGTCCATGGTGACCGGCTACC-3'; reverse primer: 5'- GATCGCGGCCGCTAG-CAGAACTGGTCATCACAG-3') with an annealing temperature of 63 °C (10 s, 25 cycles) and an extension temperature of 72 °C (45 s, 25 cycles). The PCR product containing the insert cutout SmBiT-ARRB2 and another vector plasmid (pCDNA3.1Zeo) were treated with the same restriction enzymes FD-BcuI and FD-NotI. Insert and vector DNA were obtained by 1 % agarose gel extraction and purified via NucleoSpin® Gel and PCR Clean up Kit. Ligation was carried out 30 min at RT with T4 DNA Ligase (5 U/µl). Transformation took place in XL1-Blue competent cells. Clones were picked from ampicillin-resistant agar plates after incubation overnight at 37 °C. Picked Clones grew in LB medium containing 50 µg/ml ampicillin overnight before purification using a NucleoSpin® Pasmid (NoLid) Mini kit for plasmid DNA isolation. Control digest was performed using the restriction enzyme FD-NcoI. DNA sanger sequencing

was performed (Eurofins Genomics, Ebersberg, Germany) using two primers (forward primer: 5'-CGCAAATGGGCGGTAGGCGTG-3'; reverse primer: 5'-TAGAAGGCACAGTCGAGG-3').

Cloning of pCMV_ADORA1-LgBiT

The plasmid ADORA1-Tango was a gift from Bryan Roth (Addgene plasmid # 66209; http://n2t.net/addgene:66209; PRID: Addgene 66209). The coding region for ADORA1 was amplified by addition of a HindIII site and BamHI site to the 5'- and 3'-end using a PCR (forward primer: 5'- GATCAAGCTTGATATGCCTCCCAGTATATCCG-3'; reverse primer: 5'-GATCG-GATCCGAGTCGTCAGGCCGTTC-3') with an annealing temperature of 61 °C (15 s, 25 cycles) and an extension temperature of 72 °C (30 s, 25 cycles). The PCR product containing the cutout ADORA1 and another plasmid containing LgBiT (pCMV_ADORA2B-LgBiT) were treated with the same restriction enzymes to cut out ADORA2B. Insert and vector DNA were obtained by 1% agarose gel extraction and purified via NucleoSpin® Gel and PCR Clean up Kit in the same way than described above. Ligation was carried out one hour at RT with T4 DNA Ligase (5 U/µl). Transformation took place in XL1-Blue competent cells. Clones were picked from ampicillin-resistant agar plates after incubation overnight at 37 °C. Clones grew in LB medium containing 50 µg/ml ampicillin overnight before purification using a NucleoSpin® Pasmid (NoLid) Mini kit for plasmid DNA isolation. Control digest was performed using the restriction enzyme FD-PvuII. DNA construct was confirmed by sanger sequencing (Eurofins Genomics, Ebersberg, Germany) using two primers (forward primer: 5'-CGCAAATGGGCGG-TAGGCGTG-3'; reverse primer: 5'-TAGAAGGCACAGTCGAGG-3').

100,000 HEK 293 cells per well were seeded into 12-well plate and co-transfected on the following day with the two plasmids pCMV_ADORA1-LgBiT and pCDNA3.1Zeo_SmBiT-ARRB2 using 1 mg/ml PEI. Transient transfected cells were selected using Zeocin™ (100 µg/ml) and Geneticin™ (G418, 700 µg/ml). Once cells showed resistance, growth medium without antibiotics was used.

3.2.3 Dynamic mass redistribution studies

Dynamic mass redistribution (DMR) is a method that allows label-free detection of ligand-induced changes in living cells. It requires biosensor-coated microplates that measure changes in mass of cells proximal to the sensor (Figure 4). DMR studies were performed to get a first impression if HEK 293 cells react to A_1AR stimulation.

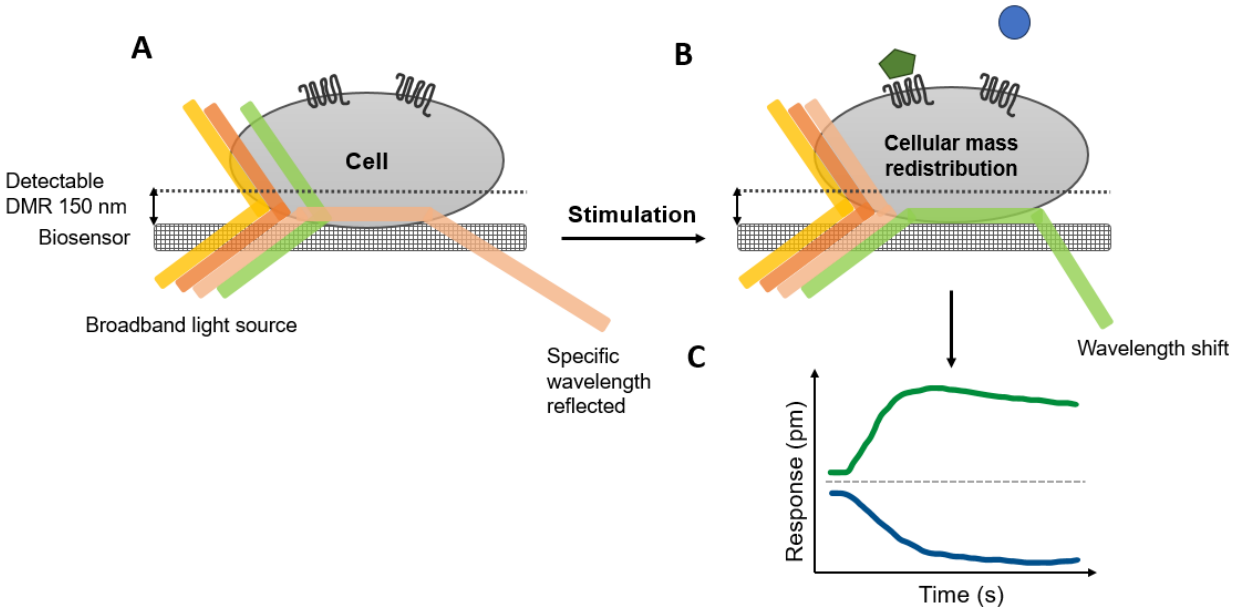

Figure 4. Schematic principle of DMR detection. (A) Resonant waveguide-grating biosensor is embedded in bottom of each well of the 384-well microplate. Broadband light illuminates the bottom of the well and the specific wavelength that is in resonance with the system is propagated and reflected. The penetration depth into the cell is 150 nm. (B) Stimulation of cells results in detectable DMR of cellular constituents or/and change of cell shape. Consequently, wavelength shift with change in refractive index and different outgoing wavelength is detected. (C) Wavelength shift (nm) can either occur as positive response (green graph) by an increase of the optical density in the sensing area of the biosensor or negative response (blue graph) by decrease of optical density in the sensing area of the biosensor. Data is usually plotted as function of time. Figure was created in PowerPoint and adapted from Schröder et al. 2011[79].

7.500 HEK Glosensor™ cells per well were seeded in a volume of 30 µl in a Corning Epic® biosensor 384 well microplate (fibronectin-coated), centrifuged (10 s, 150x g) and maintained at 37 °C for 24 hours. Medium was replaced by 30 µl HEPES-buffered Hanks' balanced salt solution (HBSS/HEPES) and plate was centrifuged (10 s, 150x g). Cells were incubated 1 hour in the Corning Epic® biosensor reader (Corning, NY, USA) at 37 °C to allow temperature equilibration. Meanwhile, agonist solutions were prepared (4x) in HBSS/HEPES. Baseline was obtained by measuring 10 time points (300 s) before 10 µl compound solution per well was added using CyBi®-SELMA semi-automatic pipetting system (Analytik Jena AG, Jena, Germany). Control cells were treated with 10 µl HBSS/HEPES instead of ligand. The wavelength shifts to monitor DMR was measured for another 70-80 minutes.

Data analysis and statistics

Raw data was baseline-corrected to HBSS/HEPES control. Baseline-corrected data (pm) was plotted over time to generate typical response profiles using GraphPad Prism. Area under the curves (AUCs) of baseline-corrected values were calculated in Excel using trapezoidal rule:

$$Area\ of\ trapezoid = \frac{1}{2}\ x\ (a + b)\ x\ w$$

In this calculation, *1/2 x (a+b)* is the average height and *w* is the width of a trapezoid. The AUC is consequently the total area (sum) of all trapezoids calculated. AUC values were applied to generate dose-response curves by non-linear regression analysis via GraphPad Prism. Additionally, a one-way analysis of variance (ANOVA) followed by post-hoc Dunnett's test was performed to determine significances using the same software. Values were considered significantly different with p values ≤ 0.05.

3.2.4 Development of cell-based assay systems

Once A_1AR is activated, several signalling cascades or other cellular mechanisms occur. To determine if these pathways are addressed by Ze 911 multiple assay systems were developed and established. All assays were performed in living human cell lines.

3.2.4.1 A_1AR-mediated β-arrestin 2 recruitment assay

This cell-based assay was established to directly detect real-time protein-protein interactions after ligand treatment specifically for A_1AR. The system uses the two compatible NanoLuc fragments called Large BiT (LgBiT) and Small BiT (SmBiT). After agonist binding and following receptor phosphorylation, β-arrestin 2 coupled to SmBiT migrates to A_1AR that is coupled to LgBiT. As soon as LgBit and SmBiT are in proximity, they bind and build a functional nanoluciferase (NanoLuc) (Figure 5). NanoLuc generates bioluminescence in presence of the substrate coelenterazine h that is converted to coelenteramide h[80].

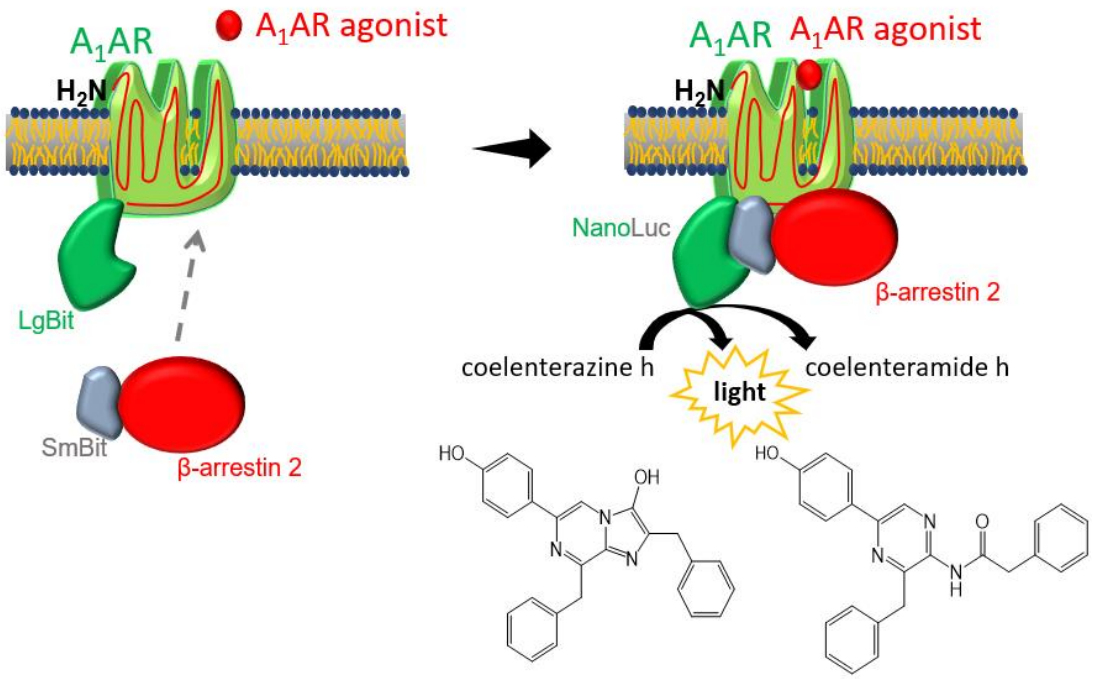

Figure 5. Principle of luciferase-based β-arrestin-2 recruitment assay. SmBiT-β-arrestin 2 migrates to A_1AR (coupled to LgBiT) after agonist binding. Binding of LgBiT and SmBiT results in a functional nanoluciferase (NanoLuc). Consequently, in the presence of substrate solution, NanoLuc generates luminescence that can be measured. Figure has been adopted from Saecker et al. 2023[61].

Stably transfected cells were seeded (25,000 cells/well) in a white clear bottom 96-well plate (Cellstar®, TC coated 96 well plate, Greiner Bio-One, Kremsmünster, Österreich) and incubated for 24 hours at 37°C and 5 % CO_2. The medium was replaced by 45 µl coelenterazine h substrate solution (2.5 µM coelenterazine h in HBSS/HEPES). The 96-well plate was immediately placed into the Tecan Spark® multimode microplate reader (Tecan Group AG, Männedorf, Switzerland) where the background luminescence was measured 3 to 5 cycles until a stable baseline signal was obtained. The measurement was paused, and cells were stimulated with 5 µl ligand solutions. Ligands were either diluted in up to 10 % DMSO or water; however, the maximum concentration of DMSO on cells was 1 %. The measurement was continued for another 55 to 57 cycles at RT.

Data analysis and statistics

Raw data from three to four independent experiments was transferred into GraphPad Prism and plotted over time. Each data point was divided by the mean of the first three values to normalize for well-to-well variabilities. For this matter, the function “remove baseline and column math” of the software was used. The solvent control was subtracted for some experiments

using the same functionality of GraphPad Prism. Next, AUC was calculated from the normalized data using either GraphPad Prism or the trapezoidal rule in Excel and plotted against the concentration (log M). A non-linear regression analysis was performed in GraphPad Prism to calculate EC_{50} and IC_{50} values. Statistical differences between groups were detected by one-way ANOVA followed by post-hoc analysis (Dunnett's). Values were considered significantly different with p values ≤ 0.05. Plug-in equations provided by Hoare et al. 2020[81,82] were used to calculate initial rates, in particular the rise and fall to baseline equation that considers drift of the data.

3.2.4.2 GloSensor™ cAMP Assay

Real-time changes in cAMP concentrations were measured using the so-called GloSensor™ technology. This sensitive system uses a circularly permuted firefly luciferase that is fused to a cAMP binding domain. Binding of cAMP to the biosensor results in a conformational shift that promotes increase of luminescence output that can be measured (Figure 6).

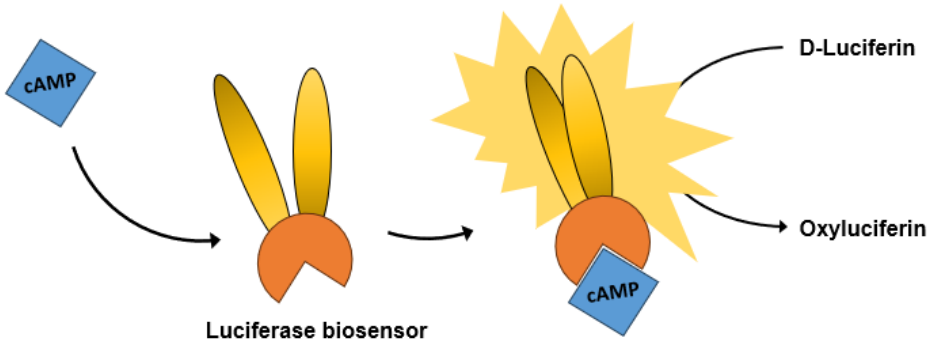

Figure 6. Principle of GloSensor™ technology. Firefly luciferase biosensor changes confirmation after binding of cAMP. This conformational shift results in substantial increase of firefly luciferase activity, consequently in luminescence output that can be measured in relative light units (RLU). Increase is proportional to amount of cAMP present. Figure was created in PowerPoint and modified according to Promega GloSensor™ technology[2].

Stably transfected cells were seeded in a white clear bottom 96-well plate (35,000 cells/well) and incubated for 24 hours at 37°C and 5 % CO_2. The medium was discarded and replaced by 25 µl substrate solution containing 4 % GloSensor™ cAMP Reagent in HEPES buffered DMEM (1:1). The cells were incubated with substrate solution for one hour at 37°C and subsequently equilibrated in the plate reader (Tecan Spark® multimode microplate reader) for one

[2] https://www.promega.de/products/cell-signaling/gpcr-signaling/glosensor-camp-cgmp-protease-biosensors/?tabset0=0&catNum=E1290 (accessed November 17th, 2024)

hour at room temperature. Afterwards, cells were stimulated with different ligands in different concentrations and measurement was started. Test compounds were directly diluted in HEPES buffered DMEM; the maximum concentration of DMSO on cells was 1 %. In addition, cells were stimulated with forskolin (FSK) and isoprenaline (Iso) to activate adenylate cyclase. Concentration of cAMP was measured subsequently via luminescence differences for 60 minutes at RT.

Data analysis and statistics

Raw data of each experiment was either directly transferred into GraphPad Prism or normalized to the mean of the first three values using Excel to eliminate well-to-well variability and plotted as function of time in GraphPad Prism. IC_{50} values and significances were calculated as described previously for β-arrestin 2 recruitment assay.

3.2.4.3 Calcium mobilization assay

Calcium mobilization assay was established to determine if Ze 911 or other A_1AR ligands mobilize Ca^{2+} intracellularly. A fluorogenic calcium-sensitive dye (Cal-520®) that crosses the plasma membrane was used to detect calcium mobilization in neuroblastoma cell line SH-SY5Y. Stimulation of cells with agonists leads to a release of intracellular calcium that significantly increases the fluorescence of the dye. SH-SY5Y cells were used because they solidly express A_1AR genuinely.

50,000 SH-SY5Y cells per well were seeded in a black clear bottom 96-well plate (96 well micro plate, PS, F-bottom, clear, black, TC, Greiner Bio-One, Kremsmünster, Österreich) and incubated for 24 hours at 37°C and 5 % CO_2. Medium was replaced by dye solution containing 10 µM Cal-520® and 0.04 % Pluronic® F-127 in 100 µl medium per well. Cells were incubated with dye solution 2 hours at 37 °C and subsequently equilibrated 30 min at RT. Ligand solutions were prepared in the meantime in a 5x concentration. Dye solution was replaced by 80 µl Locke's solution per well and 96 well-plate was transferred into Tecan spark® microplate reader. Fluorescence baseline was measured at a wavelength of 485 nM for 4 cycles (1 cycle = 15 s) before 20 µl ligand solution per well was injected by the injector system of the microplate reader resulting in in 1x concentration on cells. Immediately afterwards the measurement was continued for 11 more cycles until cycle 15 was finished.

Data analysis and statistics

Raw data of at least three independent experiments was normalized to the mean of the four baseline values using Excel and transferred into GraphPad Prism. Normalized data was plotted as function of time. AUCs were calculated in GraphPad Prism and plotted in a column graph using the calculated area and standard deviation. Statistical differences between groups were calculated via unpaired t test. Values were considered significantly different with p values ≤ 0.05.

3.2.5 Single-particle tracking of adenosine A_1 receptor

Single-particle tracking (SPT) is a powerful microscopic technique that provides information about the motion of individual fluorescence-labelled molecules (for example receptors) in living cells. Molecules are imaged by photon detector; motions are recorded in continuous matter to generate a trajectory[83]. They are recorded by a fast, very sensitive electron multiplying charge-coupled device (EMCCD) camera. A_1AR was detected after coupling to fluorescent dye Janelia Fluor® 646 HaloTag® (see 3.2.5.1 staining procedure) which can be tracked by its emission (light spots) and automatically localized based on intensity profile (Figure 7). Localization precision is usually in a range of 10 to 30 nm; this is ten times higher than the resolution limit of light microscopy. This is possible because the software detects centre of mass of the spots (maximum brightness value in the centre). Hence, spot position is determined by fitting a two-dimensional Gaussian distribution that offers higher precision. Localization of fluorescence signals is repeated on every image of the emerging image series. Consequently, detected receptors are linked from image to image to form trajectories by automatic tracking algorithms. Evaluation of the lateral receptor mobility reveals thousands of trajectories with characteristic diffusion properties like diffusion coefficients and confinement sizes.

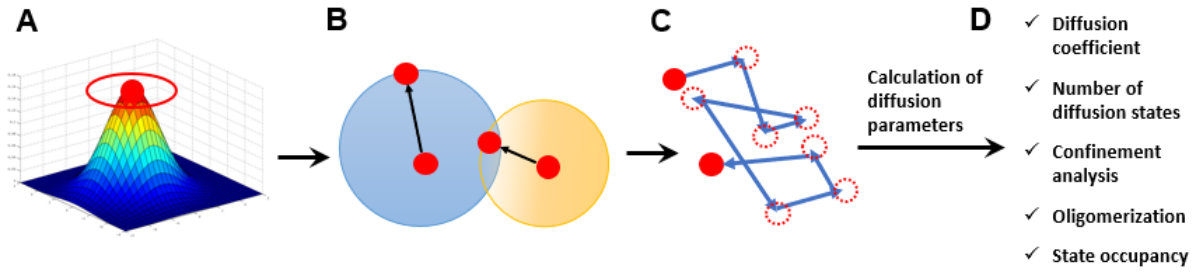

Figure 7. Principle of single-particle tracking. (A) Localization of fluorophores by software based on intensity profile. Central location (exact position) found via fitting of a 2D Gaussian distribution. (B) Identification of the same particle at different time points is achieved by using algorithms such as closest neighbour. (C) Localization of fluorophores are linked from image to image to generate trajectories. (D) Statistical analysis of the detected trajectories provides information about diffusion properties of the receptor. Figure has been created in PowerPoint and was adapted from Shen et al. 2017[83].

3.2.5.1 Staining procedure

Single clones of the previously generated cell line HEK-GloSensor™-HiBiT-A_1AR were generated by single cell dilution. Single clones were tested with Nano-Glo® HiBiT Extracellular Detection Assay to confirm the expression of HiBiT and consequently A_1AR. Afterwards, 75,000 cells per well were seeded on heat sterilized coverslips (Ø 16 mm, Marienfeld, Lauda-Königshofen, Germany) in 12-well plates. Cells were incubated for 24 h at 37 °C and 5 % CO_2. A_1AR was labelled with HaloTag®-self-labelling protein technology which has been described for GPCRs by Franken et al. 2020[84]. The fusion protein LgBiT-HaloTag® and Janelia Fluor® 646 HaloTag® ligand were diluted to a concentration of 20 nM each in growth medium without FCS and phenol red. Medium on cells was replaced by 500 µl of this dye solution and cells were incubated for 30 min at 37°C and 5 % CO_2. Coverslip with stained cells was washed 3 times in phosphate buffered saline (PBS). Afterwards, coverslip was placed into a custom mounting bracket and covered with 270 µl PBS. Single cells were searched and focused to the upper membrane in transmitted light before opening the laser shutter (637 nM) to avoid photo bleaching. Cells were treated with 30 µl ligand solution (CPA or Ze 911) directly on coverslip and imaged 15 minutes afterwards at 20 °C. A video of 1000 frames was recorded; this step was repeated twice on the same cell (3 x 1000 frames).

Time-dependent analysis of lateral diffusion was recorded in the following experiment. Influence of CPA was investigated in five time intervals after treatment (Table 10). The measurement started directly after treatment with the first cell at time point 1 (1-5 minutes after treatment). After the first time point was recorded, a new cell was searched, and the second time point (5-10 minutes after treatment) was recorded alike. For each time interval, a new cell was measured to avoid artificial processes created by long laser radiation. All in all, 5 cells and therefore time points were recorded per coverslip from 1 up to 30 minutes after treatment. The coverslip was disposed afterwards. At least three experiments were performed in the same manner.

Table 10. SPT time intervals measured after CPA treatment

Time interval	Time (min)
1	1 - 5
2	5 - 10
3	10 - 15
4	15 - 20
5	25 - 30

3.2.5.2 SPT settings, analysis and statistics

Settings

The data was recorded using an EMCCD camera (iXon DV-860DCS-BV, Andor Technology). This camera is part of a custom-built setup, including an inverted widefield epifluorescence microscope (TE2000-S, Nikon Corporation, Minato, Japan) equipped with a water immersion objective (Plan APO VC, 60x, 1.2 NA, Nikon) and a 200-mm-focal length tube lens. The effective magnification of the setup was 240x, translating to a pixel width of 100 nm. A continuous wave laser (637 nM, 50 mW, Coherent, Saxonburg, Pennsylvania) was used in combination with an acousto-optic tunable filter (AA Opto-Electronic, Orsay, France) to regulate the intensity. Image sequences were captured with a frame rate of 20 Hz for a duration of 100 s.

Spot detection and tracking

The generation of 2-dimensional particle tracks from image data was implemented with MATLAB software (R2016b, MathWorks, Natick, Massachusetts, USA). Two-dimensional movement patterns of fluorescence signals and further diffusion characteristics were extracted from the videos. The "u-track" package[85] was used to import and analyse the images. Images were processed using the following settings: 1.32 px spot radius, 3 frame rolling window time-averaging for local maxima detection, 2 frame minimum track segment length, 1 frame maximum gap length, other settings were preset.

Discrete diffusive states from particle tracks were identified using variational Bayes single particle tracking (vbSPT) MATLAB package[86]. According to their momentary diffusion speed, tracks were segmented and classified into one out of three states (S1, S2, S3) and characterized by the diffusion coefficients D1, D2 and D3. Higher order models were recognized but neglected because of their insignificant occupancy and indistinct diffusion behaviour. The following settings in the *runinput*-file were used: *timestep* = 0.05, *dim* = 2, *trjLmin* = 2, *runs* = 24, *maxHidden* = 3, *bootstrapNum* = 100, *fullBootstrap* = 0.

Confinement analysis

Confinement analysis was performed with every diffusion coefficient at every time point. Therefore, previously classified track segments were extracted and pooled by respective diffusion coefficients. To measure spatial confinement strength the packaging coefficient (Pc) was used. Packaging coefficient was described by Bussmann et al. 2023[87] and calculated at each time point *i* as follows:

$$Pc_i = \sum_{i}^{i+n-1} \frac{(x_{i+1} - x_i)^2 + (y_{i+1} - y_1)^2}{s_i^2}$$

x_i and y_i are coordinates at time *i*, x_{i+1} and y_{i+1} are coordinates at time *i+1* and *n* is the length of the time window. S_i is the surface area of the convex hull of the trajectory segment between time points *i* and *i+1*. *Si* was calculated using MATLAB (version R2016B) by the "convhull" function.

To assure stable results and an inclusion of a sufficient number of track segments, a window length of 10 time points (0.5 s) was selected. Pc_{95} values given by the 95th percentile of packing coefficients were determined by simulation of random walk data based on the earlier determined vbSPT state diffusion coefficients and segment lengths. Subsequently, derived Pc_{95}-values were used as a threshold to categorize tracks as spatially confined. Confined tracks are classified by $Pc > Pc_{95}$ and were compared by average hull areas by averaging on the 0.5 s timescale.

Spot intensity analysis

The distribution of monomers, homodimers and higher order homooligomers of A_1AR for the respective test condition was analysed via corresponding spot intensities. Spot intensities were previously generated by u-Track and plotted as histograms for each experiment. The distribution was fitted, and the different components were calculated by Gaussian mixture model in MATLAB (version R2016B). Duplication of the signal implied dimer and triplication trimer and so on. A two-compartment (homodimer) analysis was performed, higher compartment analysis (three- and four-compartment) led to non-plausible results.

Data analysis and statistics

Data generated in MATLAB was merged and transferred into GraphPad Prism. One-way ANOVA was performed on data sets followed by a post-hoc analysis (Tukey's), statistical significance was reached with p-value ≤ 0.05 compared to other group or control condition.

3.2.6 Extract characterization by high-performance liquid chromatography

High-performance liquid chromatography (HPLC) analyses were performed on an Agilent Series 1200 HPLC system equipped with a degasser (G1322A), a quaternary pump (G1311A), an autosampler (G1329A) and a photodiode array detector (G1315D). The system was operated by Agilent ChemStation Rev. B.04.01. A linear gradient was used from 100 % eluent A (water) to 100 % eluent B acetonitrile (ACN). Table 11 shows the analytic conditions and technical settings used for the characterization. A detection wavelength of 205 nM was used. The

extract was separated on a EcoCART® RP-18 (5 µM) glass cartridge (Merck, Darmstadt, Germany).

Table 11. HPLC settings for Ze 911 characterization

Time [min]	H_2O [%] (v/v)	ACN [%] (v/v)	Flow rate [ml/min]
0	100	0	1
40	80	20	1
70	50	50	1
72	0	100	1
85	0	100	1
87	100	0	1
100	100	0	1
101	100	0	1

Ze 911 was dissolved in DMSO (50 mg/ml) und diluted in water to a concentration of 5 mg/ml and analysed by HPLC method described above. The injection volume was 40 µl. Identification of the characteristic substances like valerenic acid, acetoxyvalerenic acid, hydroxyvalerenic acid, pinoresinol, pinoresinol diglucoside and olivil was performed by comparison of UV spectra and retention times of corresponding reference substances. Reference substances were dissolved in DMSO and diluted in water to a concentration of 0.1 mg/ml. The injection volume of each reference substance was 10 µl.

3.2.6.1 Adenosine in valerian extract Ze 911

Agonistic activities of Ze 911 found in the assays were comparable to synthetic agonists. That's why Ze 911 was examined for the potential content of adenosine using the above mentioned HPLC method. Either 40 µl of Ze 911 (5 mg/ml), 40 µl of Ze 911 treated with adenosine deaminase (ADA) (5 mg/ml) or 19 µl of adenosine 1 mM were injected. Identification of adenosine was carried out by comparing UV spectra and retention time to adenosine as reference substance.

4 Results

Sleep is highly dependent on adenosine regulated by adenosine A_1 receptor (A_1AR). This thesis aims for a better understanding of the effects of valerian extract Ze 911 on A_1AR. It has been shown that valerian extract acts as A_1AR agonist. However, we are still mostly in the dark which pathways may be affected and which compounds may be responsible for the sleep-improving effects. This study seeks to enhance the data situation since it is limited and one-sided so far.

4.1 HEK 293 cells respond to adenosine A_1 receptor stimulation

DMR was used to evaluate if HEK 293 cells react to A_1AR stimulation. To ensure comparability to other assays, HEK GloSensor™ cells were used. Stimulation of cells with a suitable ligand induces a change of the wavelength of outgoing light that can be measured.

To get a first impression if HEK 293 cells respond to adenosine receptor (AR) stimuli, DMR experiments with different AR agonists were performed. Figure 8A exemplarily shows raw data that was generated by Epic system software, which was transferred into GraphPad Prism and plotted over time. The wavelength shift was recorded in picometers (pm) over a certain time in seconds (s). Raw data was baseline-corrected to HBSS/HEPES control (Figure 8B). DMSO 0.25 % was included as solvent control. Stimulation with 1 µM non-specific AR agonist NECA as well as the specific A_1AR agonist CPA resulted in positive wavelength shift that was statistically significant compared to control cells. Treatment with A_1AR antagonist DPCPX (100 nM) did not result in any wavelength shift, response curve appeared on baseline level (Figure 8B+C). Since HEK 293 cells also express A_{2A}AR[97], specific A_{2A}AR agonist CGS 21680 and antagonist SCH 442416 were tested as well. No wavelength shift was detected after treatment with 100 nM SCH 442416, similar to A_1AR antagonist DPCPX. The kinetic of CGS 21680 treatment (1 µM) was different compared to CPA and NECA. The first rise of the response curve was not as steep as for the other two agonists. However, normalized responses showed that the effects of both specific agonists were comparable (Figure 8B+C). The wavelength shift of NECA and therefore the response of the cells was nearly 5 times higher than for CPA or CGS 21680. This was expected since NECA stimulated all adenosine receptors, CPA only A_1AR and CGS 21680 only A_{2A}AR. Figure 8 shows one experiment exemplarily, it was repeated with similar results. This first DMR experiment showed that HEK 293 cells respond to AR agonism. It was noticeable that the time-response curves (kinetic of the agonists) occurred to be different for CPA and CGS 21680.

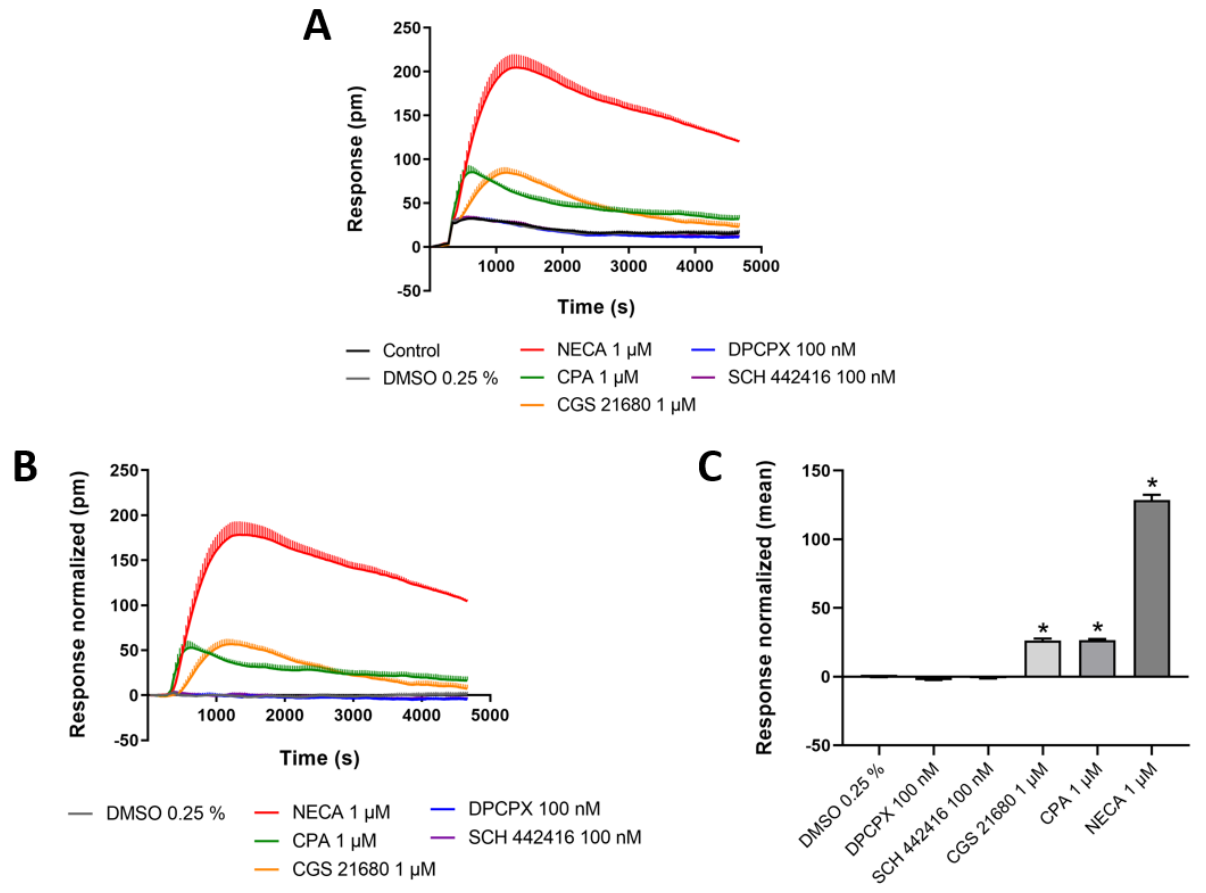

Figure 8. DMR analysis of adenosine receptor response in HEK 293 cells. DMR raw data of AR agonists and antagonists plotted over time (A, one exemplary experiment). Buffer-normalized data of ligands plotted over time (B, one exemplary experiment) and comparison of ligands to solvent control (C). Cells were stimulated with AR ligands and DMR was directly recorded afterwards for 77 min. Maximum DMR peaks were generated between 0 and 2,000 s. A_1AR agonist CPA, A_{2A}AR agonist CGS 21680 and AR agonist NECA led to positive wavelength shift. No wavelength shift was observed for A_1AR antagonist DPCPX as well as A_{2A}AR antagonist SCH 442416, responses were considered baseline level. HBSS/HEPES as well as DMSO 0.25 % served as controls, no wavelength shifts were observed. Two independent experiments were performed in quadruplicates (n=2). Data is shown in mean +/-SEM. Values were considered significantly different with p values ≤ 0.05.

In another experiment, cells were tested with different concentrations of A_1AR agonist CPA. Raw data was normalized and plotted over time in GraphPad Prism. AUCs of normalized response curves were plotted against logarithmic (log) molar concentration. A dose-dependent positive wavelength shift with an EC_{50} value of 3.4 µM was detected (Figure 9 A+B). Even though EC_{50} values of CPA are usually a little lower in the literature (low to medium nanomolar range), this result was totally acceptable for this experiment since time-dependent response of CPA in HEK 293 cells has clearly been shown. Treatment with solvent control DMSO resulted in minor negative wavelength shift. Figure 9A shows one experiment exemplarily. Experiment was repeated with similar results.

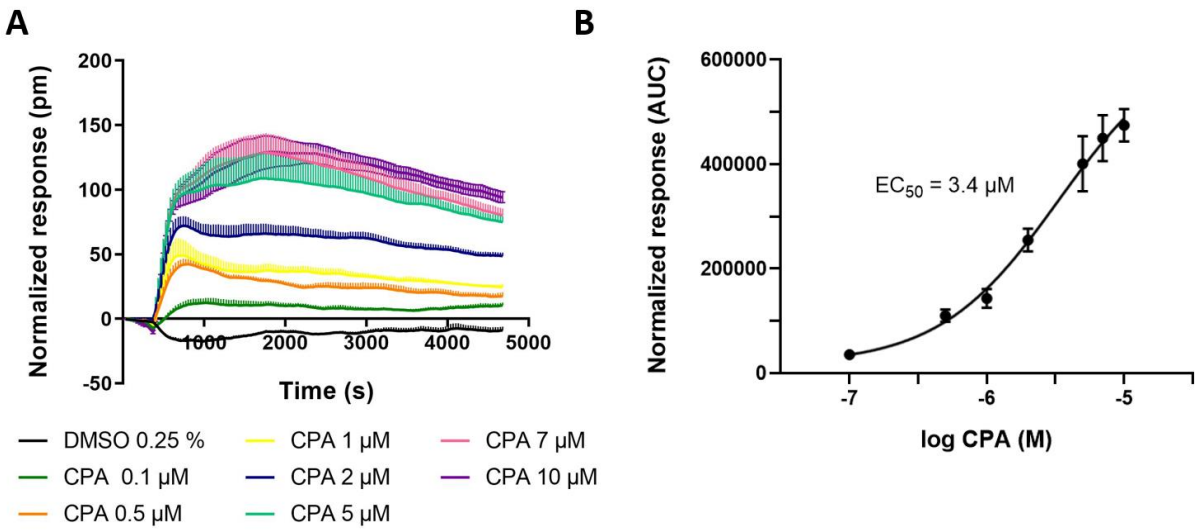

Figure 9. DMR analysis of CPA in HEK 293 cells. Normalized DMR response curves (wavelength shifts) (A, one exemplary experiment) and (B) corresponding dose-response curve with an EC_{50} value of 3.4 µM. Cells were stimulated with CPA directly before measurement and DMR was recorded for 77 min. Maximum DMR peaks were generated between 0 and 2,000 s. Data was normalized to HBSS/HEPES control. DMSO 0.25 % was included as solvent control. Two independent experiments were performed in quadruplicates (n=2). Data is shown in mean +/-SEM.

After getting a first impression and the confirmation that cells respond to A_1AR stimulation, valerian extract Ze 911 was tested. Cells were prepared equally and directly treated before measurement was started. Like other AR agonists, Ze 911 led to a positive dose-dependent wavelength shift (Figure 10). At a concentration of 0.001 mg/ml Ze 911 and higher, a significant increase in wavelength shift was observed (Figure 10B). Data was normalized to HBSS/HEPES control and DMSO 1% was used as solvent control. A small positive wavelength shift was detected for DMSO treated cells. It was noticeable that the kinetic of Ze 911 was different compared to the kinetic of CPA or other tested AR agonists. The rising of the curve was steeper, and the maximum was detected earlier after treatment with Ze 911. Figure 10 shows one experiment exemplarily. The experiment was repeated twice with similar results. These first DMR studies confirmed that HEK 293 cells are stimulated by synthetic A_1AR agonist as well as the extract Ze 911.

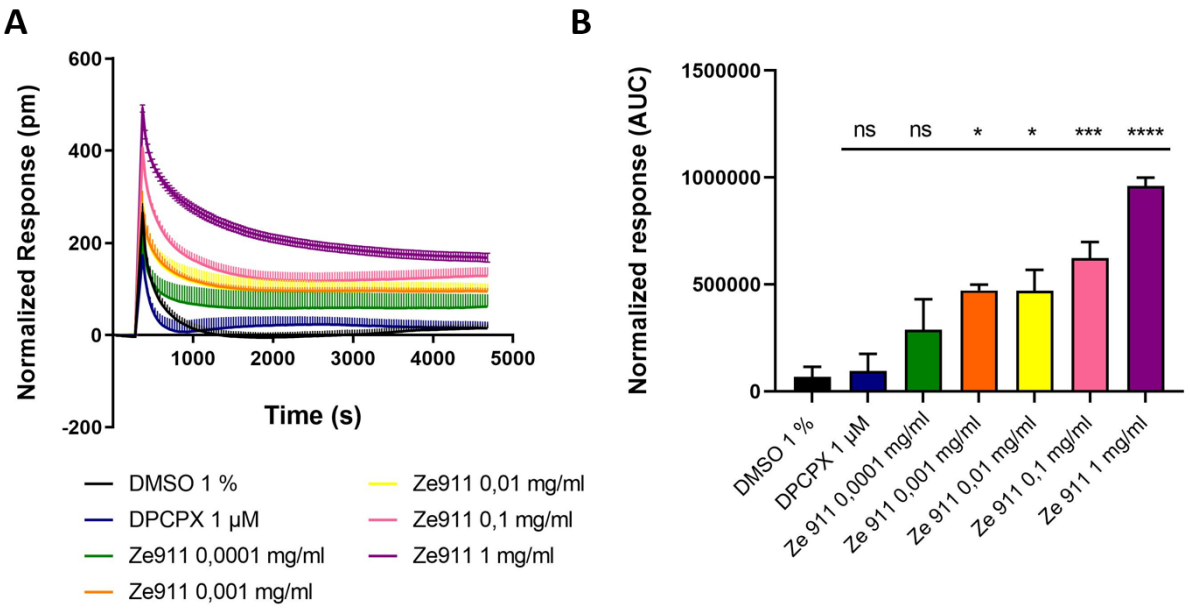

Figure 10. DMR analysis of Ze 911 in HEK 293 cells. Normalized DMR response curves (A, one exemplary experiment) and corresponding AUCs with statistical significances (B). Cells were stimulated with Ze 911 directly before measurement and DMR was recorded for 77 min. Maximum DMR peaks were generated between 0 and 1,000 s. Data was normalized to HBSS/HEPES control. DMSO 1 % was included as solvent control. Three independent experiments were performed in quadruplicates (n=3). Data is shown in mean +/-SEM. Values were considered significantly different with p values ≤ 0.05.

Since DMR is a complex label-free technique, it is referred to as a “black box”. The events reflected by DMR signal are sometimes hard to identify due to its complexity. However, the experiments above generated the answers that needed to be achieved. It has been proven that HEK 293 cells respond to A_1AR stimulus in a concentration-dependent manner. This concentration-dependent response was also detected after treatment with Ze 911.

The establishment of a specific A_1AR assay was the next experimental step. Since the existing data mainly deals with the inhibitory effect of valerian on cAMP concentration, a different approach was selected and conducted.

4.2 Establishment of β-arrestin 2 recruitment assay

To our best knowledge, no data about valerian extract influencing A_1AR β-arrestin 2 dependently has been published by now. Therefore, an assay that was designed to study A_1AR mediated β-arrestin 2 recruitment in real-time was developed using NanoBiT® technology. LgBiT was fused to the C-terminus of A_1AR and SmBiT to N-terminus of β-arrestin 2. Since nothing is known about Ze 911 potentially recruiting β-arrestin 2 and little is known about A_1AR-mediated β-arrestin signalling in general, the assay was validated with several ligands.

Treatment of cells with natural unspecific AR agonist adenosine (Ado) as well as the synthetic unspecific AR agonist NECA resulted in dose-dependent β-arrestin 2 recruitments with EC_{50} values of 780 ± 158 nM and 121 ± 24.5 nM respectively calculated from the AUC values (Figure 11A and 11B respectively). Specific A_1AR agonism also led to robust dose-dependent β-arrestin 2 recruitment (Figure 11C). The calculated EC_{50} of CPA (130 ± 22.6 nM) is similar to EC_{50} of NECA, both appeared to be significantly lower compared to adenosine. Next, the non-nucleoside partial A_1AR agonist capadenoson was tested for β-arrestin 2 recruitment. It resulted in less pronounced dose-dependent recruitment with an EC_{50} of 209 ± 60.7 nM and in conclusion to a lower efficiency compared to full agonist CPA (Figure 11D). At least three independent experiments were performed in triplicates (n=3).

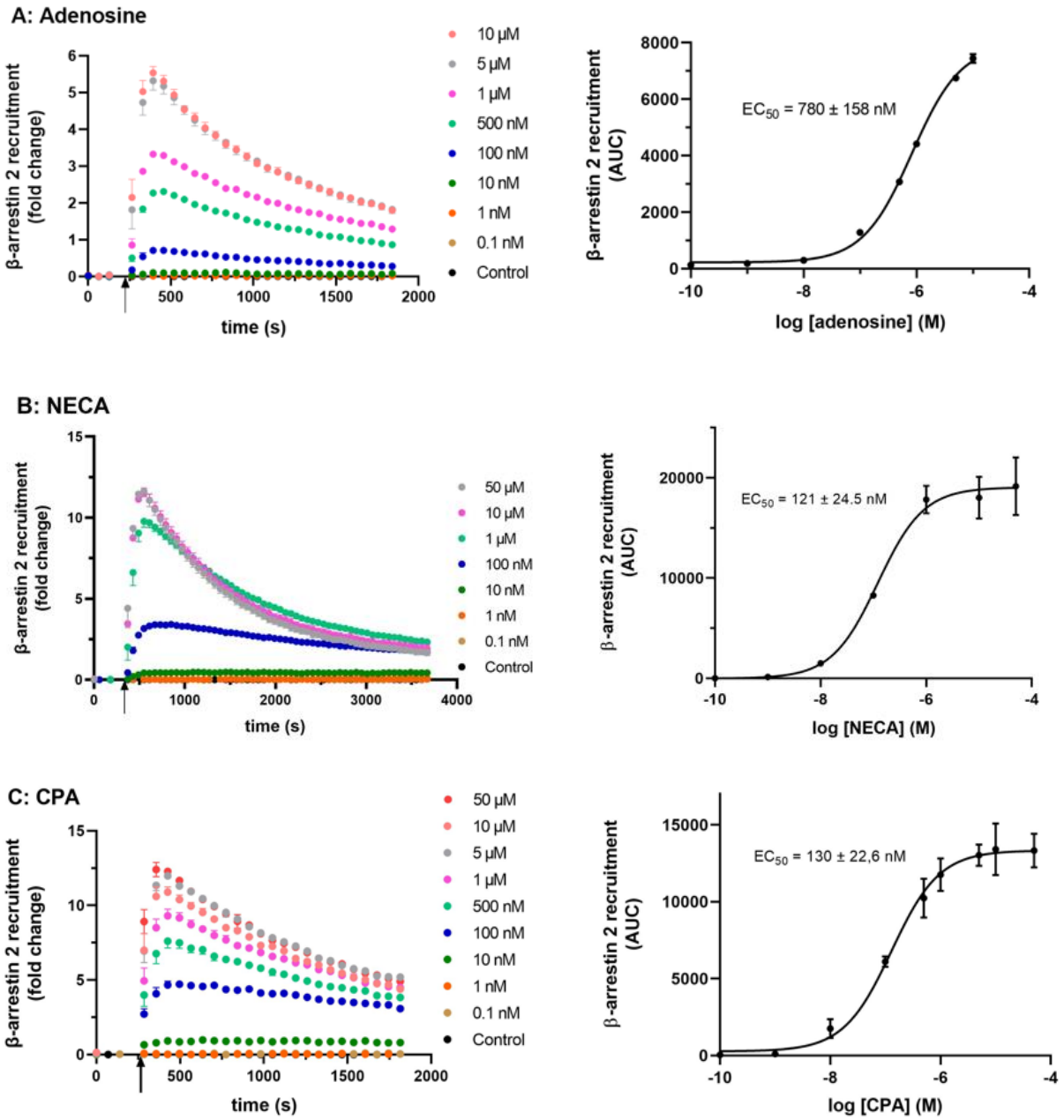

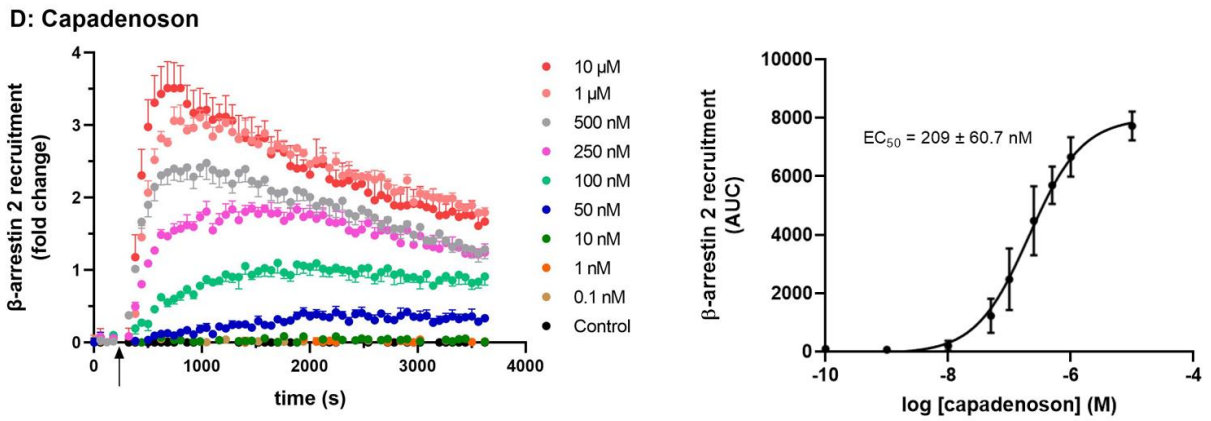

Figure 11. Concentration dependencies of A_1AR agonists in β-arrestin 2 recruitment assay. Treatment with two non-specific AR agonists adenosine (A), NECA (B) and the two specific agonists CPA (C) and capadenoson (D) resulted in dose-dependent β-arrestin 2 recruitments. Agonists were added at the timepoints indicated by the arrow. Luminescence was measured up to one hour and a solvent control of 0.1 % DMSO was included. Graphs on the left side show exemplarily data from one experiment. Dose-response curves on the right side were calculated from all three experiments using AUCs. Data is given in mean +/- SD. Three independent experiments were performed in triplicates (n=3). Figure has been adapted from Saecker et al. 2023[61].

Assay specificity was tested using DPCPX, a specific A_1AR antagonist. DPCPX reversed the CPA-mediated recruitment dose-dependently with an IC_{50} value of 105 nM ± 44 nM (Figure 12A+B). In addition, agonists of all four adenosine receptors were tested. NECA, CPA and adenosine led to a significant recruitment of β-arrestin 2 whereas CGS 21680 (specific A_{2A}AR agonist), BAY-60-6583 (specific A_{2B}AR agonist) and 2-Chloro-IB-MECA (2-MECA, specific A_3AR agonist) did no recruit β-arrestin 2 significantly (Figure 12C). Isoprenaline (Iso, β-adrenergic receptor agonist) was used as independent unrelated control, no recruitment of β-arrestin 2 was detected. This experiment proved that the assay is specific for A_1AR.

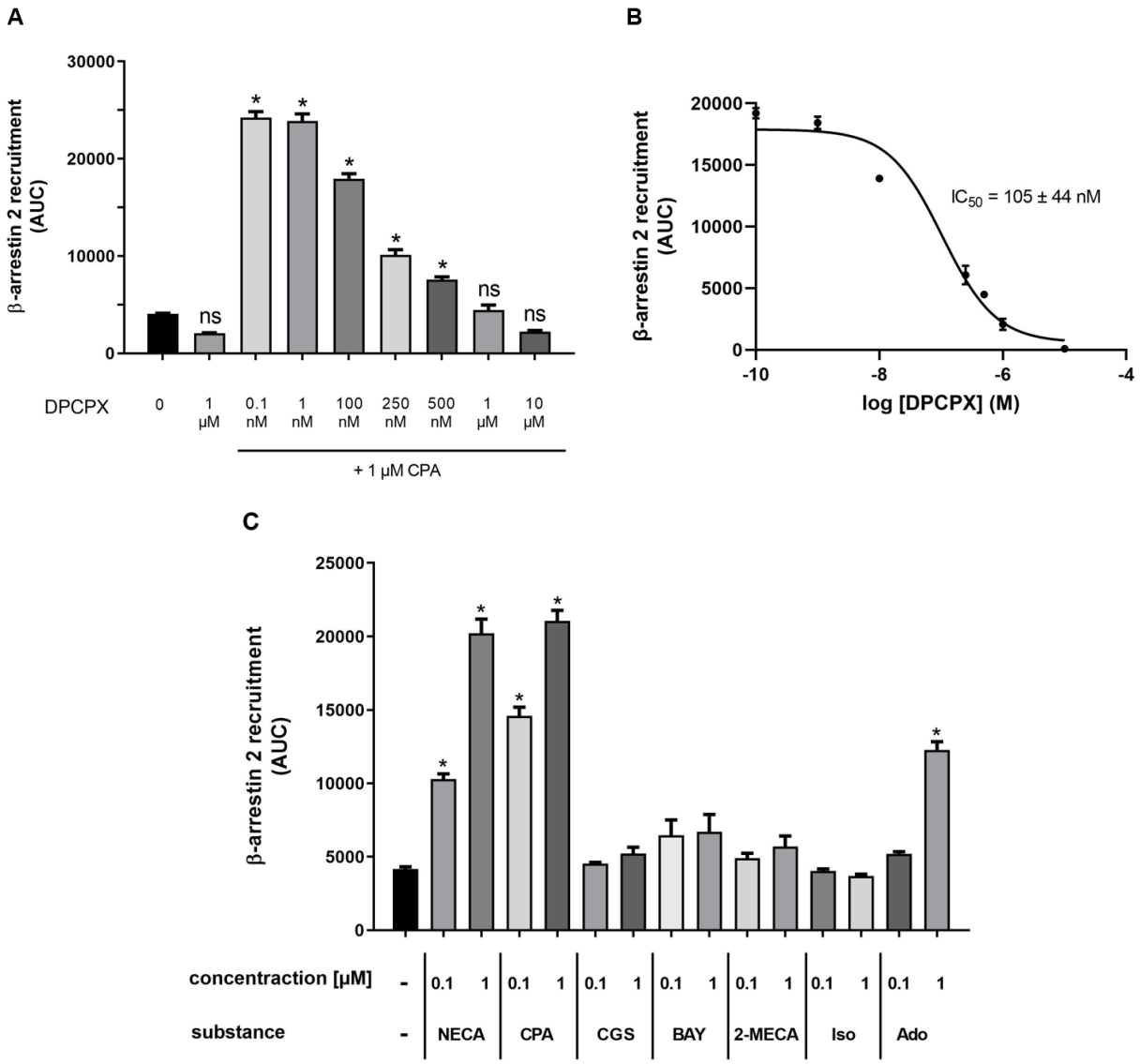

Figure 12. Specificity testing of β-arrestin 2 recruitment assay. (A) Influence of DPCPX on CPA stimulated cells. Cells were incubated with 1 µM CPA and different concentrations of DPCPX. CPA-mediated recruitment was reversed dose-dependently by DPCPX with an IC_{50} of 105 ± 44 nM (B). Luminescence was measured up to one hour and a solvent control of 0.1 % DMSO was included. Values are given in mean +/- SEM (n=3 independent experiments performed in triplicates). (C) Different AR agonists tested in two different concentrations, 0.1 and 1 µM respectively. Isoprenaline was tested as unrelated control. Values are given in mean +/- SEM (n=3 independent experiments in triplicates). Values were considered significantly different with p values ≤ 0.05. Figure B+C have been adapted from Saecker et al. 2023[61].

After the specificity of the assay was verified, finally valerian extract Ze 911 was tested using the same experimental conditions. Ze 911 treatment resulted in a robust dose-dependent recruitment of β-arrestin 2 with an EC_{50} value of 66 ± 14 µg/ml (Figure 13). Comparing the fold

changes of Ze 911 and CPA, Ze 911 appeared to be less efficient. This however was expectable since CPA is a synthetic specific A_1AR agonist whereas Ze 911 is classified as a complex mixture of many substances that unfolds several potential effects at different targets.

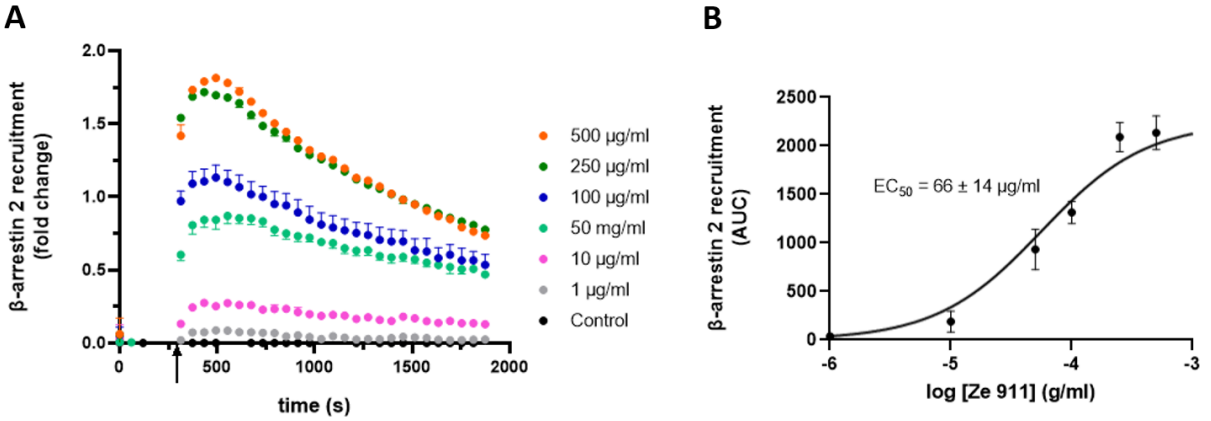

Figure 13. Concentration dependence of Ze 911 in β-arrestin 2 recruitment assay. Different concentrations of Ze 911 were added at the time point indicated by the arrow (A). Luminescence was measured 30 min and a solvent control of 0.1 % DMSO was included. Dose-response curve was calculated from the corresponding AUCs (B). Values are given in mean +/- SEM (n=3 independent experiments in triplicates). Figure has been adopted from Saecker et al. 2023[61].

4.2.1 Adenosine found in valerian extract Ze 911

Adenosine is found in nearly all kinds of living organisms[88,89]. It occurs in almost every human cell but also in plants, fungi or insects for example[89–91]. The results above (Figure 13) were quite promising for Ze 911 since the kinetic profile looked very similar to other adenosine receptor agonists. The most obvious explanation for the observed effect of Ze 911 on A_1AR-mediated β-arrestin 2 recruitment would therefore be the presence of adenosine in the extract. Consequently, it was essential to analyse Ze 911 for the potential content of adenosine. The HPLC analysis of the extract including adenosine as reference substance indeed confirmed the presence of adenosine in Ze 911 (see 4.6.1).

This result was verified in the β-arrestin 2 recruitment assay. The extract was incubated 30 min at RT with ADA and tested in the β-arrestin 2 recruitment assay. Figure 14 shows that the signal induced by Ze 911 was completely eliminated after treatment with ADA. The response curves of ADA-treated cells appeared slightly below baseline level indicating that ADA further eliminated basal adenosine concentrations (Figure 14).

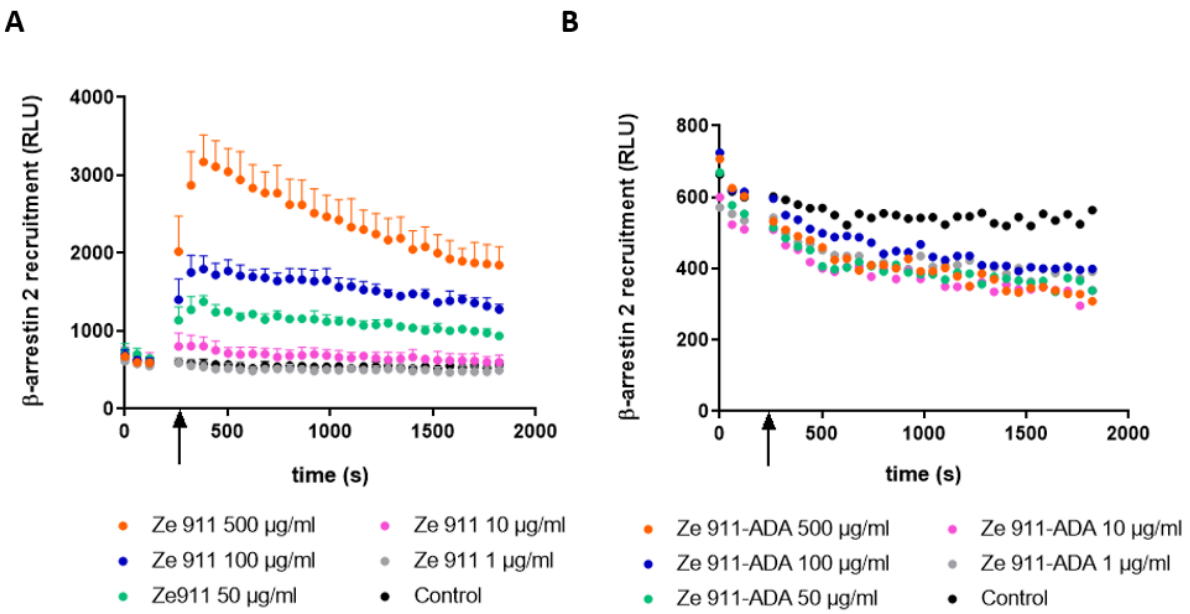

Figure 14. Agonistic effect of Ze 911 reversed by ADA in β-arrestin 2 recruitment assay. Dose-dependent β-arrestin 2 recruitment after treatment with different concentrations of Ze 911 (A) and reversed recruitment after Ze 911-ADA-treatment (B). Different concentrations were added at the time points indicated by the arrow. Luminescence was measured 30 min after treatment and a solvent control of 1 % DMSO was included. Luminescence of ADA-treated cells was recorded slightly below baseline level. Values are given in mean +/- SEM.

To our best knowledge it has never been described that adenosine is a component of valerian extract. It can be assumed that the strong agonistic effect in the β-arrestin 2 recruitment assay results from the adenosine in the extract. This finding was a game changer for further experiments. The focus shifted from agonistic to potential modulatory A_1AR effects of Ze 911. As a result of this finding, the industry partner of this study, Zeller Söhne AG Switzerland, prepared an adenosine-free extract. This adenosine-free extract was further fractionated and investigated for modulatory properties. Particularly one fraction was very promising, modulatory A_1AR effect was identified by them using a cAMP assay. This potent fraction primarily contained one substance class: dicaffeoylquinic acids (DQAs). The occurrence of DQAs in Ze 911 that was used in this work was confirmed by LC/MS-MS (see supplementary material and data 8.2.). This LC/MS-MS experiment was kindly performed by a colleague at the IBMB Bonn.

DQAs became a promising substance class for further investigations since they were found in Ze 911 and they can pass the blood brain barrier[92]. In addition, there is evidence that chlorogenic acids, as part of DQAs, improve sleep quality[93]. For this purpose, it was worthy to identify DQAs in Ze 911 and investigate their potentials in detail.

4.2.2 Modulatory properties of DQAs on A_1AR

The positive allosteric A_1AR modulator VCP 171 was tested in the β-arrestin 2 recruitment assay to verify the ability of measuring modulatory effects. The combination of different concentrations NECA and VCP 171 led to a significant higher recruitment of β-arrestin 2 compared to NECA alone (Figure 15). VCP 171 single treatment did not recruit β-arrestin 2. This experiment proved that the established assay is suitable to detect modulatory effects in a concentration-dependent manner.

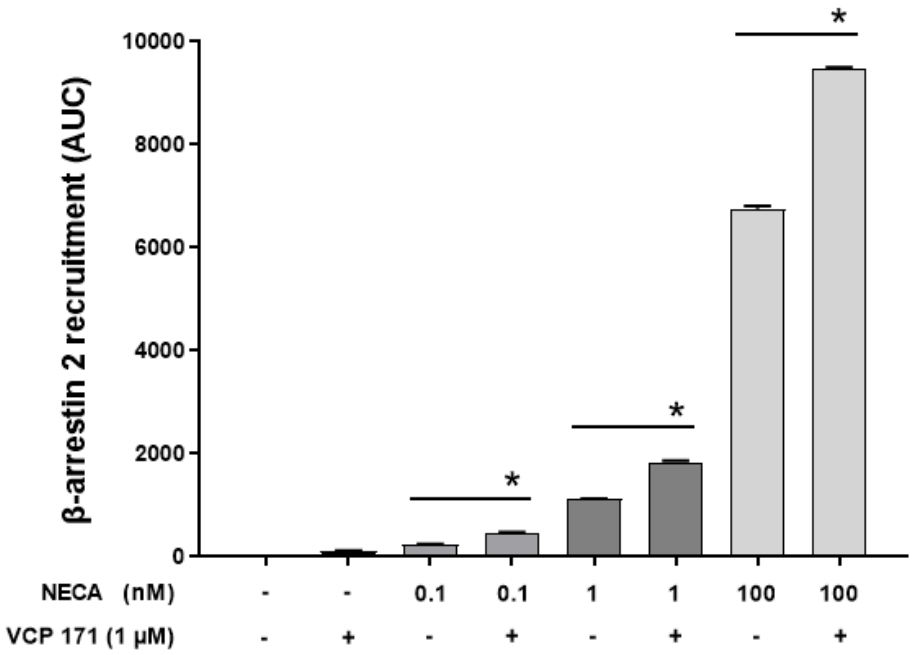

Figure 15. Modulatory properties of VCP 171 in combination with NECA in β-arrestin 2 recruitment assay. Cells were treated with 1 µM VCP 171 and either 0.1, 1 or 100 nM NECA. Luminescence was measured directly after treatment for 1 h at RT and a solvent control of 0.1 % DMSO was included. Three independent experiments were performed in triplicates (n=3). Values are given in mean ± SEM. Values were considered significantly different with p values ≤ 0.05. Figure has been adapted from Saecker et al. 2023[61].

In the next experiment, single DQAs were tested for their modulatory properties. To get a first impression a single concentration of the natural A_1AR ligand adenosine (0.25 µM) was tested in combination with either 0.1 mg/ml 1,5-DQA, 3,4-DQA, 3,5-DQA or 4,5-DQA. Figure 16 shows that 3,4-DQA and 4,5-DQA increased β-arrestin 2 recruitment significantly in combination with adenosine compared to adenosine single treatment whereas 1,5-DQA and 3,5-DQA showed no such effect. No recruitment of β-arrestin 2 has been detected after treatment with a mix of all four DQAs (0.1 mg/ml each) that was included as control (Figure 16).

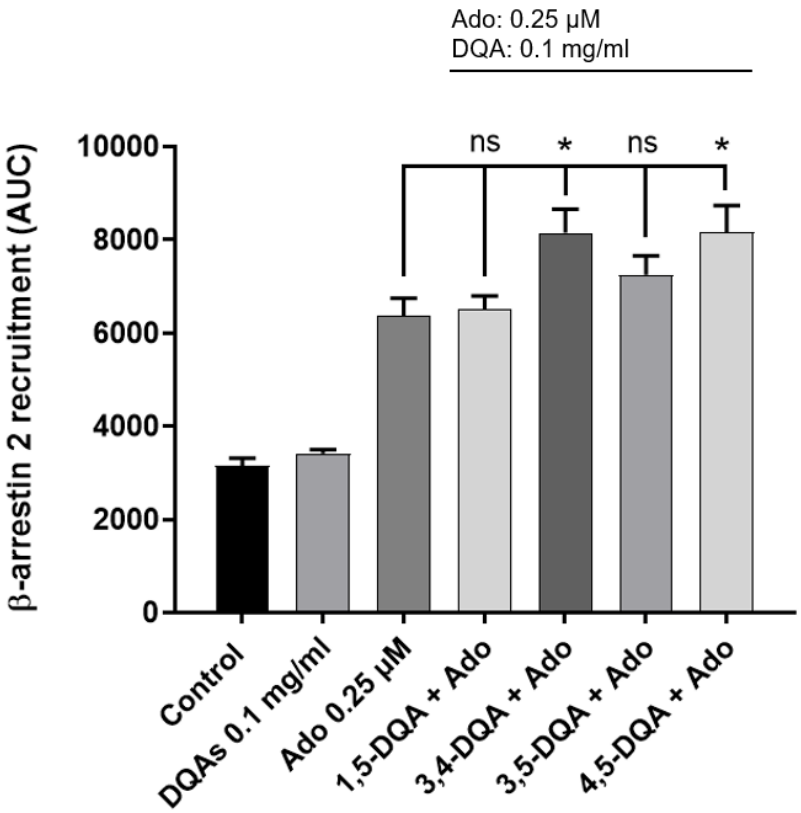

Figure 16. Adenosine-mediated β-arrestin 2 recruitment increased by certain DQAs in β-arrestin 2 recruitment assay. Cells were treated with 0.25 µM adenosine (Ado) in combination with 0.1 mg/ml of either 1,5-, 3,4-, 3,5-, or 4,5-DQA. A mix of all four DQAs (0.1 mg/ml each) was included as control condition besides DMSO solvent control (0.1 %). Luminescence was measured directly after treatment for 1 h at RT. Values are given in mean +/- SEM (n=3 independent experiments in triplicates). Values were considered significantly different with p values ≤ 0.05.

In the following experiment, DQAs were tested individually with and without adenosine instead of using a control that contained a mix of all four DQAs. Separately tested DQAs did not result in recruitment of β-arrestin 2 (Figure 17). The combinations however resulted in significant increases of recruitment again for 3,4- and 4,5-DQA but not for 1,5-DQA. Since 1,5- and 3,5-DQA showed no increased recruitment in the experiment before (Figure 16), only 1,5-DQA was tested again in this experiment as negative control. Protocatechuic acid (PCA), the metabolic product of DQAs, was also tested separately and in combination with 0.25 µM adenosine. The combination of adenosine and 0.1 mg/ml PCA resulted in a significant increase of β-arrestin 2 recruitment compared to adenosine single treatment (Figure 17).

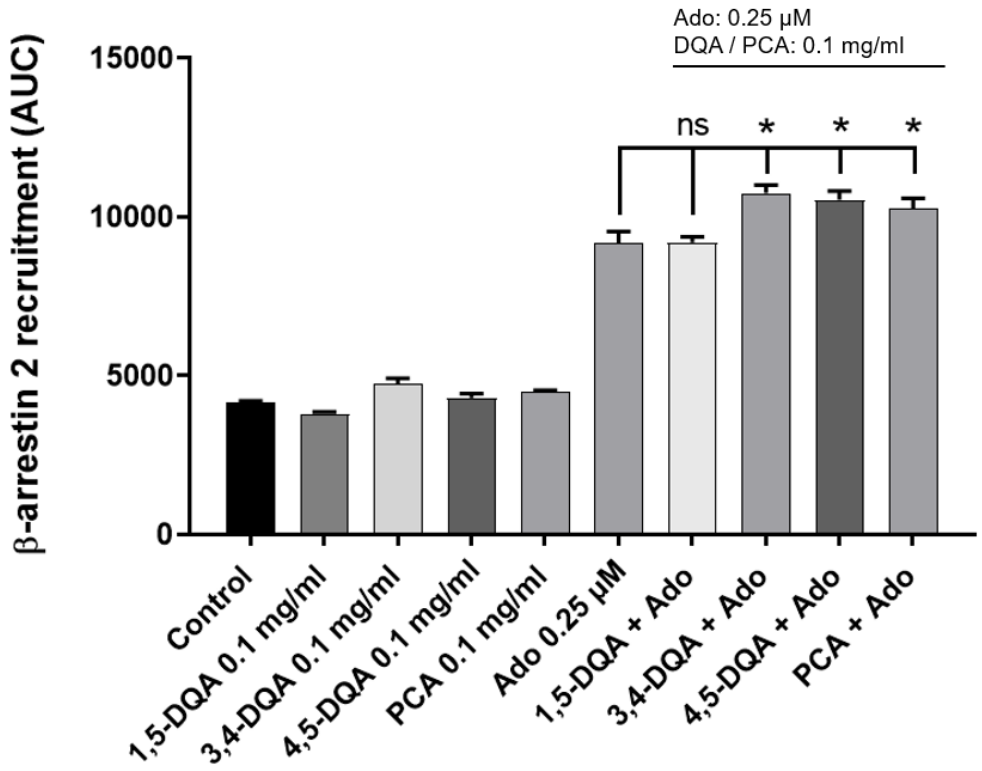

Figure 17. Modulatory properties of certain DQAs and PCA detected in β-arrestin 2 recruitment assay. Cells were treated with 0.1 mg/ml of either 1,5-DQA, 3,4-DQA, 4,5-DQA or PCA separately or in combination with 0.25 µM adenosine. Luminescence was measured directly after treatment for 1 hour at RT and a solvent control of 0.1 % DMSO was included. Values are given in mean +/- SEM (n=3 independent experiments in triplicates). Values were considered significantly different with p values ≤ 0.05.

Since 3,4-DQA and 4,5-DQA showed a modulatory effect in prior experiments, 3,4-DQA was further investigated exemplarily in detail. 3,4-DQA showed a dose-dependent modulatory effect in combination with adenosine (Figure 18). Concentrations of 0.01 mg/ml 3,4-DQA and higher in combination with 0.25 µM adenosine showed significant increase in β-arrestin 2 recruitment compared to adenosine alone (Figure 18A). Interestingly, DQAs did not influence the activation phase in the beginning of the measurement but they prevented deactivation of A_1AR. This was exemplarily shown for a high and a low concentration of 3,4-DQA in Figure 18B. The first part of the curve was not altered (compared to adenosine single treatment) while there was a distinct difference after the activation phase. This again showed the importance of the inspection of several time points. Inspecting only the AUC for example would neglect interesting changes of the receptor kinetic.

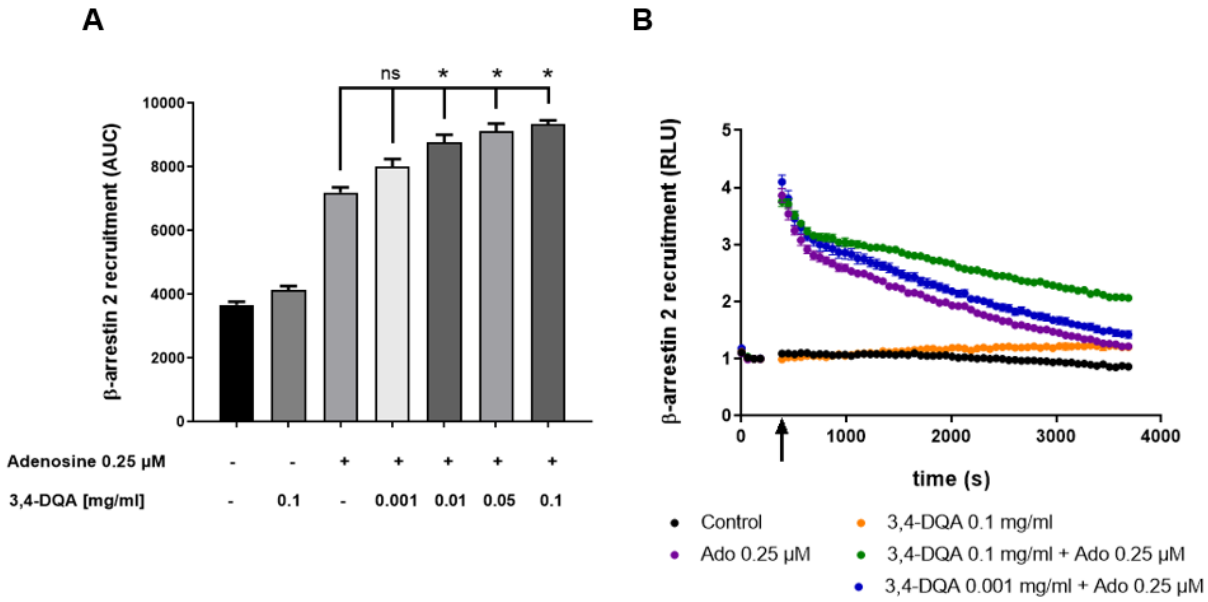

Figure 18. Concentration-dependent modulatory effect of 3,4-DQA in combination with adenosine in β-arrestin 2 recruitment assay. Cells were treated with 0.25 µM adenosine (Ado) and different concentrations of 3,4-DQA at the time point indicated by the arrow. (A) Concentrations of 0.01 mg/ml DQA and higher in combination with Ado resulted in significant increase of recruitment compared to Ado alone while 0.001 mg/ml 3,4-DQA showed no significant modulatory effect. Response of 3,4-DQA single treatment was similar to the response of the solvent control (0.1 % DMSO). (B) Kinetic representation of high and low concentration of 3,4-DQA in combination with Ado. Luminescence was measured directly after treatment for 1 h at RT. Values are given in mean +/- SEM (n=3 independent experiments in triplicates). Values were considered significantly different with p values ≤ 0.05.

Different concentrations of adenosine were tested in the following experiment in combination with a single concentration of 3,4-DQA (0.1 mg/ml). The modulatory effect of 3,4-DQA was noticeably in combination with small concentrations of adenosine (10 nM – 250 nM) whereas it was not shown for high adenosine concentrations (> 250 nM) (Figure 19). The smaller the concentration of adenosine, the greater the modulatory effect of 3,4-DQA.

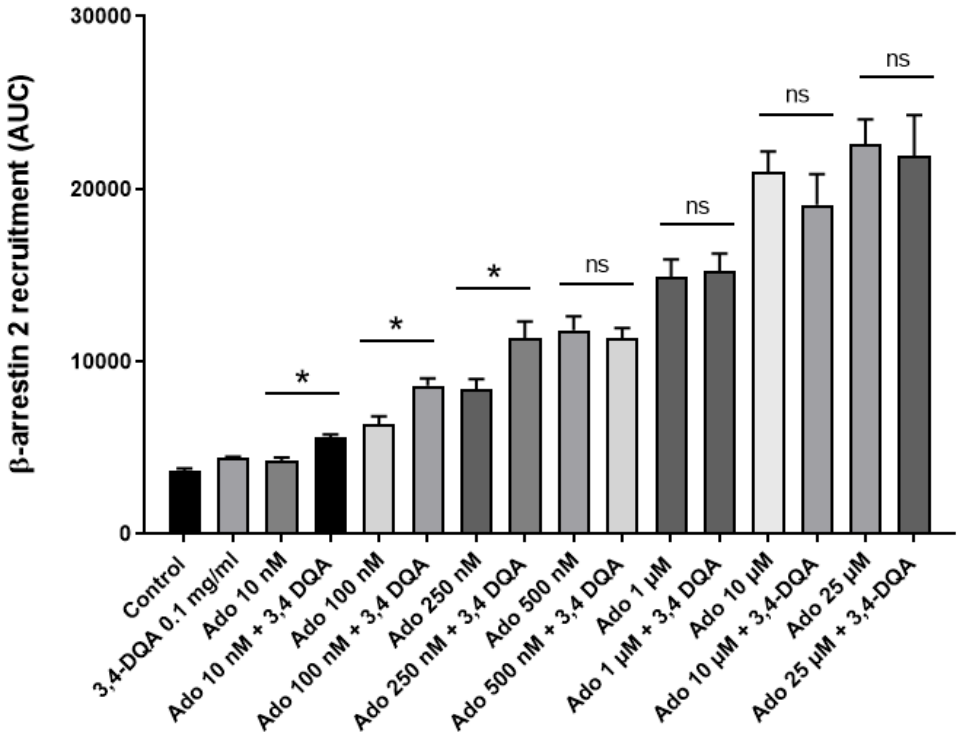

Figure 19. Small concentrations of adenosine-mediated recruitment modulated by 3,4-DQA. Cells were treated with different concentrations of adenosine (10 nM – 25 µM) and a single concentration of 3,4-DQA (0.1 mg/ml). Modulatory properties of 3,4-DQA were detected in combination with small concentrations of adenosine (10 nM – 250 nM) while high concentrations of adenosine were not modulated by 3,4-DQA. Luminescence was measured directly after treatment for 1 h at RT and a solvent control of 0.1 % DMSO was included. Values are given in mean +/- SEM (n=3 independent experiments in triplicates). Values were considered significantly different with p values ≤ 0.05.

Since the agonistic effect of Ze 911 is explainable by the adenosine content present in the extract, an additional independent modulatory effect was an important finding for this work. In the upcoming experiments, both, DQAs and the whole extract Ze 911 were tested.

4.2.3 Initial rate investigations of A_1AR ligands in β-arrestin 2 recruitment assay

Calculation of the AUC contains both, activation/inactivation and downstream signalling processes of the receptor. However, it can be useful to compare only the activation phase of the receptor after treatment. This provides information about the efficacy of the ligands. Hoare et al. 2020[81,82] developed and provided an evaluation tool for G-protein- and arrestin-mediated signalling in living cells that allows calculation of receptor activation and inactivation separately. The analysis tool containing certain plug-in equations provides different parameters. The “initial rate” is the slope of a straight line adapted to the activation phase and a parameter for effi-

ciency. Agonists were tested at saturating concentrations (10 µM) and initial rates were calculated with the respective equation. The calculated initial rates of adenosine (10.4 ± 0.3-fold change/min), NECA (12.9 ± 0.3-fold change/min) and CPA (10.3 ± 0.3-fold change/min) were very similar (Figure 20). The initial rate of capadenoson (2.5 ± 0.1-fold change/min) however was approximately 4 times lower (Figure 20). Even though, adenosine has a much higher EC_{50} compared to NECA and CPA, the efficiency in receptor activation measured as initial rate is just as high as for the other two agonists.

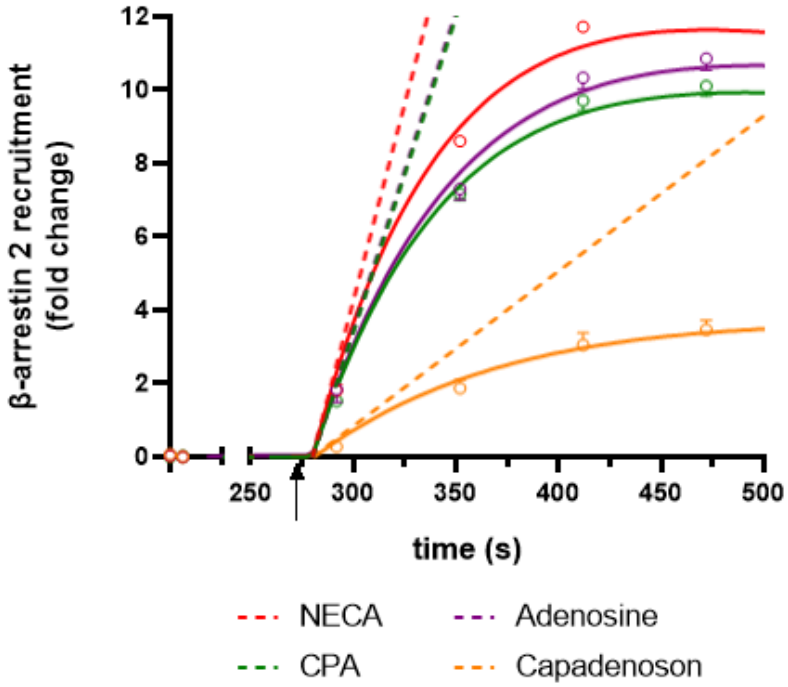

Figure 20. Initial rates of A_1AR agonists analysed by rise-and-fall to baseline equation with drift. Cells were treated using saturating concentrations of each agonist (10 µM) at the time point indicated by the arrow. Luminescence was measured directly after treatment for 1 h at RT and a solvent control of 0.1 % DMSO was included. Dashed lines represent initial rates that were calculated from the fitted curves. Values are given in mean +/- SEM (n=3 independent experiments in triplicates). Figure has been adopted from Saecker et al. 2023[61].

Interestingly, adenosine in combination with 3,4-DQA did not result in a higher initial rate compared to adenosine alone (2.20 ± 0,001 and 2.50 ± 0.003-fold-change/min respectively). Data is not shown in Figure 20. However, the AUC of the combination was significantly higher than for adenosine alone (Figure 18). This also fits to Figure 18B since the response curves are equally steep in the beginning. As mentioned before, 3,4-DQA seems to prevent the receptor from inactivation/internalization. The initial rate of Ze 911 (7.10 ± 0.008-fold-change/min) was comparable to the other adenosine receptor agonists. Data is also not shown in Figure 20.

This work aimed to get a better understanding of Ze 911 influencing adenosine A_1 receptor. To get the whole picture, it was reasonable to investigate both, β-arrestin 2 recruitment as well as G protein-dependent signalling pathways that might be affected by Ze 911. Hence, G protein dependent cAMP concentration and Ca^{2+} mobilization were studied in the upcoming experiments.

4.3 Ze 911 decreased cAMP concentration in cell-based assay

The transfected cAMP biosensor allowed the detection of cellular cAMP changes. Since A_1AR is G_i-coupled, stimulation inhibits adenylate cyclase and decreases cAMP concentration. Besides A_1AR, HEK 293 cells express $A_{2A}AR$ and $A_{2B}AR$[97] that stimulate adenylate cyclase. Therefore, cells were additionally transfected with A_1AR to compensate signals of other adenosine receptors.

Cells were transfected with pCDNA3.1Zeo_HiBiT-ADORA1 and pGloSensor™-22F cAMP plasmid. Stably transfected cells were tested with Nano-Glo® HiBiT extracellular detection system (Promega GmbH, Walldorf, Germany). The detection kit contains LgBiT, the complementary polypeptide to HiBiT. Luminescence is proportional to amount of HiBiT-tagged protein on cell surface. Even though both tested clones showed a robust signal, luminescence of clone one was considerably more prominent (Figure 21). Therefore, clone one was used for the following experiments.

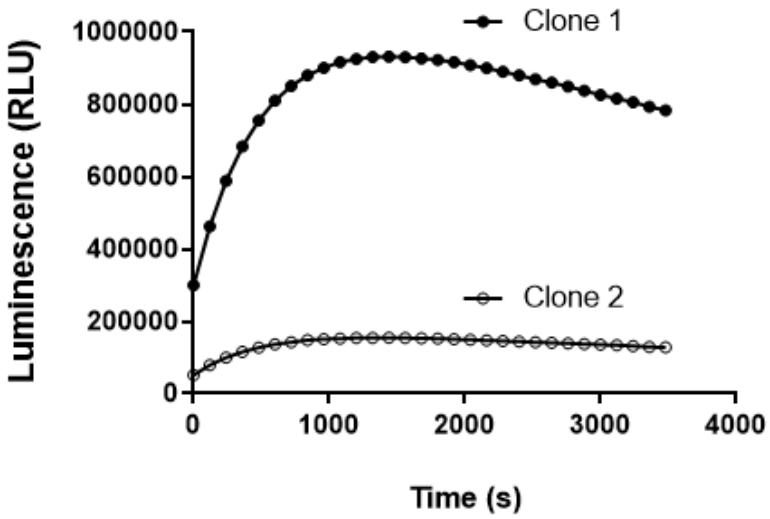

Figure 21. Verification of stably transfected cell line using Nano-Glo® HiBiT extracellular detection assay. Cells were seeded in 96-well plate and treated with LgBiT and corresponding substrate solution from the assay kit. Luminescence was measured 1 h at RT. Robust luminescence signal was measured for both clones.

In the first experiment, cells were tested for A_1AR response. Figure 22A shows the time flow of the assay. Cells were incubated with luciferase substrate for 2 hours before ligand treatment and measurement. Beside ligand treatment, adenylate cyclase was stimulated with 1 µM forskolin. Additionally, cells were treated with 1 µM isoprenaline that stimulates β-AR because the luminescence signal of forskolin alone was not strong enough. A solid luminescence signal was mandatory since an A_1AR-mediated decrease of luminescence was to be measured. Treatment of cells with A_1AR agonist CPA resulted in a significant decrease of cAMP concentration which was reversed by A_1AR antagonist DPCPX (Figure 22A+B). Control cells were treated with 1 µM isoprenaline and 1 µM forskolin only. Figures show one experiment exemplarily. Three independent experiments were performed in triplicates (n=3) with similar results. This also applies for following cAMP experiments if not stated otherwise.

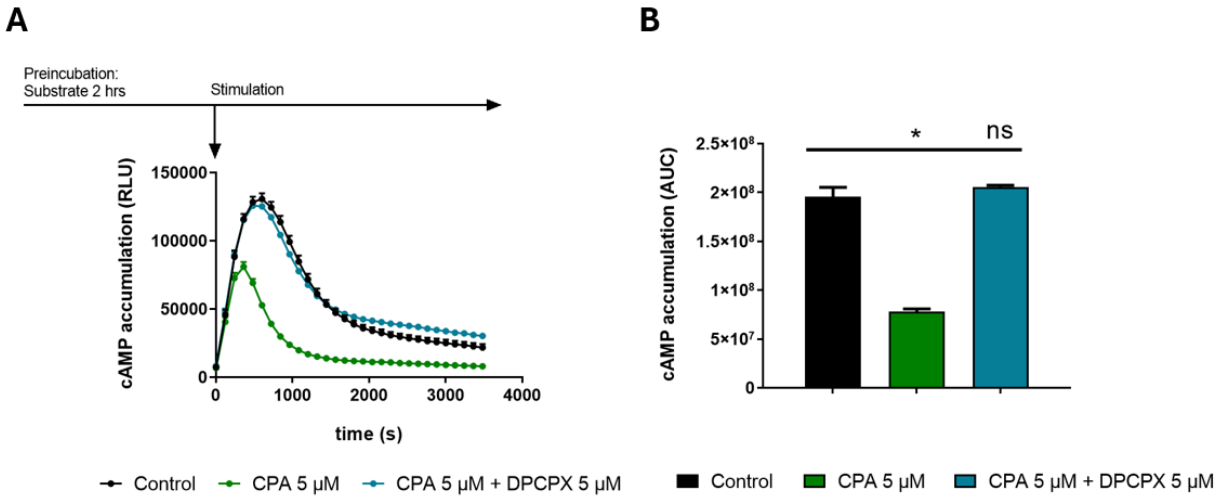

Figure 22. CPA-mediated inhibition of cAMP accumulation reversed by DPCPX. (A) Principle of the assay including time-response curves and corresponding AUCs (B). Cells were treated with either 5 µM CPA or 5 µM CPA in combination with 5 µM DPCPX directly before measurement. Additionally, cells were stimulated with 1 µM forskolin and 1 µM isoprenaline at the same time. Luminescence was measured for 1 hour at RT and a control containing 0.1 % DMSO was included. Figure shows one experiment exemplarily. Three independent experiments were performed in triplicates (n=3). Values are given in mean ± SEM. Values were considered significantly different with p values ≤ 0.05.

The following experiment showed that CPA treatment resulted in a dose-dependent decrease of cAMP concentration with an IC_{50} of 16 ± 0.14 nM (Figure 23A+B). Since the established assay responded well to A_1AR stimulation, Ze 911 was tested in the next experiment. Treatment with different concentrations of Ze 911 also resulted in a dose-dependent decrease of cAMP accumulation with an IC_{50} of 35 ± 0.12 µg/ml (Figure 23C+D). The agonistic activity of Ze 911 on G_i-dependent signalling was therefore confirmed. This result was expectable because of the adenosine concentration present in the extract.

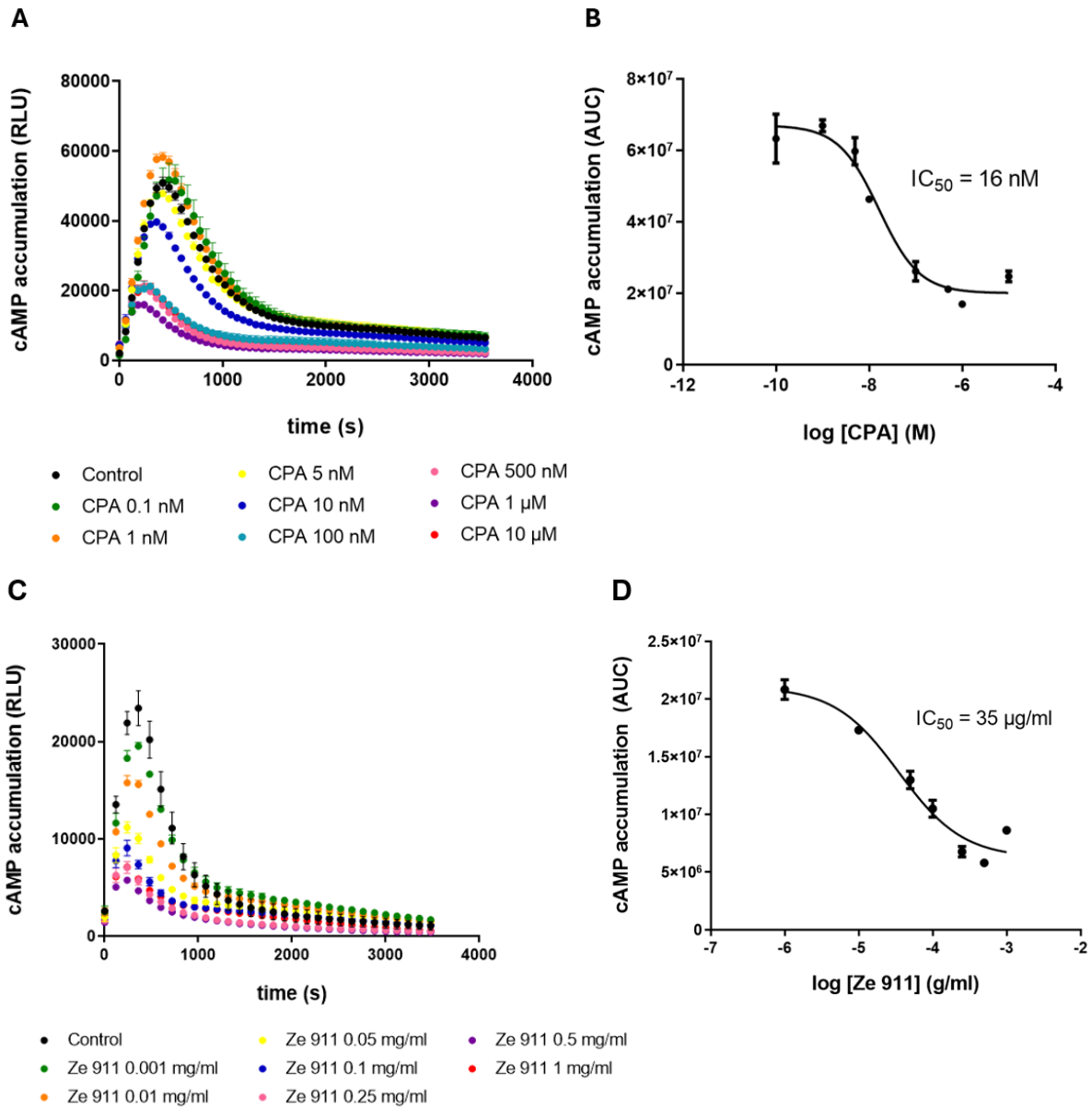

Figure 23. Dose-dependent decrease of cAMP accumulation by CPA and Ze 911. (A) cAMP accumulation after CPA treatment and corresponding dose-response curve (B). (C) cAMP accumulation after treatment with Ze 911 and corresponding dose-response curve (D). Cells were treated with concentration series of either CPA or Ze 911. Luminescence was measured for 1 h at RT and a control containing 1 % DMSO was included. All test conditions also contained 1 µM forskolin und 1 µM isoprenaline. IC_{50} values were calculated in GraphPad Prism using a nonlinear regression model (dose-response inhibition). Figure shows one experiment exemplarily. Three independent experiments were performed in triplicates (n=3). Values are given in mean +/- SEM. Figure has been adapted from Saecker et al. 2023[61].

Specific A_1AR and non-specific AR agonists were tested afterwards using saturating concentrations (1 µM). CPA and the partial A_1AR agonist capadenoson showed the strongest decrease in cAMP accumulation (Figure 24). Setting control to 100 % cAMP concentration, CPA

decreases cAMP concentration to 39 %, capadenoson to 44 %, adenosine to 72 % and NECA to 78 %.

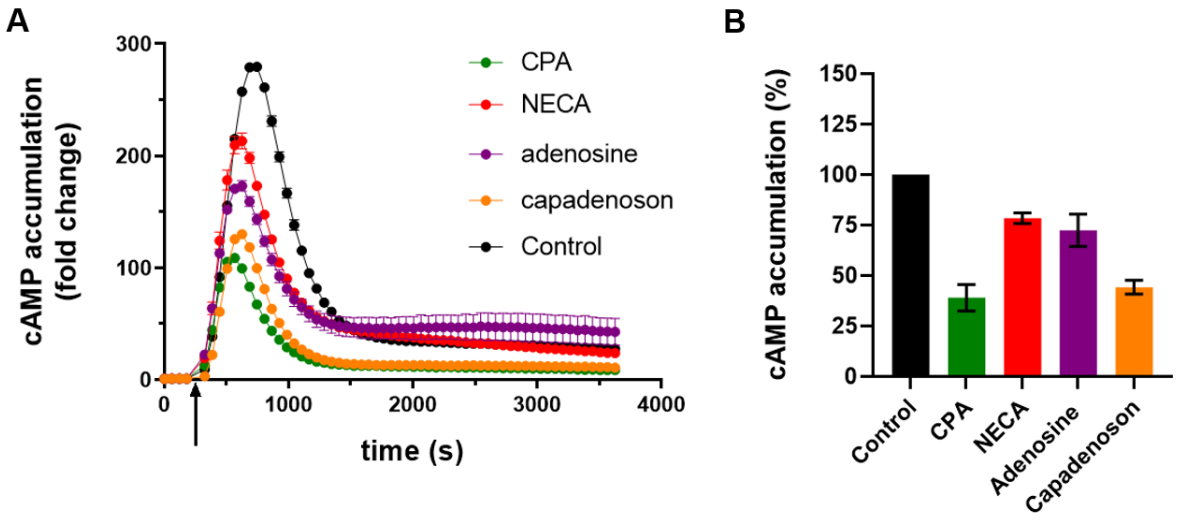

Figure 24. Comparison of adenosine receptor agonists regarding cAMP accumulation. (A) Time-response curves of agonists and comparison of cAMP accumulation after treatment (B). Cells were treated with either CPA, NECA, adenosine or capadenoson in saturating concentrations (1 µM). Luminescence was measured for 1 h at RT and a control containing 1 % DMSO was included. All test conditions also contained 1 µM forskolin und 1 µM isoprenaline. Three independent experiments were performed in triplicates (n=3). Values are given in mean +/- SEM.

Subsequently, cells were tested with A_1AR positive allosteric modulator VCP 171. Even though the concentration of the combination NECA (100 nM) and VCP 171 (1 µM) resulted in a stronger decrease of cAMP concentration compared to NECA alone, it was not significant (Figure 25). In addition, VCP 171 single treatment also decreased cAMP concentration. This implies that it is more difficult to measure modulatory properties using this assay. Calculated AUC values were normalized to control condition.

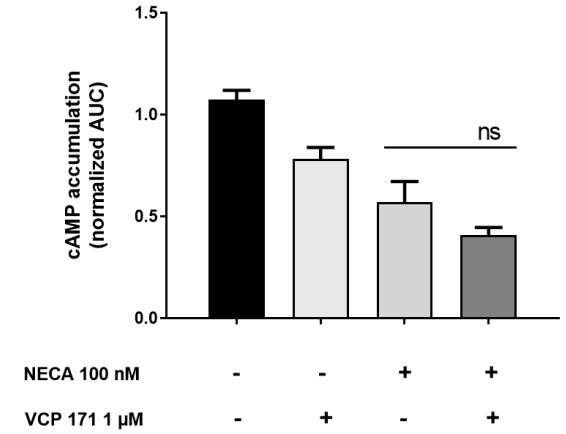

Figure 25. No modulatory properties of VCP 171 on cAMP accumulation mediated by NECA. Cells were treated with either 1 µM VCP, 100 nM NECA or both combined. Luminescence was measured for 1 h at RT and a control containing 0.25 % DMSO was included. All test conditions also contained 1 µM forskolin und 1 µM isoprenaline. Two independent experiments were performed in triplicates (n=2). Values are given in mean +/- SEM.

Even though no modulatory effect of VCP 171 was detected, 3,4-DQA was tested on the cells separately as well as in combination with adenosine 0.25 µM. Concentrations were selected similar to those tested in β-arrestin recruitment assay. The results however were not as stable as for the other conditions. Single treatment with 3,4-DQA resulted in slight increase of cAMP accumulation. No differences in cAMP accumulations have been detected for the combination of adenosine and 3,4-DQA compared to adenosine single treatment (Figure 26). Modulatory effect of 3,4-DQA was therefore not detectable in G protein dependent cAMP assay, at least using these certain concentrations. Experiment was repeated once in triplicates with similar results (n=2).

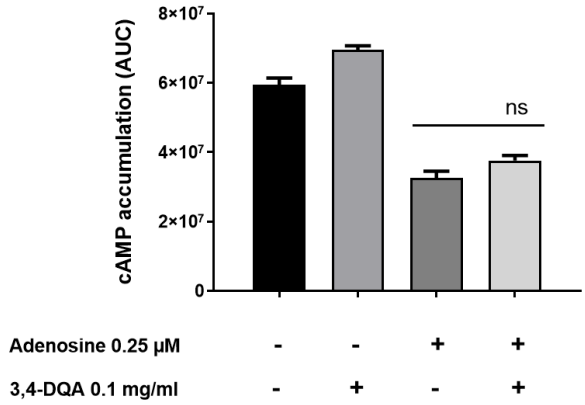

Figure 26. No modulatory properties of 3,4-DQA on cAMP accumulation mediated by adenosine. Cells were treated with either 0.25 µM adenosine, 0.1 mg/ml 3,4-DQA or a combination of both. Luminescence was measured for 1 h at RT and a control containing 1 % DMSO was included. All test conditions also contained 1 µM forskolin und 1 µM isoprenaline. Two independent experiments were performed in triplicates (n=2). Values are given in mean +/- SEM.

4.4 Calcium mobilization after Ze 911 treatment

Figure 1 shows that among other things A_1AR activation mobilizes Ca^{2+}. Recent studies prove that calcium plays an important role in the regulation of sleep[94–96]. SH-SY5Y cells that express A_1AR genuinely were tested in a calcium assay using the fluorescence-based calcium dye Cal-520®.

Figure 27 shows in detail how the assay was performed. Normalized data was plotted over time in GraphPad Prism. In the beginning, 4 cycles a 15 s fluorescence were measured under control conditions (cells in 80 µl Locke's solution) starting at time point 0 s. Afterwards, 20 µl ligand solution or Locke's solution were injected by Tecan Spark® injection system and measurement was continued until cycle 15 was finished. First experiments showed that CPA single treatment did not result in calcium mobilization (Figure 27). No fluorescence enhancement has been measured compared to control cells. The non-selective muscarinic receptor agonist methacholine was used as positive control for calcium mobilization. After injection of methacholine, the fluorescence signal increased rapidly. Experiments were always repeated twice in triplicates (n=3) if not stated otherwise.

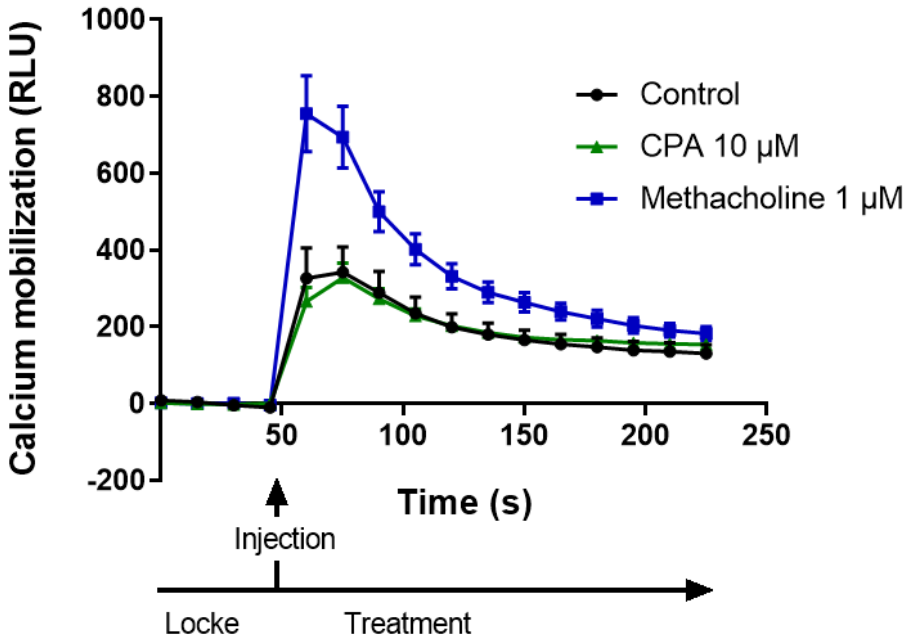

Figure 27. No calcium mobilization detected in SH-SY5Y cells after CPA treatment. Cells were incubated with 10 µM calcium dye Cal-520® 2.5 h before fluorescence was measured. Baseline was measured 4 cycles a 15 s (starting at time point 0 s) at 485 nM. Injector system injected 20 µl CPA (10 µM) or methacholine (1 µM) and measurement was continued for 12 more cycles a 15 s. Locke's solution was included as control treatment. Three independent experiments were performed in triplicates (n=3) and values are given in mean +/- SEM.

Interestingly, methacholine-mediated calcium mobilization was increased by CPA. The combination resulted in fluorescence enhancement compared to methacholine single treatment (Figure 28A). This modulating effect was even more prominent for Ze 911. The combination of Ze 911 and methacholine resulted in a significant increase of fluorescence compared to methacholine alone (Figure 28B+C). In addition, Ze 911 single treatment mobilized calcium unlike CPA. The effect of Ze 911 and methacholine is more than additive. These results implied that Ze 911 contains agonistic as well as modulating substances mobilizing calcium.

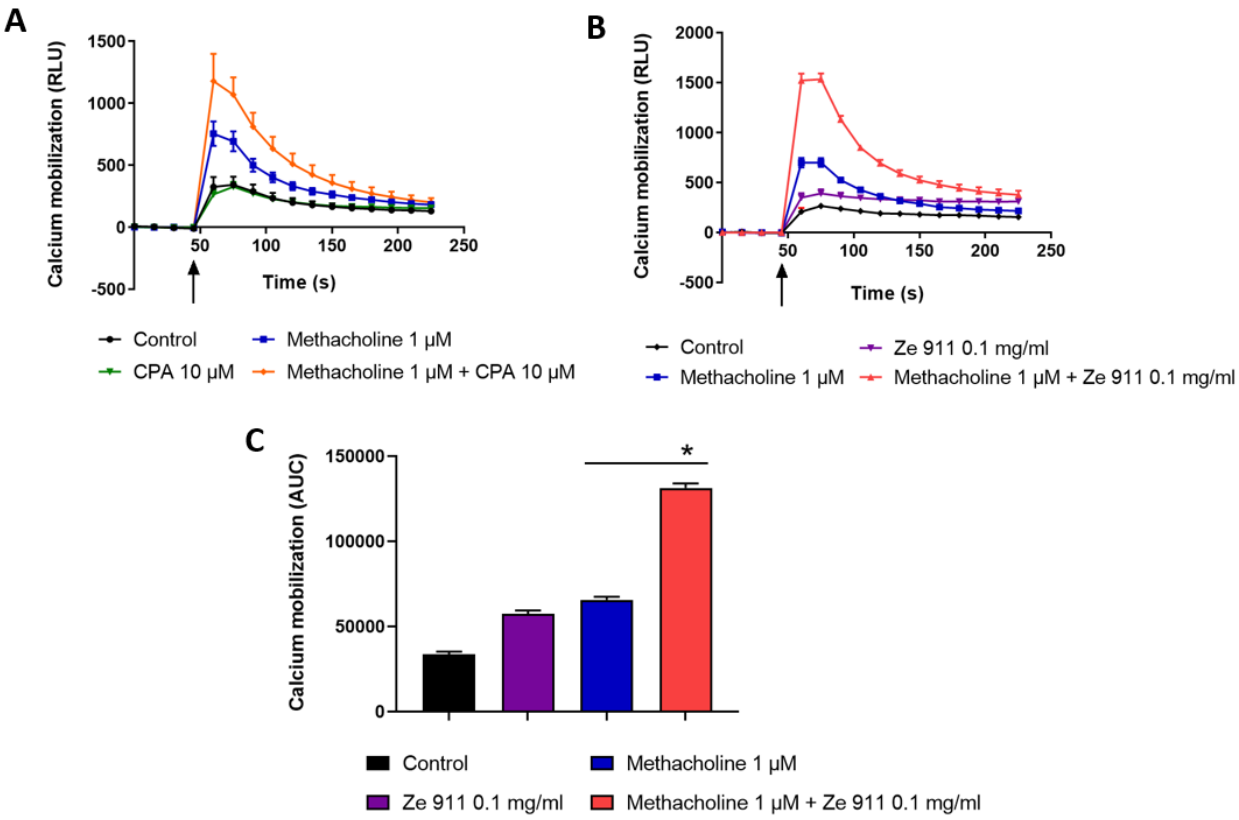

Figure 28. Modulatory effect of CPA (A) and Ze 911 (B+C) on methacholine-mediated calcium mobilization in SH-SY5Y cells. Cells were incubated with 10 µM calcium dye Cal-520® 2.5 h before fluorescence was measured. Baseline was measured 4 cycles a 15 s (starting at time point 0 s) at 485 nm. Injector system injected 20 µl CPA (10 µM), methacholine (1 µM), Ze 911 (0.1 mg/ml), a combination of CPA and methacholine or a combination of Ze 911 and methacholine and measurement was continued for 11 more cycles. Locke's solution was included as control treatment. Three independent experiments were performed in triplicates (n=3) and values are given in mean +/- SEM. Values were considered significantly different with p values ≤ 0.05.

Valerian extract pretreated with adenosine deaminase (Ze 911-ADA) and 3,4-DQA were tested for calcium mobilization thereafter. Figure 29 shows that the combination of Ze 911-ADA and methacholine resulted in significant fluorescence increase compared to methacholine single treatment. To confirm the involvement of A_1AR, cells were treated with A_1AR antagonist

DPCPX in combination with methacholine and Ze 911-ADA. The fluorescence signal of Ze 911-ADA in combination with methacholine was slightly decreased by DPCPX, but not significantly (Figure 29). It can be speculated that adenosine in Ze 911 plays a role but is not the only component responsible for the effect. Therefore, treatment with antagonist showed that A_1AR might play a role but is not the only regulator of calcium mobilization in these experiments. It is likely that one of the approximately 200 substances in Ze 911 mobilizes calcium by a different pathway.

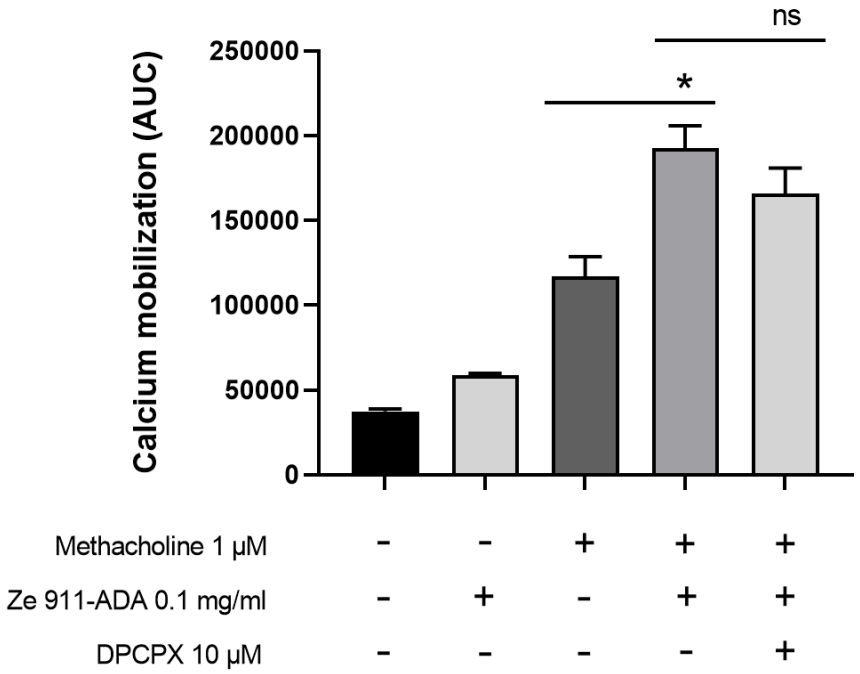

Figure 29. Ze 911-ADA modulates methacholine-mediated calcium mobilization in SH-SY5Y cells. Cells were incubated with 10 µM calcium dye Cal-520® 2.5 h before fluorescence was measured. Baseline was measured 4 cycles a 15 s (starting at time point 0 s) at 485 nM. Injector system injected 20 µl methacholine, Ze 911-ADA, a combination of Ze 911-ADA and methacholine or a combination of Ze 911-ADA, DPCPX and methacholine and measurement was continued for 11 more cycles. Locke's solution was included as control treatment. Three independent experiments were performed in triplicates (n=3) and values are given in mean +/- SEM. Values were considered significantly different with p values ≤ 0.05.

Subsequently, since 3,4-DQA showed a robust modulatory effect in the β-arrestin 2 recruitment assay it was also tested for possible modulatory effects concerning calcium mobilization. Cells treated with methacholine and 3,4-DQA showed a different kinetic in the assay compared to other substances that were tested. 3,4-DQA did not affect the first rise of the curve (first response after treatment) but prolonged the phase of calcium mobilization (Figure 30A). The difference calculated by the AUC scratched at the limit of significance ($p = 0.0568$). Therefore,

single time point analysis was performed afterwards. Significant differences have been detected for single time point investigations (Figure 30C). 3,4-DQA significantly increased calcium mobilization of methacholine from 60 s until 105 s after treatment. Single treatment with 3,4-DQA did not result in calcium mobilization (Figure 30A+B).

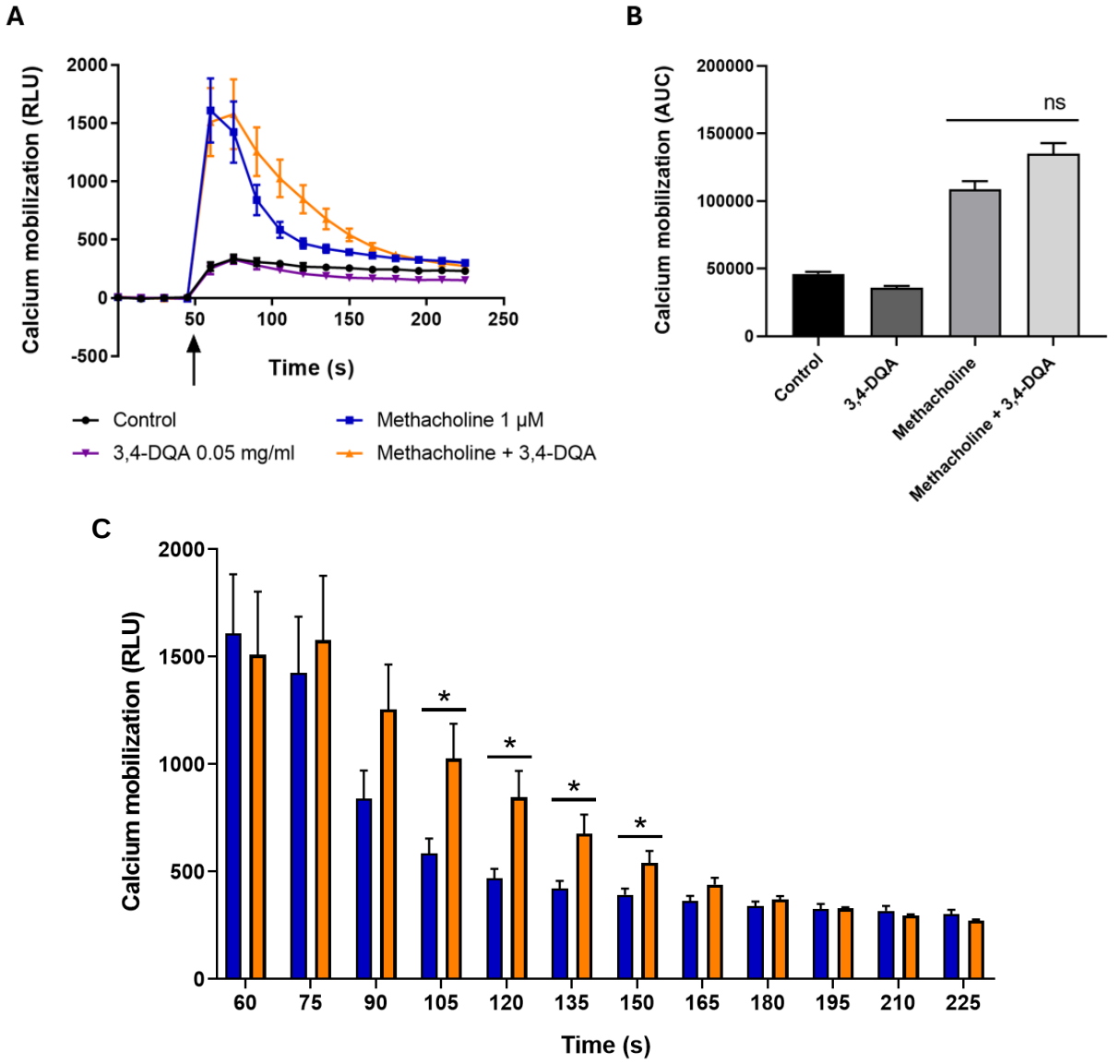

Figure 30. Modulating effect of 3,4-DQA on methacholine-mediated calcium mobilization in SH-SY5Y cells. Cells were incubated with 10 µM calcium dye Cal-520® 2.5 hours before fluorescence was measured at 485 nm. Baseline was measured 4 cycles a 15 s. Afterwards, injector system injected 20 µl methacholine, 3,4-DQA or a combination of methacholine and 3,4-DQA and measurement was continued for 11 more cycles (A). AUC analyses (B) did not show significant differences while single point investigation (C) resulted in significant differences between 60 s and 105 s after treatment. Locke's solution was included as control treatment. Three independent experiments were performed in triplicates (n=3) and values are given in mean +/- SEM. Values were considered significantly different with p values ≤ 0.05.

4.5 Lateral diffusion behaviour of A_1AR after treatment

HEK-GloSensor™-HiBiT-A_1AR cells were labelled with HaloTag®-self-labelling protein technology and analysed in SPT setup that operated with a 637 nm laser. This method has already been successfully established for GPCRs by Franken et al. 2020[84]. The following experiments aimed to detect receptor dynamics after stimulation with A_1AR ligands. Three independent experiments were performed measuring and examining at least three cells each (n=3).

4.5.1 Investigation of diffusion states using a three-state model

Among other things, SPT measurements allow the observation of different receptor states that are characterized by diffusion coefficients, spatial confinement and oligomerization for instance. A_1AR receptor can be found in three distinct receptor states on HEK 293 cells. These states are classified as follows: an immobile state called S1, a rather slow-diffusing state called S2, and a fast-diffusing state called S3. These states are defined by diffusion coefficients and corresponding state occupancy values. In the first experiment, cells were treated with either 1 µM CPA, 0.1 mg/ml Ze 911 or PBS (control) and incubated 15 minutes before measurement was started. Incubation time of 15 minutes was chosen since assays performed above implicated that a lot of signalling happens in the first 15 minutes. Cells that were only treated with buffer control PBS showed the following diffusion coefficients: 0.018 ± 0.003 µm²/s for S1, 0.040 ± 0.003 µm²/s for S2 and 0.125 ± 0.009 µm²/s for S3. Treatment with CPA or Ze 911 did not change diffusion coefficients in any of the three states significantly (Figure 31).

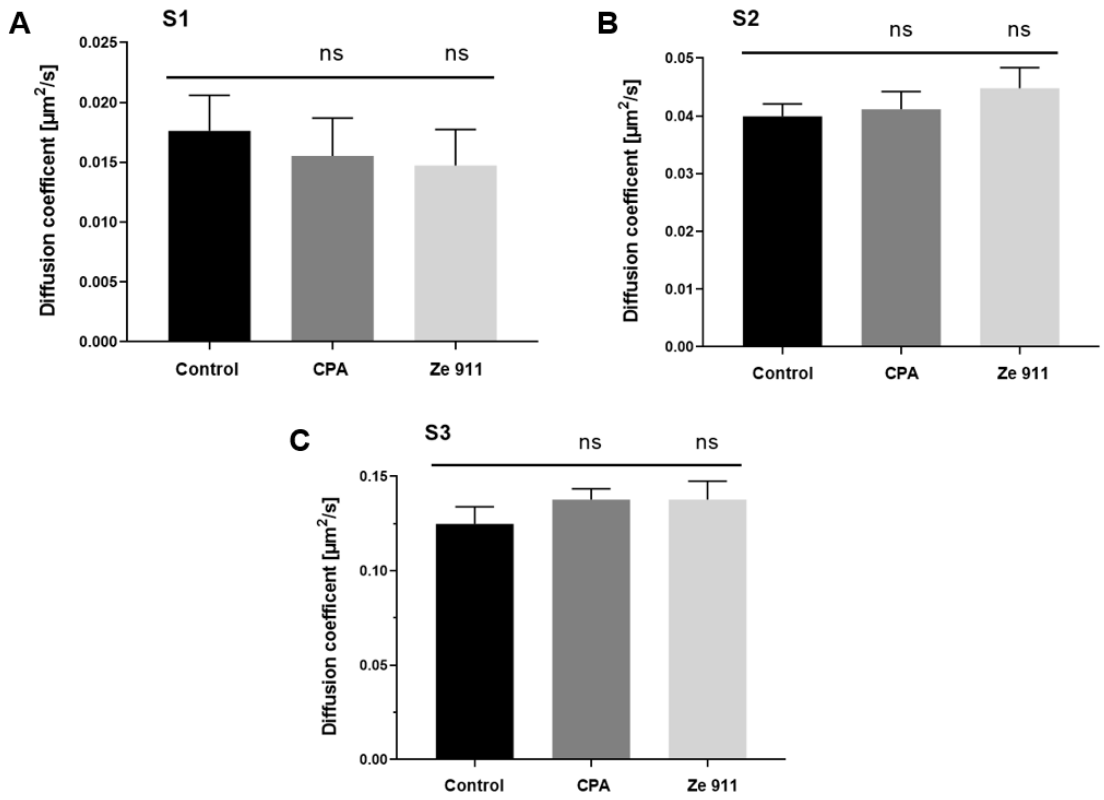

Figure 31. Diffusion behaviour of A_1AR on HEK 293 cells after agonist treatment. Diffusion coefficients corresponding to states S1 (A), S2 (B) and S3 (C) on plasma membrane of HEK-GloSensor™-HiBiT-A_1AR cells. Cells were either treated with PBS (control), 1 µM CPA or 0.1 mg/ml Ze 911 15 min before measurement was started. Data was obtained by vbSPT analysis in MATLAB (version R2016b). At least three independent experiments were performed. Values are given in mean +/- SEM.

4.5.2 Receptor state occupancy not altered after agonist stimulation

Besides diffusion coefficients, vbSPT analysis also considers and calculates the relative number of particles in the certain states S1, S2 or S3. The distribution of A_1AR in the different states after treatment is shown in Figure 32. Cells were treated with agonists 15 minutes before measurement was started. No significant changes in number of particles have been observed after treatment with CPA or Ze 911 including all three states. Occupancies were comparable to control cells (Figure 32B).

A

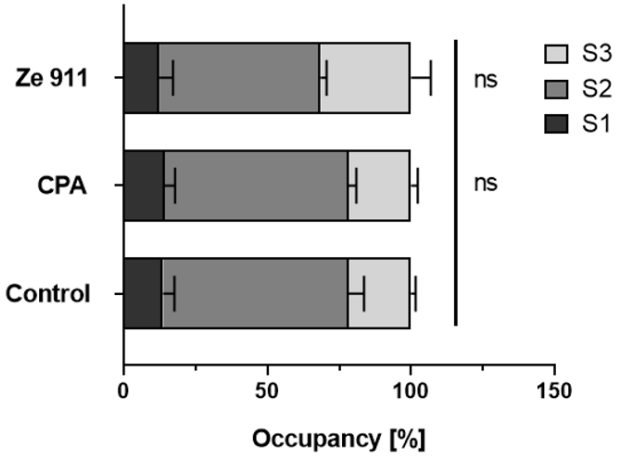

B

	Occupancy S1 (%)	Occupancy S2 (%)	Occupancy S3 (%)
Control	16.662 ± 3.958	64.530 ± 5.441	21.808 ± 1.656
CPA	14.288 ± 3.520	64.092 ± 2.546	21.620 ± 2.365
Ze 911	12.339 ± 4.828	56.178 ± 2.063	31.482 ± 6.895

Figure 32. Occupancies of different diffusion states after treatment. Receptor state occupancies for S1, S2 and S3 15 minutes after treatment with either PBS (control), 1 µM CPA or 0.1 mg/ml Ze 911 (A) with corresponding tabulated values (B). Occupancies of different receptor states are expressed in percentages. Data was obtained by vbSPT analysis in MATLAB (version R2016b). At least three independent experiments were performed. Values are given in mean +/- SEM.

4.5.3 Impact of A_1AR stimulation on spatial confinement

Impact of A_1AR stimulation on spatial confinement of diffusion was investigated to further characterize lateral diffusion of the receptor. Confinement analysis based on packing coefficient (Pc) was described in 3.2.5.2. Even though, confinement analysis was performed for every diffusion state, robust statistical analyses of spatial confinement was only possible for S1 and S2. Number of track segments in S3 were too little for reliable statistical analysis. For cells treated with buffer control, 34.893 ± 8.968 % of evaluated trajectories were identified to be confined in state S1 and 8.527 ± 1.424 % in state S2. Besides confined fraction (%), the mean of confinement size of the diffusion area was determined which was given as the square root of the convex hull area in nm. Mean confinement size of control cells was 65.086 ± 6.481 nm in state S1 and 103.707 ± 0.760 nm in state S2. No significant changes in confined fraction and confinement size were detected after treatment with CPA or Ze 911 compared to control (Figure 33). Confined fraction in state S1 is nearly the same for all three tested conditions (Figure 33A) whereas a tendency of increasing confined fraction after A_1AR stimulation was detected in state S2 (Figure 33B). Mean confinement sizes were comparable for the three tested conditions in state S1 as well as S2 (Figure 33C+D).

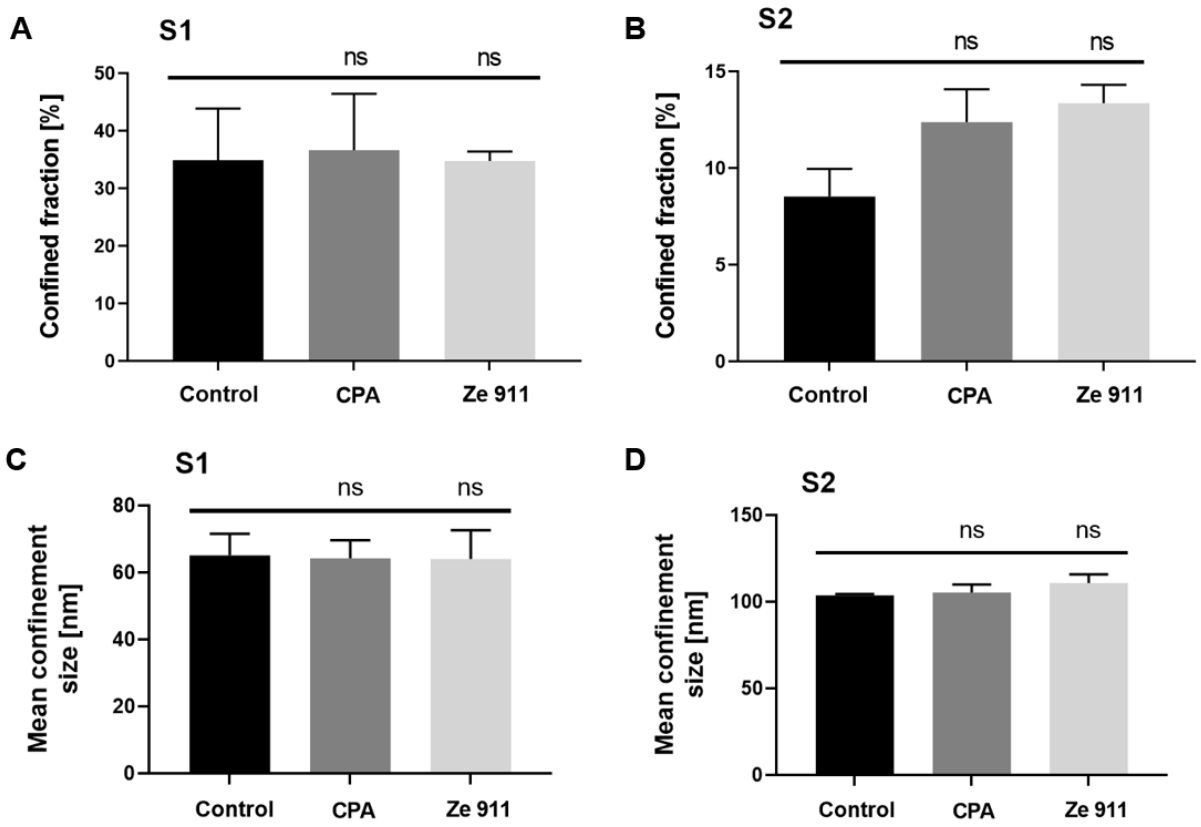

Figure 33. Confinement of A_1AR on HEK 293 cells after treatment. Confined fractions in percentages (A+B) and corresponding mean confinement sizes (C+D) in nm for states S1 and S2 on membrane of HEK-GloSensor™-HiBiT-A_1AR cells 15 min after treatment with either 1 µM CPA, 0.1 mg/ml Ze 911 or PBS (control). At least three independent experiments were performed. Values are given in mean ± SEM.

4.5.4 Homodimerization of A_1AR after stimulation

The last SPT evaluation step was the investigation of ligand treatment on A_1AR homooligomerization states on the cell surface. The previously generated fluorescence intensity distributions of the vbSPT data was investigated by a mixed Gaussian fitting to determine fractions and corresponding mean intensities of the corresponding monomers and potential homooligomers. They were identified by rising mean intensities. Doubled mean intensity signalized the presence of homodimers, tripled mean intensity signalized the presence of homotrimers and so on. The oligomerization analysis revealed that only monomers and homodimers were present at the surface of the investigated cells with a proportion of approximately 1:5. Homotrimers or higher oligomers were not identified. PBS treated control cells showed a distribution of mainly monomers with 78.702 ± 2.134 %. Homodimers occurred with 21.298 ± 2.134 % in a lower ratio. After treatment with CPA or Ze 911 an increase of homodimer occurrence has been observed compared to control cells (Figure 34). However, the changes were not statistically significant.

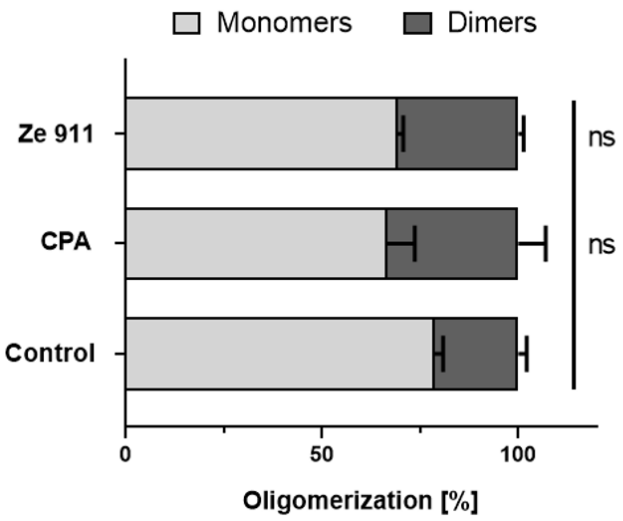

	Monomers (%)	Dimers (%)
Control	78.702 ± 2.134	21.298 ± 2.134
CPA	66.635 ± 6.964	33.365 ± 6.964
Ze 911	69.330 ± 1.329	30.670 ± 1.329

Figure 34. Fractions of monomers and homodimers of HiBiT-A_1AR on HEK 293 cells after treatment. Cells were either treated with 1 µM CPA, 0.1 mg/ml Ze 911 or PBS 15 min before measurement. Fluorescence intensities were fitted by a mixed Gaussian model and plotted as percentages (A). Values were separately tabulated (B). Values were not significantly different from each other and given in mean ± SEM. At least three independent experiments were performed.

No differences in the lateral mobility of HiBiT-A_1AR has been detected on HEK 293 cells concerning the investigated diffusion properties above. This was surprising since agonist stimulation usually has a measurable impact on lateral mobility. The other assays showed that time-dependency is an important parameter that should be considered. Whereas calcium mobilizations was mainly detected after the first 2 minutes after stimulations, the peak of cAMP response was measured after approximately 15 minutes. Recruitment of β-arrestin 2 peaked at around 5-10 minutes with a longer activation phase compared to the other assays. Since time does play an important role, a time-dependent analysis of lateral mobility was planned next to ensure that no effects were overseen. Therefore, the well-descried A_1AR agonist CPA was inspected at five different time points after treatment. These timepoints are listed in Table 10. Hence, CPA was measured directly after treatment until 30 minutes thereafter. It is not recommended to measure much longer than 30 min on one coverslip because of laser-induced photobleaching.

4.5.5 Time-dependent investigation of lateral diffusion of A_1AR after CPA treatment

4.5.5.1 Impact of time-dependent A_1AR stimulation on diffusion coefficients

In the first experiment, cells were treated with 1 µM CPA and measured in a time interval from 1 to 30 minutes directly after treatment. Cells treated with CPA showed diffusion coefficients between 0.0151 and 0.0206 µm²/s for S1, 0.0411 and 0.0436 µm²/s for S2 and 0.1364 and

0.1609 µm²/s for S3. The diffusion coefficients in the different states remained the same for all five investigated time intervals (Figure 35). No significant differences between groups have been observed.

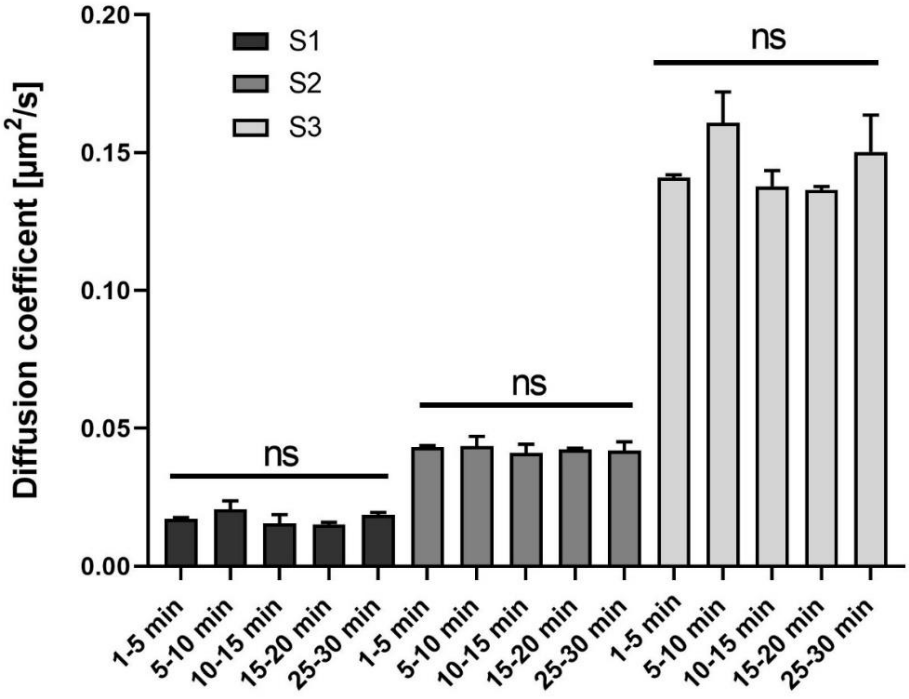

Figure 35. Time-dependent diffusion behaviour of A_1AR on HEK 293 cells after CPA treatment. Diffusion coefficients corresponding to states S1-S3 including five different time intervals on plasma membrane of HEK-GloSensor™-HiBiT-A_1AR cells. Cells were treated with 1 µM CPA directly before measurement and recorded 1-30 minutes afterwards. Data was obtained by vbSPT analysis in MATLAB (version R2016b). At least three independent experiments were performed and values are given in mean ± SEM.

4.5.5.2 Impact of time-dependent A_1AR stimulation on receptor state occupancy

State occupancies after CPA treatment for all five different time intervals were investigated. The number of particles in state S1 and S2 did not change over time after treatment. However, in the fast-diffusing state S3, a significant difference was detected (Figure 36A). The occupancy of S3 significantly increased between time interval 2 and time interval 4 from 18.261 ± 1.492 % to 30.016 ± 1.355 % (Figure 36B). Another significant difference has been observed between time interval three and time interval four from 21.620 ± 2.365 % to 30.016 ± 1.355 % (Figure 36B).

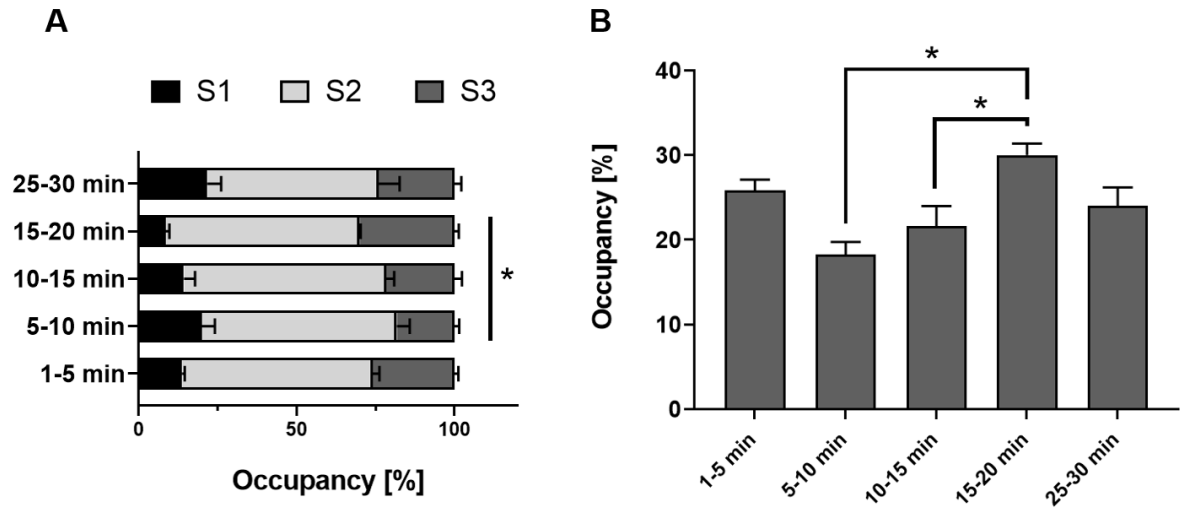

Figure 36. Time-dependent occupancies of different diffusive states after CPA treatment. Receptor state occupancies for S1, S2 and S3 including five time intervals after treatment with 1 µM CPA (A). Increase of receptor state occupancies in state S3 from time interval two to time interval four (B). Occupancies of different receptor states are expressed in percentages. Data was obtained by vbSPT analysis in MATLAB (version R2016b). At least three independent experiments were performed. Values are given in mean ± SEM. Values with $p \leq 0.05$ were considered statistically significant.

4.5.5.3 Impact of time-dependent A_1AR stimulation on spatial confinement

For CPA treated cells the confined fraction in the time intervals of 1 to 30 minutes reached from 22.518 ± 3.423 % to 44.879 ± 3.793 % for S1 and from 6.734 ± 0.188 % to 14.326 ± 2.148 % for S2. A significant increase of confined fraction has been detected from time interval one to time interval five in state S2 (Figure 37B). There is a tendency of increasement from the beginning to the end of the time intervals. However, no other statistical significances have been detected in S2. Confined fraction did not change over time in S1 (Figure 37A). Besides confined fraction, the mean of confinement size was determined. It is given as the square root of the convex hull area in nm. Figure 37C and D show that the confinement size remained constant for S1 as well as S2 including all five time intervals. For S1, the mean confinement size was between 64.227 ± 5.493 nm and 71.946 ± 6.292 nm and for S2 between 103.022 ± 5.020 nm and 110.439 ± 7.164 nm.

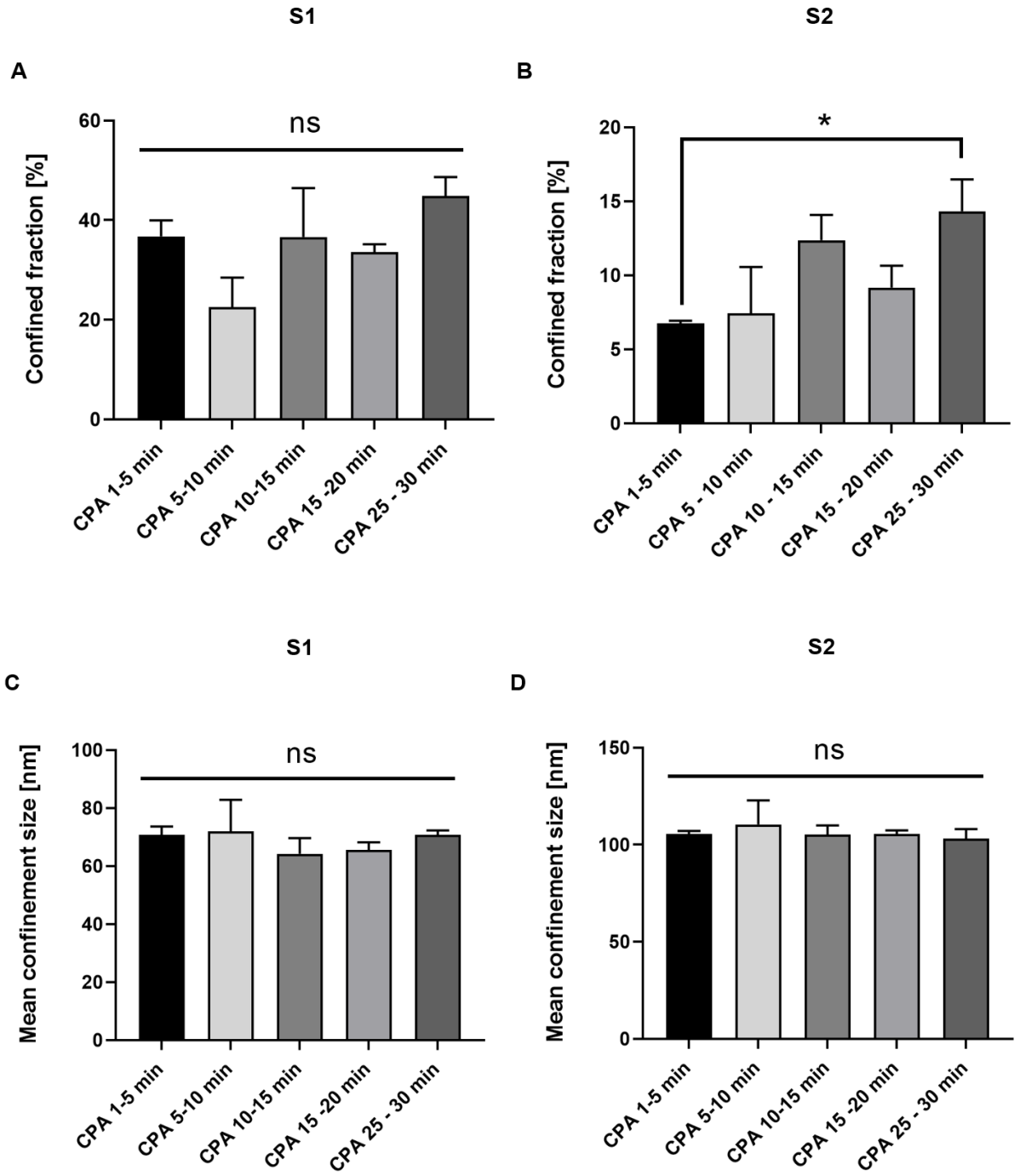

Figure 37. Time-dependent confinement of HiBiT-A_1AR after CPA treatment. Confined fractions in percentages (A+B) and corresponding mean confinement sizes (C+D) in states S1 and S2 on membrane of HEK-GloSensor™-HiBiT-A_1AR cells after CPA treatment. Cells were treated with 1 µM CPA and SPT measurements were performed 1 to 30 minutes afterwards. At least three independent experiments were performed. Values are given in mean ± SEM. Values with $p \leq 0.05$ were considered statistically significant.

4.5.5.4 Impact of time-dependent A_1AR stimulation on homodimerization

The proportion of monomers compared to homodimers was approximately 1:5. Oligomerization states did not change significantly over time after CPA treatment (Figure 38A and B). There is a tendency of an increasing number of homodimers over time and a decreasing number of monomers over time (Figure 38B). The difference from time interval 2 to time interval 3 scratched the significance (p = 0.0804 monomers and p = 0.0785 homodimers).

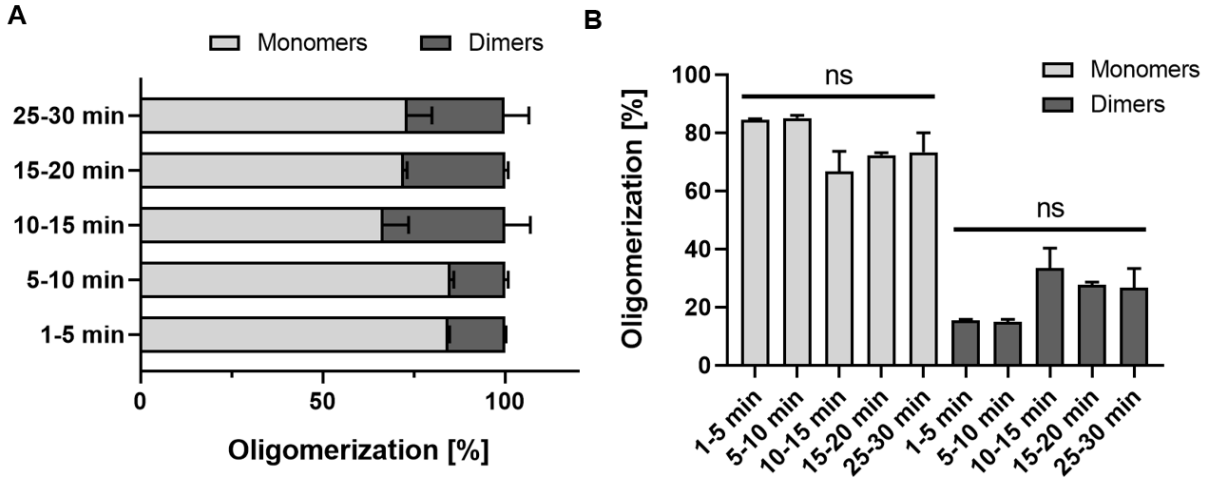

Figure 38. Fractions of monomers and homodimers of HiBiT-A_1AR on HEK 293 cells after CPA treatment. Cells were treated with 1 µM CPA directly before measurement including a time interval of 1 to 30 minutes. Fluorescence intensities were fitted by a mixed Gaussian model and plotted as percentages. Values were not significantly different from each other and given in mean ± SEM. At least three independent experiments were performed.

The results showed that time-dependent investigation of lateral mobility does make sense after A_1AR stimulation. Especially the investigation of receptor state occupancy and confinement showed that longer incubation times resulted in significant changes. Inspecting only one time point (endpoint) sometimes comes with the disadvantage of missing important information about certain receptor characteristics including diffusion and signal transduction.

4.6 HPLC fingerprint of Ze 911

Valerian extract Ze 911 was analysed and characterized using HPLC (method described in Table 11) to identify main components and corresponding peaks. This was achieved by comparing retention times and UV absorption spectra using reference substances. Valerenic acid (t = 72.2 min), Acetoxyvalerenic acid (t = 62.9 min), (+)-Pinoresinol (t = 44.5 min), Pinoresinol diglucoside (t = 26.0 min) and (-)-Olivil (t = 27.7 min) were successfully identified (Figure 39).

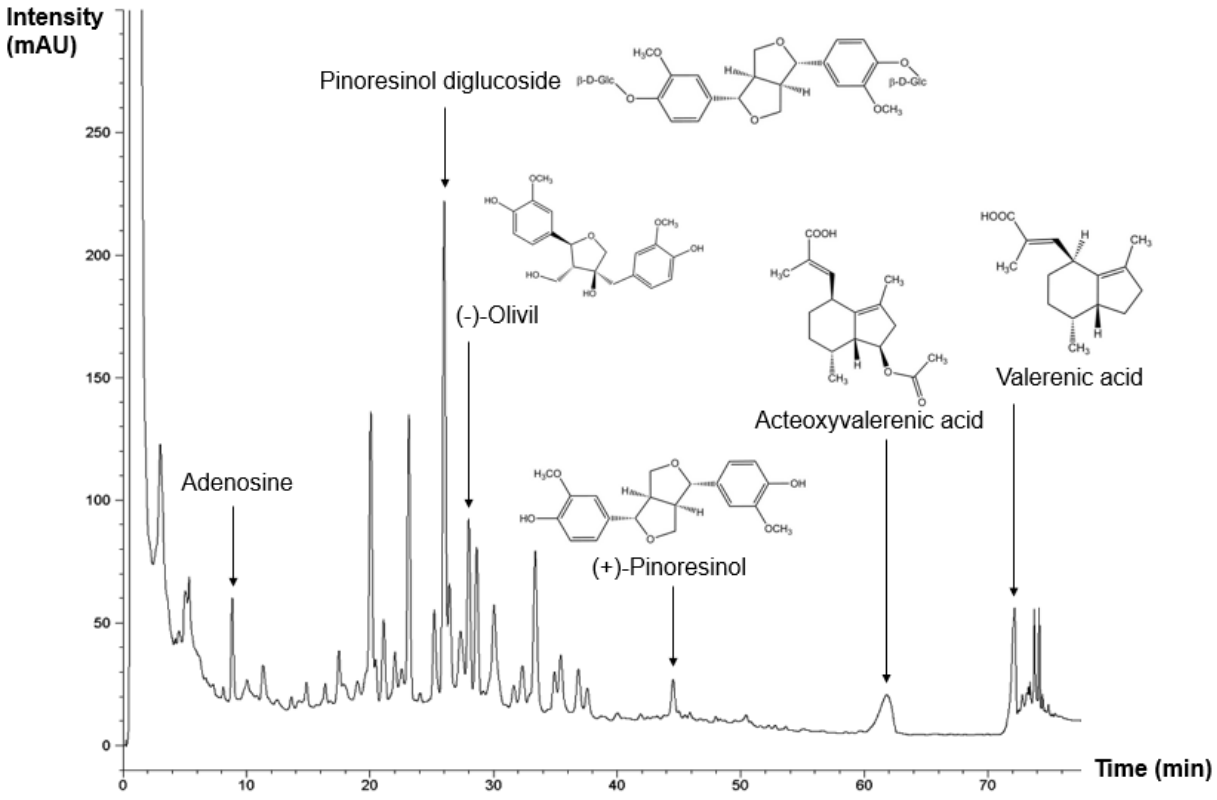

Figure 39. HPLC Chromatogram of Ze 911. Ze 911 was dissolved in DMSO and diluted in water to a concentration of 5 mg/ml. 40 µl solution was injected into the system. Reference substances were dissolved in DMSO and diluted in water. They were injected using a concentration of 0.1 mg/ml. Characteristic peaks occurred at corresponding retention times (min).

4.6.1 Adenosine detected in Ze 911

To confirm the content of adenosine in Ze 911, HPLC analysis of Ze 911 and Ze 911 treated with ADA were performed and compared. Adenosine was injected as reference substance and identified by retention time and corresponding UV absorption spectrum. Figure 40A shows the chromatogram of adenosine with a retention time at t = 8.9 min. This specific peak also appeared in the chromatogram of Ze 911 (Figure 40B) whereas it was missing in the chromatogram of Ze 911-ADA (Figure 40C). This experiment confirmed the results from the β-arrestin 2 assay and ensured the presence of adenosine in Ze 911.

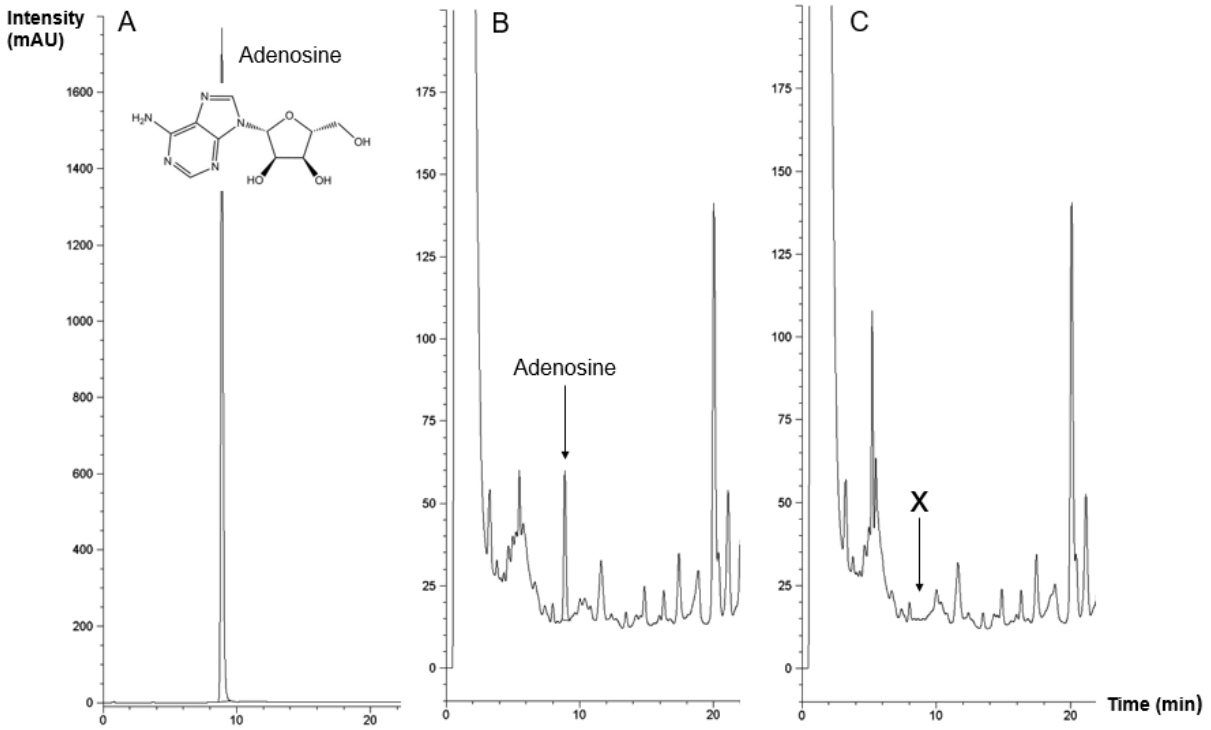

Figure 40. Adenosine peak detected in Ze 911. Ze 911 (B), Ze 911-ADA (C) and adenosine as reference substance (A) have been injected into HPLC system. The two extracts were diluted in water to a concentration of 5 mg/ml. Adenosine was diluted in water to a concentration of 1 mM. The injection volume of the two extracts was 40 µl and for adenosine 18.7 µl (equals 5 µg). Characteristic adenosine peaks have appeared at corresponding retention time (8.9 min) except for Ze 911-ADA.

5 Discussion

Valeriana officinalis has a long tradition as mild sleep-inducing agent. One of the characteristics of a medicinal plant extract is the complexity of its ingredients and therefore possible targets and effects. Finding and defining the substances of interest is difficult and tedious. Another challenge might be the growing conditions such as location and weather. It is desirable that these conditions are consistent to ensure unchanged composition of active substances in the resulting extract. It is known that valerian extract is binding to and interacting with adenosine A1 receptors (A_1AR). In 2002, Müller et al.[16] showed that valerian extract acts as partial A_1AR agonist. Moreover, it has been shown that the hydrophilic polar extracts might be preferential over non-polar extracts[14]. Isovaltrate, a lipophilic component of valerian extract, acted as inverse agonist that might counteract the sleep-inducing effect[14]. Schumacher et al. 2002[15] identified an olivil derivate (4'-O-β-d-glucosyl-9-O-(6''-deoxysaccharosyl)olivil) that interacts with A_1AR as partial agonist. Controversially, the study group Sendker et al. 2020[70] investigated several valerian extracts for the above mentioned olivil derivate with no success. All investigated batches seem to lack this particular olivil derivate. These findings from the last two decades left us with the motivation to find new answers concerning active substances in valerian extract including their effect to improve the current data situation. The agonistic effect of valerian extract on A_1AR has been shown by measurement of second messenger cAMP[16]. To our knowledge no data of valerian extract Ze 911 potentially influencing A_1AR β-arrestin dependent has been published so far.

HEK 293 cells genuinely express adenosine A_1, A_{2A} and A_{2B} receptor[97]. While A_1AR inhibits adenylate cyclase and consequently cAMP accumulation, A_{2A}AR and A_{2B}AR stimulate adenylate cyclase and therefore increase cAMP accumulation. To verify if HEK 293 cells respond to A_1AR ligands like Ze 911, dynamic mass redistribution studies were conducted. Even though, as a label-free technique, DMR is often considered a "black box", the measurements were quite promising for the concerns of this study. Stimulation with NECA, CPA and CGS 21680 resulted in positive wavelength shifts of different magnitudes. The wavelength shift of NECA was clearly higher compared to the other two specific agonists. This was expectable since NECA stimulates all adenosine receptors expressed on HEK 293 cells. The dose-dependent positive wavelength shifts of CPA and subsequently Ze 911 provided valid information about A_1AR agonism. It was noticeable that the graphs with corresponding respond curves of CPA and Ze 911 differed from each other. A steep peak right after treatment was observed for cells stimulated with Ze 911 unlike CPA. This phenomenon was possibly driven by the higher amount of DMSO in the sample solutions of Ze 911. This finding demonstrated the importance of applying a correct solvent in every experiment. Navarro et al. 2020[98] showed a positive

wavelength shift for A_{2A}AR agonism using DMR. The strongest wavelength shift was generated by A_{2A}AR agonist PSB-0777 whereas it was moderate for adenosine and NECA. The difference in wavelength shift produced by NECA might be explainable by cells used. Navarro et al. 2020[98] worked with A_{2A}AR overexpressing HEK 293 cells while non-transfected HEK 293 cells were tested in this study.

After proving the presence and activity of A_1AR on HEK 293 cells, a tool that worked A_1AR-specific was developed. The goal was to generate data that provides information about A_1AR-mediated β-arrestin 2 recruitment. Besides receptor internalization and desensitization, these adaptor proteins are known to play a role in GPCR signalling[54,55]. In fact, it has been shown that signalling provoked by β-arrestins is very diverse[99]. There is evidence that β-arrestins are involved in orexin signalling which is important for the regulation of the sleep-wake cycle[100]. It has been shown that β-arrestins are recruited after activation of orexin receptors (OX_1R and OX_2R)[63]. However, the data situation is limited and the exact purpose of β-arrestins in sleep regulation still eludes us. Nevertheless, these findings demonstrate the importance of signal transduction triggered by β-arrestin recruitment.

To study the interaction between A_1AR activation and corresponding β-arrestin 2 recruitment a NanoBiT® assay was developed. An EC_{50} value of 780 nM for the natural nonspecific AR agonist adenosine was determined for β-arrestin 2 recruitment. Since A_1AR couples to G_i proteins and therefore inhibits adenylate cyclase, other study groups usually investigated IC_{50} values instead of EC_{50} values. For example, Fredholm et al. 2001[101] determined an IC_{50} value of 310 nM for adenosine by measuring changes in cAMP formation in A_1AR-overexpressing CHO cells. The assays are only partially comparable since different cells and different readouts were addressed. Whereas Fredholm et al.[101] measured G protein dependent inhibition of adenylate cyclase recruitment of β-arrestin 2 was measured in this study. Additionally, endogenously produced adenosine or inosine must be considered that may vary using different cell lines, culture conditions and assays methodologies. However, since both values were determined in a similar medium to large nanomolar range, they are generally comparable. Afterwards, the specific A_1AR agonist CPA was tested and an EC_{50} value of 130 nM was determined for β-arrestin 2 recruitment. Müller et al. 2002[16] determined an IC_{50} value of 24 nM for inhibition of cAMP production by CPA. Different conditions using different assays must be considered again. Müller et al. 2002[16] measured inhibition of cAMP accumulation on isolated membranes of A_1AR overexpressing CHO cells treated with adenosine deaminase (ADA) while measurements in this study were performed in living A_1AR NanoBiT®-βarr2 HEK cells. For comparison reasons, a cAMP assay in living HEK GloSensor™ cells was performed additionally in this work. In this assay, an IC_{50} value of 16 nM was determined for CPA, which perfectly fitted to

the above-mentioned results from Müller et. al 2002[16]. It was noticeable, that the difference between β-arrestin 2 recruitment and cAMP inhibition were true for CPA as well as adenosine. The determined EC_{50} value of 121 nM for the non-specific agonist NECA was comparable to the one of CPA in the β-arrestin 2 recruitment assay (130 nM). Cordeaux et al. 2000[102] determined an IC_{50} value of 115 nM for NECA in CHO cells by measuring inhibition of cAMP accumulation, which is comparable to result determined in this study. Assay specificity was proven by A_1AR antagonist DPCPX. CPA-mediated recruitment was dose-dependently reversed by DPCPX with an IC_{50} value of 105 nM. Calzetta et al. 2011[103] also conducted a study to investigate the suppression of the effect of CPA by DPCPX in isolated human bronchial tissue. A concentration of 100 nM DPCPX totally reversed the CPA-mediated response. In this study, the response of CPA is completely abolished at a concentration of 1 µM DPCPX. This difference is explainable by a different experimental procedure including different test conditions. Calzetta et al. 2011[103] worked with bronchial tissue samples from patients while HEK 293 cells were investigated in this study.

The understanding of β-arrestins and their role in several signalling pathways of GPCRs has become a focus of scientific research not only in the progression of diseases but also in drug safety characteristics. Favouring either one or several transduction pathways can improve the safety and efficacy of a drug and is also known as biased signalling. This phenomenon was extensively studied for β-adrenergic receptor blocker carvedilol that acts β-arrestin biased[104,105]. Several study groups also showed a positive effect of ligand bias concerning safety for A_1AR[57,106]. Wall et al. 2022[107] discovered an A_1AR-selective agonist named benzyloxy-cyclopentyladenosine (BnOCPA) that acts analgesic but does not cause hypotension, bradycardia or respiratory depression. Capadenoson, a non-nucleoside A_1AR selective biased agonist with improved safety profile[108], was tested in this present study. To our knowledge, there is no data published for β-arrestin 2 recruitment mediated by capadenoson-activated A_1AR. Robust partial agonism was determined in the NanoBiT® assay for capadenoson whereas full agonism was detected for adenylate cyclase inhibition in the cAMP assay. Adenylate cyclase inhibition by capadenoson is comparable to full agonist CPA. Baltos et al. 2016[57] showed that capadenoson resulted in slightly higher cAMP inhibition and reduction of ERK1/2 and Akt phosphorylation compared to NECA. This fits the generated data in the adenylate cyclase inhibition assay conducted in this study. Since A_1AR-mediated ERK1/2 phosphorylation is partly dependent on β-arrestin, the effect found by Baltos et al. 2016[57] could be explained by capadenoson-reduced recruitment of β-arrestin 2 presented in this work.

It has been shown that β-arrestin 2 recruitment was approximately twice as high for CPA and NECA compared to capadenoson considering calculated AUCs. Calculation of AUCs includes

receptor activation, deactivation and internalization. To investigate the efficacy of agonists it can be useful to measure and characterize the activation phase of the receptor only. Therefore, so-called initial rates that represent activation kinetics before counter-regulations take place have been determined for the different agonists with the help of plug-in equations by Hoare et al. 2020[81,82]. The initial rate of CPA (10.3 ± 0.3-fold change/min) was 5 times higher compared to the one of capadenoson (2.5 ± 0.1-fold change/min). The difference in initial rates is therefore even more prominent than the difference of the calculated AUCs that include counter-regulations of the receptor. Consequently, the calculation of initial rates might be the more sensitive method for the comparison of different agonists in the β-arrestin 2 recruitment assay.

After testing and validating the system with agonists and antagonists, guaranteeing high specificity for A_1AR, Ze 911 was tested. It has been already shown that valerian extract has an agonistic activity at A_1AR[14–16]. The data available focused on the influence of valerian extract or its single components on cAMP accumulation or receptor binding. Data for A_1AR-mediated β-arrestin 2 recruitment after treatment with valerian extract has not been published by now to our best knowledge. Müller et al. 2002[16] determined an IC_{50} value measuring cAMP accumulation of 900 µg/ml for valerian extract VE-1 (Ze 911), whereas it was 35 µg/ml in the GloSensor® cAMP assay used in this study. They investigated membrane preparations from overexpressing CHO cells while the assay used in this work was performed in living A_1AR-overexpressing HEK cells expressing a cAMP biosensor. Even though the IC_{50} values vary, both study groups showed individually the agonistic effect of valerian extract on A_1AR. Interestingly, the determined EC_{50} value of Ze 911 in the β-arrestin 2 recruitment assay (66 µg/ml) was only twice as high compared to inhibition of cAMP accumulation. CPA for instance, had a significantly higher difference comparing both assays, in fact approximately 5 times. It can be speculated that Ze 911 has a slight bias towards the recruitment of β-arrestins compared to CPA.

After the detection of the strong agonistic effect of Ze 911, a HPLC fingerprint analysis of the extract was essential. Since adenosine appears in a variety of species, it was a not surprising to find it in Ze 911. This outcome was a perfect explanation for the solid agonistic effect for both, β-arrestin 2 recruitment and inhibition of cAMP accumulation. To our knowledge it has not been described that valerian extract contains adenosine. This also explains the adenosine-like action of valerian described by Brattström et al. 2007[109]. Pretreating Ze 911 with adenosine deaminase completely abolished the response in β-arrestin 2 recruitment assay. Since adenosine has poor bioavailability[110] and is therefore not the most promising drug candidate, it was fundamental to find other possible effects of Ze 911 on adenosine A1 receptor. Besides agonistic effects it became obvious to investigate the extract for potential modulatory effects. The

industry partner of this work, Zeller Söhne AG, prepared an adenosine-free extract and discovered a potent fraction that mainly contained one substance class: dicaffeoylquinic acids (DQAs). The core facility Analytical Proteomics of the IBMB kindly analysed Ze 911 for the presence of DQAs (1,5-DQA, 3,4-DQA, 3,5-DQA and 4,5-DQA) in Ze 911 using liquid chromatography tandem-mass spectrometry (LC-MS/MS). Masses (m+1) and corresponding fragment ions were identified (see supplemental material and data 8.2.). DQAs are interesting concerning the regulation of the sleep-wake cycle since they can pass the blood brain barrier[92]. Additionally, it has been shown that DQAs improved sleep quality as part of beverages in a clinical randomized, double-blind, placebo-controlled crossover study[93]. The four identified DQAs in Ze 911 were tested in the established β-arrestin 2 recruitment assay. The combination of adenosine and 3,4-DQA or 4,5-DQA resulted in significantly higher recruitment compared to adenosine single treatment. For 1,5-, and 3,5-DQA no such effect was determined. A possible explanation for this result could be the steric hindrance since the stereochemistry of 1,5-DQA und 3,5-DQA differs from the other two DQAs. Single treatment with DQAs did not result in β-arrestin 2 recruitment. To investigate these modulatory properties in more detail, different concentrations of 3,4-DQA as well as adenosine have been tested. A dose-dependent modulatory effect of 3,4-DQA has been detected. Additionally, cells treated with low concentrations of adenosine in combination with 3,4-DQA showed a solid modulation by 3,4-DQA whereas cells treated with high concentrations of adenosine were not modulated by 3,4-DQA. This was expected since high concentrations are dominated by agonistic effect of adenosine itself. Interestingly, 3,4-DQA did not influence the activation phase of the recruitment - it rather prolonged the effect after activation and therefore prevented the receptor from deactivation. This modulatory effect of DQAs was not detectable for inhibition of cAMP accumulation. The inhibition caused by adenosine single treatment was similar for the combination of adenosine and 3,4-DQA. It was also not possible to detect a modulating effect using the synthetic positive allosteric A_1AR modulator VCP 171 in the cAMP assay, whereas it worked well for β-arrestin 2 recruitment. This is remarkable, since these results show that the established β-arrestin 2 assay can be quickly adapted from measuring agonistic to modulatory properties. The agonistic effect of NECA was increased by 25 % using VCP 171 which fits the literature data[111].

The NanoBiT® system for the investigation of β-arrestin 2 recruitment has been used for other adenosine receptors[112]. However, for A_1AR only internalization was determined using this technology[113], interactions with β-arrestins have not been investigated. In the field of biased agonism, A_1AR was analysed by downstream signalling pathways like ERK1/2 instead of the interaction between the receptor and β-arrestins directly[57,106]. The signal-to-noise ratio of the developed β-arrestin 2 assay is very high. Increases of the signal by a factor of 10 can easily be determined by the essay. This is a great tool for the establishment of recruitment assays

measuring physiological expression levels in future experiments. White et al. 2019[114] already showed, that the implementation of a Nanoluciferase (NanoLuc) into a cell at a genomic level is possible using CRISPR/Cas9. This is a great advantage, since they were able to achieve successful results under endogenous promotion of NanoLuc-A_{2B}AR.

As mentioned above, the literature data of adenylate cyclase inhibition was confirmed for CPA and Ze 911. The established cAMP assay used the expression of a cAMP biosensor plasmid (pGloSensor™-22 cAMP). Additionally, cells were overexpressing A_1AR to level out the signal of the other endogenous expressed adenosine receptors. Activity of adenylate cyclase was inhibited dose-dependently by CPA and Ze 911. However, measurement of modulatory activity was not possible, neither for VCP 171 nor for 3,4-DQA. A problem could have been the number of different substances used in the assay. Measuring a G_i effect is dependent on a stimulating substance in the first place (forskolin and isoprenaline in this case). Additionally, adding an agonist and a modulating substance might exceed the possibilities of the assay system. Several study groups also used this cAMP assay to investigate GPCRs with agonistic and antagonistic substances[115,116]. Goulding et al. 2018[117] described a potential allosteric modulatory effect of the A_{2B}AR-selective antagonist PSB 603 detected in the cAMP GloSensor™ assay. Comparing two antagonists, ZM 241385 (A_{2A}AR antagonist) was able to completely inhibit agonist effect of NECA, while PSB 603 (A_{2B}AR antagonist) only partially inhibited agonistic effect of NECA, suggesting that this mechanism could be explained by a negatively cooperative effect on the biding affinity of agonists at the orthosteric site. However, Goulding et al. 2018[118] only suspected that the effect they measured might be modulatory, there is no prove since they did not use a modulating agent for comparison or confirmation respectively. In addition, measuring this inhibiting effect of an A_{2A}AR / A_{2B}AR-mediated G_s response might be less prone to errors compared to a G_i response measuring inhibitory signals. It is not surprising that 3,4-DQA treatment did not result in measurable modulating properties since it could be biased towards β-arrestin signalling. VCP 171 however, was suspected to produce a modulatory effect, also on cAMP level.

To get a holistic picture of Ze 911-mediated effects on A_1AR, calcium mobilization was investigated after treatment. It is known that G_i-coupled receptors, including A_1AR, evoke calcium mobilization[118]. The connection between sleep and calcium signalling was extensively studied by several study groups[94,119]. Sleep deprivation in mice resulted in diminished calcium signalling and consequently insufficient Ca^{2+} supply[119]. Significant reduction of intracellular calcium mobilization has been shown after 48 h sleep deprivation in splenocytes[120]. Additionally, it has been shown that activation of A_1AR stimulates calcium release from intracellular stores[120]. One of the main components found in Valeriana officinalis named pinoresinol diglucoside induced

calcium mobilization by activation of lysophosphatidic acid receptors[121]. The results generated in this study showed that CPA as well as Ze 911 rather modulate calcium mobilization. Single treatment with Ze 911 or CPA did not result in significant calcium mobilization whereas it was clearly detected by positive control methacholine. However, the effect of methacholine was modulated by CPA and Ze 911. The combination of both substances resulted in increased calcium mobilization compared to methacholine single treatment. Interestingly, the positive modulatory effect on methacholine was significant for Ze 911 whereas it was detectable but not significant for CPA. This indicates that Ze 911 might contain other substances that influence calcium mobilization via AR independent pathways. This finding was strengthened by the results generated by Ze 911 pretreated with adenosine deaminase (Ze 911-ADA). The combination also increased the calcium signal mediated by methacholine significantly compared to methacholine single treatment. DPCXP was able to inhibit this increase slightly but not significant, indicating that A_1AR plays a role but is not the only operator explaining this modulatory effect. Interestingly, 3,4-DQA resulted not in increased calcium concentration in the beginning but prolonged the mobilization phase itself showing a slightly different kinetic than other test substances. This effect was investigated in more detail inspecting every time point individually. Significant increases of methacholine-mediated calcium mobilization have been detected in the time slot between 60 s and 105 s after treatment. This phenomenon of not influencing the beginning of the mobilization but prolonging the effect was also detected in the β-arrestin assay. It can be speculated that DQAs might prevent the receptor from deactivation or internalization. Unlike the results in this work, Ethier and Madison 2006[122] showed mobilization of calcium by CPA on human bronchial muscle cells. Since different cells and experimental setup have been used, results are only partly comparable. However, it would be worth studying the effect of CPA modulating methacholine in more detail. Mobilization of calcium in SH-SY5Y cells by muscarinic receptors has been described before[123].

Single-particle tracking (SPT) has been frequently used to investigate lateral mobility of GPCRs[124–126]. Protein-protein interactions that take place at the plasma membrane are highly dependent and influenced by lateral mobility of several components in the membrane[127]. SPT is a powerful technique to analyse and quantify for example diffusion properties of receptors. The membrane is divided by a network of actin filaments in accordance with the “membrane skeleton fence model”. The network of actin filaments belongs to the cytoskeleton of the cell and is located close to plasma membrane[128]. Additionally, numerous transmembrane proteins are anchored to actin-based membrane skeleton network. They act as rows of pickets that briefly appear as diffusion barriers in the membrane[129]. Moreover, microdomains are found in the bilayer of the membrane which also act as semi-permeable diffusion barriers. Microdomains are rich in cholesterol and defined by a high membrane rigidity and density of signal

proteins[130,131]. The lateral mobility of the receptor therefore depends on many different components. Signal proteins and receptors are not distributed equally but rather located in individual microdomains. Protein-protein interactions might be favoured in functional microdomains since protein clusters can be formed (hots pots)[132]. Sungkaworn et al. 2017[132] showed that diffusion barriers that resulted at least partly out of actin filaments and clathrin-coated pits favoured the formation of hot spots. These hot spots contained GPCRs as well as G proteins resulting in increased signal transduction. Receptors in microdomains either diffuse or leave it by so-called "hop diffusion". Suzuki et al. 2005[133] nicely described hop diffusion for μ-opiod receptor. In general, different states of the receptors are found inside as well as outside of microdomains that are defined by specific diffusion behaviours. SPT experiments were conducted to investigate lateral mobility of A_1AR after stimulation with CPA or Ze 911. Therefore, HEK-GloSensor™-HiBiT-A_1AR cells were investigated using HaloTag®-self-labelling protein technology. The red fluorescent dye Janelia Fluor® HaloTag® Ligand 646 was used for imaging. The usability of this technique for single-particle tracking has been demonstrated for GPCRs by Franken et al. 2020[84]. Even though HaloTag® labelling is not frequently used in SPT experiments, it has a wide range of applications[134]. Lillo et al. 2020[135] for example used HaloTag® to investigate the influence of A_3AR on A_{2A}AR in competition experiments.

Based on localized fluorescence, signals were analysed using "u-track" in MATLAB to identify trajectories. The vbSPT algorithm divided trajectories into segments according to their momentary diffusion speed as described by Persson et al. 2013[86]. These segments were divided accordingly and diffusion coefficients as well as corresponding occupancies were determined. Compared to other approaches in single-molecule tracking like the hidden Markov model, vbSPT analysis has the advantage of being able to process information from data sets with short trajectories. This is crucial for experiments with fluorescent dyes, because they tend to bleach out due to laser irritation. This results statistically in a higher proportion of short trajectories. The data generated in this study by vbSPT analysis created segments that were further classified into the three diffusion states S1, S2 and S3. The states were differentiated into an immobile state (S1), a rather slow diffusion sate (S2) and a fast diffusion sate (S3). Every state had a specific diffusion coefficient and corresponding state occupancy value.

A_1AR-overexpressing HEK 293 cells were treated with either CPA or Ze 911 and SPT measurement was started after an incubation time of 15 minutes. Diffusion coefficients of agonist-treated cells were comparable to PBS-treated control cells in all three diffusion states. The number of particles also remained the same for all investigated conditions in the certain states S1, S2 and S3. Aatz et al. 2022[136] also detected three diffusion states for 5-HT_{2A} receptor on SH-SY5Y cells using a similar SPT model. Stimulation of cells resulted in increase of receptors

in immobile state S1 and decrease in fast-diffusing state S3. Unlike in this study, they pre-incubated SH-SY5Y cells with St. John's wort extract (STW3-VI) six days prior measurement. Therefore, experiments are only partly comparable. However, changes in diffusion coefficients or number of particles after agonist treatment have been suspected in this work as well since downstream signalling processes for example result in altered diffusion properties. Sungkaworn et al. 2017[132] observed an increased fraction of α2a-adrenergic receptors in immobile state S1 and slow diffusive state S2 during interaction with $G_{\alpha i}$ subunits. The "lack of change" after treatment in this work could be explained by the incubation time of 15 minutes before the measurement was started. Results of other assays in this study have shown that time does play an important role in the response kinetic. While calcium mobilization took place in the very first seconds to minutes after treatment, the peak of β-arrestin 2 recruitment was measured approximately 5-10 minutes after treatment.

Spatial confinement was determined for every diffusion state S1, S2 and S3. However, number of track segments in S3 were too little to be included in statistical analysis, robust statistical analyses of spatial confinement was therefore only possible for receptors in S1 and S2. Even though a tendency of increasing confined fractions after CPA and Ze 911 treatment was detected (Figure 33B), the effect was not significantly different from the control condition. Mean confinement sizes after treatment were comparable to control in S1 and S2. Investigation of β_1-adrenergic receptor (β_1AR) in C6 cells also showed spatial confinement in state S1 and S2 whereas it was not detectable in S3[137]. The confined fractions of β_1AR in the two states were higher in the study of Bussmann 2021[137] whereas corresponding confinement sizes were in a similar range. Besides testing different cells, they incubated the cells over a period of five days with St. John's wort extract (Ze 117) before SPT measurement was started. Longer incubation times may have a different impact on the plasma membrane and therefore diffusion properties. Schwenzer et al. 2018[138] detected an increase in spatial confinement on β_2-adrenergic receptor overexpressing HEK 293 cells (HEK-β_2AR) in state S2 and S3 with consistent confinement sizes. However, the results are only partly comparable to this study since a different receptor was investigated. Unlike A_1AR, β_2AR is G_s-coupled leading to different signal transduction pathways.

Homooligomers were identified by fluorescence intensity distributions and curve fitting with a mixed Gaussian model. The analysis resulted in two fractions identified as monomers and homodimers. Homotrimers or higher order oligomers were not identified. The distribution of monomers and homodimers of A_1AR after CPA or Ze 911 treatment differed slightly from control cells. The number of homodimers increased after treatment; the values scratched the significance (Figure 34). Li et al. 2019[139] also showed the occurrence of A_1AR homodimers that

could be activated by agonists like NECA or adenosine. It has been shown that the agonist affinity can be increased if A_1AR homodimers are present[140]. In fact, Gracia et al. 2013[140] detected that low concentrations of A_1AR antagonist caffeine increased agonist-induced signalling in a homodimer while high concentrations of caffeine inhibit signalling as expected. Canals et al. 2004[141] investigated A_{2A}AR homodimers on HEK 293 cells and found out that more than 90 % of the receptors are in dimeric state at the cell surface. Unlike in this study, they investigated dimer occurrences using bioluminescence resonance energy transfer / fluorescence resonance energy transfer. The distribution difference of monomers and homodimers between A_1AR and A_{2A}AR on the surface could be explained by the receptor type itself. A_1AR binds to inhibitory G proteins, while A_{2A}AR binds to stimulatory G proteins that might has an impact on homodimer formation. The investigation of (homo)dimerization and (homo)oligomerization states of receptors including consequences for downstream signalling processes is therefore an important factor.

The first SPT experiments revealed small differences between control cells and A_1AR-stimulated cells. However, none of the investigated parameters including diffusion coefficients, receptor state occupancy, spatial confinement and homodimerization of A_1AR turned out to be significantly different from control cells. The other conducted assays in this study showed that the first few minutes after treatment were informative because significant differences have been detected in that period of time. In the β-arrestin 2 recruitment assay for example, a very steep activation phase right after treatment has been observed. After the peak was reached at approximately 5-10 min after treatment, the curve descended evenly in approximately 30 minutes. Hence, a time-dependent approach was developed including five time intervals (1 to 30 minutes after treatment, see Table 10). It is not recommended to measure one coverslip longer than 30 minutes because of photo bleaching. The time-dependent experiment was carried out with the well-described A_1AR agonist CPA.

Diffusion coefficients did not change over time after CPA treatment, they remained the same for all three investigated A_1AR states (Figure 35). An increasing number of receptors in state S1 has been observed between time interval one (1-5 min after treatment) and two (5-10 min after treatment), even though it was not significant. At the same time, a decrease in number of receptors has been detected in S3. An increase of receptors in S1 implies a potential regulatory response of the cell. However, the only significant increase of number of receptors has been detected in fast diffusion state S3. The number of receptors in S3 increased significantly from 18.261 ± 1.492 % (time interval two, 5-10 min after treatment) to 30.016 ± 1.355 % (time interval four, 20-25 min after treatment) while they decreased in state S1 for the same time intervals. This suggests that receptor state distributions, that regulate receptor interactions, mainly

took place in the first ten minutes. As already described above, other study groups detected an increase of receptors in slow diffusion state S1 after agonist treatment[132,136]. They, however, only inspected one time point (endpoint) after treatment and not a time interval. Additionally, incubation times were tremendously longer compared to this study.

Spatial confinement was determined for every diffusion state and time interval after treatment. Confined fractions and corresponding confinement sizes were detectable in S1 and S2. A tendency of increasing confided fractions in S1 and S2 over time has been observed after treatment (Figure 37 A+B). One significant increase has been detected in slow-diffusive state S2 between time intervals one (1-5 min after treatment) and five (25-30 min after treatment) (Figure 37B). For confinement analysis, it is therefore preferable to choose longer incubation times before starting the measurement. Especially for plant extracts, incubation times are often much longer. Bussmann et al.[137] or Aatz et al.[136] for example incubated St. John's wort extract for several days. Therefore, it would be interesting, to investigate lateral mobility of A_1AR after a longer incubation time with Ze 911. However, St. John's wort extract is used for the treatment of depression, and it is known that the full effect occurs after a few weeks of medication[142,143]. Therefore, longer incubation times before inspecting lateral mobility of the receptor was a logical approach. Since valerian extract is used for mild sleep disorders, it is desirable to have a rather fast effect, consequently shorter incubation times were selected in this work. It is safe to say that these findings demonstrated the great advantage of time-dependent investigations and consequently the effect of different incubation times of an agonist. Future experiments should address the investigation of time-dependent lateral mobility after treatment with Ze 911 and the A_1AR-modulating DQAs.

The inspection of monomer and homodimer formation of A_1AR in the five different time-intervals after treatment showed that there is a strong tendency of increasing homodimer formation for the last three time intervals compared to the first two time intervals (Figure 38). Effects on homodimerization after agonist treatment have been shown for several different receptors including fibroblast growth factor receptor 1 (FGFR1)[144], human purinergic G protein-coupled receptor P2Y1[145] and α-adrenergic receptors[146] for example. In the last decades, there has been a debate whether GPCRs occur most frequently in monomers, homodimers, heterodimers or even oligomers and if those formations play a role in signalling cascades. Time-dependent formations after treatment have not been studied extensively yet, this might be addressed in future experiments. Especially for sleep-inducing agents like valerian extract, these results are promising since "time" does play a superior role in the process of falling asleep. A sleep-inducing drug, no matter if herbal or chemical, should unfold its effects shortly after intake.

6 Conclusion and Outlook

Even though human beings must sleep, the complex mechanisms behind it still eludes us. Sleeping disorders can be treated with herbal medicinal products like valerian extract preparations. Even though, several clinical studies have proven the effect of valerian extract, the mechanism of action is still not fully understood and therefore definitely worth inspecting in more detail. Valerian preparations are used frequently since decades for mild sleep disorders. Nevertheless, the extract is not recommended in the medical guidelines for the treatment of sleep disorders. This underlines that the current data situation needs to be improved. Identification of the substances responsible for the sleep-inducing effects and involved signalling pathways come with great benefits. Valid data that is available for physicians, pharmacists and patients creates safety and confidence in prescribing and recommending herbal products that contain valerian extract for mild sleep disorders rather than chemical alternatives. Additionally, if potent components of the extracts are identified one can think about plant extracts that are enriched with those substances in the future.

This work has shown that there is still a lot of unknow potential concerning the identification of valerian extracts' effective substances including their mode of action. Detecting adenosine in the extract was a challenge for the investigated target and future experiments. Even though, adenosine is a ubiquitous molecule that plays a superior role in the sleep-wake cycle and is found in almost every part of the human body, it has a poor bioavailability which makes it a rather challenging drug candidate. However, this finding also opened new doors including the identification of A_1AR-modulating substances present in Ze 911 named dicaffeolquinic acids (DQAs). Especially determining that DQAs modulate the effect of adenosine-mediated β-arrestin 2 recruitment is promising since DQAs can pass the blood brain barrier. The hypothesis that DQAs positively modulate the effect of endogenous adenosine at A_1AR in the brain regions responsible for sleep would be a bright outlook. Besides recruitment of β-arrestin 2, Ze 911 and DQAs also modulated methacholine-mediated calcium mobilization. This was a very interesting finding and might be addressed in the future since this assay was not A_1AR specific and the results showed that there are more potential targets that could be investigated. Especially the fact that Ze 911 pretreated with adenosine deaminase modulated calcium mobilization revealed that there are other components than adenosine involved in this effect. The information gained from SPT experiments intensified the importance of time-dependent investigations rather than end point analysis. Especially because cell membranes are highly complex structures, and the diffusion properties of receptors can be modulated by the composition of the membrane and its environment. Therefore, it would be interesting to investigate time-dependent influence of valerian extract on diffusion properties of A_1AR since it already has been

shown that plant extracts like St. John's wort for example has an impact on lateral diffusion of receptors that are relevant for depression after a longer incubation time. In this work, no significant changes have been shown on receptor homooligomerization after treatment. However, a tendency of increased homodimer formation was detected after treatment. Focussing on the formation of homooligomers and heterooligomers of A_1AR in the context of sleep would be an interesting attempt for the future as well.

Safe approaches and therapies for sleep disorders remains an important topic for the society. Even though a tiny step towards unfolding the sleep-inducing effects of valerian extract has been made, there still is a lot of room for further investigations.

7 References

(1) Saper, C. B.; Cano, G.; Scammell, T. E. Homeostatic, circadian, and emotional regulation of sleep. *The Journal of comparative neurology* **2005**, *493* (1), 92–98. DOI: 10.1002/cne.20770.

(2) Carley, D. W.; Farabi, S. S. Physiology of Sleep. *Diabetes spectrum : a publication of the American Diabetes Association* **2016**, *29* (1), 5–9. DOI: 10.2337/diaspect.29.1.5.

(3) Brown, R. E.; Basheer, R.; McKenna, J. T.; Strecker, R. E.; McCarley, R. W. Control of sleep and wakefulness. *Physiological reviews* **2012**, *92* (3), 1087–1187. DOI: 10.1152/physrev.00032.2011.

(4) Saper, C. B.; Chou, T. C.; Scammell, T. E. The sleep switch: hypothalamic control of sleep and wakefulness. *Trends in neurosciences* **2001**, *24* (12), 726–731. DOI: 10.1016/s0166-2236(00)02002-6.

(5) Strecker, R. E.; Morairty, S.; Thakkar, M. M.; Porkka-Heiskanen, T.; Basheer, R.; Dauphin, L. J.; Rainnie, D. G.; Portas, C. M.; Greene, R. W.; McCarley, R. W. Adenosinergic modulation of basal forebrain and preoptic/anterior hypothalamic neuronal activity in the control of behavioral state. *Behavioural brain research* **2000**, *115* (2), 183–204. DOI: 10.1016/s0166-4328(00)00258-8.

(6) Berro, L. F.; Fidalgo, T. M.; Rowlett, J. K.; Tardelli, V. S. Editorial: Benzodiazepine addiction: from lab to street. *Frontiers in psychiatry* **2023**, *14*, 1287352. DOI: 10.3389/fpsyt.2023.1287352. Published Online: Sep. 22, 2023.

(7) Vallianatou, K. Benzodiazepines and hypnotics. *Medicine* **2024**, *52* (9), 592–595. DOI: 10.1016/j.mpmed.2024.06.005.

(8) Wang, S.-H.; Chen, W.-S.; Tang, S.-E.; Lin, H.-C.; Peng, C.-K.; Chu, H.-T.; Kao, C.-H. Benzodiazepines Associated With Acute Respiratory Failure in Patients With Obstructive Sleep Apnea. *Frontiers in pharmacology* **2018**, *9*, 1513. DOI: 10.3389/fphar.2018.01513. Published Online: Jan. 7, 2019.

(9) Gyllenhaal, C.; Merritt, S. L.; Peterson, S. D.; Block, K. I.; Gochenour, T. Efficacy and safety of herbal stimulants and sedatives in sleep disorders. *Sleep medicine reviews* **2000**, *4* (3), 229–251. DOI: 10.1053/smrv.1999.0093.

(10) Gupta, R.; Das, S.; Gujar, K.; Mishra, K. K.; Gaur, N.; Majid, A. Clinical Practice Guidelines for Sleep Disorders. *Indian journal of psychiatry* **2017**, *59* (Suppl 1), S116-S138. DOI: 10.4103/0019-5545.196978.

(11) Yuan, C.-S.; Mehendale, S.; Xiao, Y.; Aung, H. H.; Xie, J.-T.; Ang-Lee, M. K. The gamma-aminobutyric acidergic effects of valerian and valerenic acid on rat brainstem neuronal activity. *Anesthesia and analgesia* **2004**, *98* (2), 353–358. DOI: 10.1213/01.ANE.0000096189.70405.A5.

(12) Benke, D.; Barberis, A.; Kopp, S.; Altmann, K.-H.; Schubiger, M.; Vogt, K. E.; Rudolph, U.; Möhler, H. GABA A receptors as in vivo substrate for the anxiolytic action of valerenic acid, a major constituent of valerian root extracts. *Neuropharmacology* **2009**, *56* (1), 174–181. DOI: 10.1016/j.neuropharm.2008.06.013. Published Online: Jun. 17, 2008.

(13) Mulyawan, E.; Ahmad, M. R.; Islam, A. A.; Massi, M. N.; Hatta, M.; Arif, S. K. Analysis of GABRB3 Protein Level After Administration of Valerian Extract (Valeriana officinalis) in BALB/c mice. *Pharmacognosy Journal* **2020**, *12* (4), 821–827. DOI: 10.5530/pj.2020.12.118.

(14) Lacher, S. K.; Mayer, R.; Sichardt, K.; Nieber, K.; Müller, C. E. Interaction of valerian extracts of different polarity with adenosine receptors: identification of isovaltrate as an inverse agonist at A1 receptors. *Biochemical pharmacology* **2007**, *73* (2), 248–258. DOI: 10.1016/j.bcp.2006.09.029. Published Online: Oct. 6, 2006.

(15) Schumacher, B.; Scholle, S.; Hölzl, J.; Khudeir, N.; Hess, S.; Müller, C. E. Lignans isolated from valerian: identification and characterization of a new olivil derivative with partial agonistic activity at A(1) adenosine receptors. *Journal of natural products* **2002**, *65* (10), 1479–1485. DOI: 10.1021/np010464q.

(16) Müller, C. E.; Schumacher, B.; Brattström, A.; Abourashed, E. A.; Koetter, U. Interactions of valerian extracts and a fixed valerian-hop extract combination with adenosine receptors. *Life sciences* **2002**, *71* (16), 1939–1949. DOI: 10.1016/s0024-3205(02)01964-1.

(17) Saini, A.; Patel, R.; Gaba, S.; Singh, G.; Gupta, G. D.; Monga, V. Adenosine receptor antagonists: Recent advances and therapeutic perspective. *European journal of medicinal chemistry* **2022**, *227*, 113907. DOI: 10.1016/j.ejmech.2021.113907. Published Online: Oct. 13, 2021.

(18) Cunha, R. A. Adenosine as a neuromodulator and as a homeostatic regulator in the nervous system: different roles, different sources and different receptors. *Neurochemistry international* **2001**, *38* (2), 107–125. DOI: 10.1016/s0197-0186(00)00034-6.

(19) Layland, J.; Carrick, D.; Lee, M.; Oldroyd, K.; Berry, C. Adenosine: physiology, pharmacology, and clinical applications. *JACC. Cardiovascular interventions* **2014**, *7* (6), 581–591. DOI: 10.1016/j.jcin.2014.02.009. Published Online: May. 14, 2014.

(20) Sheth, S.; Brito, R.; Mukherjea, D.; Rybak, L. P.; Ramkumar, V. Adenosine receptors: expression, function and regulation. *International journal of molecular sciences* **2014**, *15* (2), 2024–2052. DOI: 10.3390/ijms15022024. Published Online: Jan. 28, 2014.

(21) Young, J. D.; Yao, S. Y. M.; Baldwin, J. M.; Cass, C. E.; Baldwin, S. A. The human concentrative and equilibrative nucleoside transporter families, SLC28 and SLC29. *Molecular aspects of medicine* **2013**, *34* (2-3), 529–547. DOI: 10.1016/j.mam.2012.05.007.

(22) Boison, D. Adenosine as a neuromodulator in neurological diseases. *Current opinion in pharmacology* **2008**, *8* (1), 2–7. DOI: 10.1016/j.coph.2007.09.002. Published Online: Oct. 17, 2007.

(23) Ranjan, R.; Dwivedi, H.; Baidya, M.; Kumar, M.; Shukla, A. K. Novel Structural Insights into GPCR-β-Arrestin Interaction and Signaling. *Trends in cell biology* **2017**, *27* (11), 851–862. DOI: 10.1016/j.tcb.2017.05.008. Published Online: Jun. 23, 2017.

(24) Gerwins, P.; Fredholm, B. B. ATP and its metabolite adenosine act synergistically to mobilize intracellular calcium via the formation of inositol 1,4,5-trisphosphate in a smooth muscle cell line. *The Journal of biological chemistry* **1992**, *267* (23), 16081–16087.

(25) Fredholm, B. B.; IJzerman, A. P.; Jacobson, K. A.; Klotz, K. N.; Linden, J. International Union of Pharmacology. XXV. Nomenclature and classification of adenosine receptors. *Pharmacological reviews* **2001**, *53* (4), 527–552.

(26) Gessi, S.; Merighi, S.; Varani, K.; Borea, P. A. Adenosine receptors in health and disease. *Advances in pharmacology (San Diego, Calif.)* **2011**, *61*, 41–75. DOI: 10.1016/B978-0-12-385526-8.00002-3.

(27) Fredholm, B. B.; IJzerman, A. P.; Jacobson, K. A.; Linden, J.; Müller, C. E. International Union of Basic and Clinical Pharmacology. LXXXI. Nomenclature and classification of adenosine receptors--an update. *Pharmacological reviews* **2011**, *63* (1), 1–34. DOI: 10.1124/pr.110.003285. Published Online: Feb. 8, 2011.

(28) Fastbom, J.; Pazos, A.; Probst, A.; Palacios, J. M. Adenosine A1-receptors in human brain: characterization and autoradiographic visualization. *Neuroscience letters* **1986**, *65* (2), 127–132. DOI: 10.1016/0304-3940(86)90291-0.

(29) Alexander, S. P.; Reddington, M. The cellular localization of adenosine receptors in rat neostriatum. *Neuroscience* **1989**, *28* (3), 645–651. DOI: 10.1016/0306-4522(89)90011-0.

(30) Gebicke-Haerter, P. J.; Christoffel, F.; Timmer, J.; Northoff, H.; Berger, M.; van Calker, D. Both adenosine A1- and A2-receptors are required to stimulate microglial proliferation. *Neurochemistry international* **1996**, *29* (1), 37–42.

(31) Borea, P. A.; Gessi, S.; Merighi, S.; Vincenzi, F.; Varani, K. Pharmacology of Adenosine Receptors: The State of the Art. *Physiological reviews* **2018**, *98* (3), 1591–1625. DOI: 10.1152/physrev.00049.2017.

(32) Pasquini, S.; Contri, C.; Merighi, S.; Gessi, S.; Borea, P. A.; Varani, K.; Vincenzi, F. Adenosine Receptors in Neuropsychiatric Disorders: Fine Regulators of Neurotransmission and Potential Therapeutic Targets. *International journal of molecular sciences* **2022**, *23* (3). DOI: 10.3390/ijms23031219. Published Online: Jan. 22, 2022.

(33) Zhong, L.; Peng, Q.; Zeng, X. The role of adenosine A1 receptor on immune cells. *Inflammation research : official journal of the European Histamine Research Society … [et al.]* **2022**, *71* (10-11), 1203–1212. DOI: 10.1007/s00011-022-01607-w. Published Online: Sep. 5, 2022.

(34) Yan, L.; Burbiel, J. C.; Maass, A.; Müller, C. E. Adenosine receptor agonists: from basic medicinal chemistry to clinical development. *Expert opinion on emerging drugs* **2003**, *8* (2), 537–576. DOI: 10.1517/14728214.8.2.537.

(35) Müller, C. E.; Jacobson, K. A. Recent developments in adenosine receptor ligands and their potential as novel drugs. *Biochimica et biophysica acta* **2011**, *1808* (5), 1290–1308. DOI: 10.1016/j.bbamem.2010.12.017. Published Online: Dec. 23, 2010.

(36) Glukhova, A.; Thal, D. M.; Nguyen, A. T.; Vecchio, E. A.; Jörg, M.; Scammells, P. J.; May, L. T.; Sexton, P. M.; Christopoulos, A. Structure of the Adenosine A1 Receptor Reveals the Basis for Subtype Selectivity. *Cell* **2017**, *168* (5), 867-877.e13. DOI: 10.1016/j.cell.2017.01.042.

(37) Jagannath, A.; Varga, N.; Dallmann, R.; Rando, G.; Gosselin, P.; Ebrahimjee, F.; Taylor, L.; Mosneagu, D.; Stefaniak, J.; Walsh, S.; Palumaa, T.; Di Pretoro, S.; Sanghani, H.; Wakaf, Z.; Churchill, G. C.; Galione, A.; Peirson, S. N.; Boison, D.; Brown, S. A.; Foster, R. G.; Vasudevan, S. R. Adenosine integrates light and sleep signalling for the regulation of circadian timing in mice. *Nature communications* **2021**, *12* (1), 2113. DOI: 10.1038/s41467-021-22179-z. Published Online: Apr. 9, 2021.

(38) Liu, Z.-W.; Gao, X.-B. Adenosine inhibits activity of hypocretin/orexin neurons by the A1 receptor in the lateral hypothalamus: a possible sleep-promoting effect. *Journal of neurophysiology* **2007**, *97* (1), 837–848. DOI: 10.1152/jn.00873.2006. Published Online: Nov. 8, 2006.

(39) Virus, R. M.; Djuricic-Nedelson, M.; Radulovacki, M.; Green, R. D. The effects of adenosine and 2'-deoxycoformycin on sleep and wakefulness in rats. *Neuropharmacology* **1983**, *22* (12A), 1401–1404. DOI: 10.1016/0028-3908(83)90231-9.

(40) Monti, D.; Carley, D. W.; Radulovacki, M. Adenosine analogues modulate the incidence of sleep apneas in rats. *Pharmacology, biochemistry, and behavior* **1995**, *51* (1), 125–131. DOI: 10.1016/0091-3057(94)00395-Y.

(41) Ticho, S. R.; Radulovacki, M. Role of adenosine in sleep and temperature regulation in the preoptic area of rats. *Pharmacology, biochemistry, and behavior* **1991**, *40* (1), 33–40. DOI: 10.1016/0091-3057(91)90317-u.

(42) Elmenhorst, D.; Meyer, P. T.; Winz, O. H.; Matusch, A.; Ermert, J.; Coenen, H. H.; Basheer, R.; Haas, H. L.; Zilles, K.; Bauer, A. Sleep deprivation increases A1 adenosine receptor binding in the human brain: a positron emission tomography study. *The Journal of neuroscience : the official journal of the Society for Neuroscience* **2007**, *27* (9), 2410–2415. DOI: 10.1523/JNEUROSCI.5066-06.2007.

(43) Alam, M. N.; Szymusiak, R.; Gong, H.; King, J.; McGinty, D. Adenosinergic modulation of rat basal forebrain neurons during sleep and waking: neuronal recording with microdialysis. *The Journal of physiology* **1999**, *521 Pt 3* (Pt 3), 679–690. DOI: 10.1111/j.1469-7793.1999.00679.x.

(44) Thakkar, M. M.; Engemann, S. C.; Walsh, K. M.; Sahota, P. K. Adenosine and the homeostatic control of sleep: effects of A1 receptor blockade in the perifornical lateral hypothalamus on sleep-wakefulness. *Neuroscience* **2008**, *153* (4), 875–880. DOI: 10.1016/j.neuroscience.2008.01.017. Published Online: Jan. 19, 2008.

(45) Oishi, Y.; Huang, Z.-L.; Fredholm, B. B.; Urade, Y.; Hayaishi, O. Adenosine in the tuberomammillary nucleus inhibits the histaminergic system via A1 receptors and promotes non-rapid eye movement sleep. *Proceedings of the National Academy of Sciences of the United States of America* **2008**, *105* (50), 19992–19997. DOI: 10.1073/pnas.0810926105. Published Online: Dec. 9, 2008.

(46) Satoh, S.; Matsumura, H.; Koike, N.; Tokunaga, Y.; Maeda, T.; Hayaishi, O. Region-dependent difference in the sleep-promoting potency of an adenosine A2A receptor agonist. *The European journal of neuroscience* **1999**, *11* (5), 1587–1597. DOI: 10.1046/j.1460-9568.1999.00569.x.

(47) Basheer, R.; Strecker, R. E.; Thakkar, M. M.; McCarley, R. W. Adenosine and sleep-wake regulation. *Progress in neurobiology* **2004**, *73* (6), 379–396. DOI: 10.1016/j.pneurobio.2004.06.004.

(48) DeWire, S. M.; Ahn, S.; Lefkowitz, R. J.; Shenoy, S. K. Beta-arrestins and cell signaling. *Annual review of physiology* **2007**, *69*, 483–510. DOI: 10.1146/annurev.physiol.69.022405.154749.

(49) Gurevich, V. V.; Gurevich, E. V. GPCR Signaling Regulation: The Role of GRKs and Arrestins. *Frontiers in pharmacology* **2019**, *10*, 125. DOI: 10.3389/fphar.2019.00125. Published Online: Feb. 19, 2019.

(50) Shenoy, S. K.; Lefkowitz, R. J. β-Arrestin-mediated receptor trafficking and signal transduction. *Trends in pharmacological sciences* **2011**, *32* (9), 521–533. DOI: 10.1016/j.tips.2011.05.002. Published Online: Jun. 15, 2011.

(51) Klaasse, E. C.; IJzerman, A. P.; Grip, W. J. de; Beukers, M. W. Internalization and desensitization of adenosine receptors. *Purinergic signalling* **2008**, *4* (1), 21–37. DOI: 10.1007/s11302-007-9086-7. Published Online: Nov. 13, 2007.

(52) Rajagopal, S.; Shenoy, S. K. GPCR desensitization: Acute and prolonged phases. *Cellular signalling* **2018**, *41*, 9–16. DOI: 10.1016/j.cellsig.2017.01.024. Published Online: Jan. 28, 2017.

(53) Verzijl, D.; Ijzerman, A. P. Functional selectivity of adenosine receptor ligands. *Purinergic signalling* **2011**, *7* (2), 171–192. DOI: 10.1007/s11302-011-9232-0. Published Online: May. 5, 2011.

(54) Luttrell, L. M. Activation and targeting of mitogen-activated protein kinases by G-protein-coupled receptors. *Canadian journal of physiology and pharmacology* **2002**, *80* (5), 375–382. DOI: 10.1139/Y02-045.

(55) Luttrell, L. M.; Daaka, Y.; Lefkowitz, R. J. Regulation of tyrosine kinase cascades by G-protein-coupled receptors. *Current opinion in cell biology* **1999**, *11* (2), 177–183. DOI: 10.1016/s0955-0674(99)80023-4.

(56) Premont, R. T.; Inglese, J.; Lefkowitz, R. J. Protein kinases that phosphorylate activated G protein-coupled receptors. *FASEB journal : official publication of the Federation of American Societies for Experimental Biology* **1995**, *9* (2), 175–182. DOI: 10.1096/fasebj.9.2.7781920.

(57) Baltos, J.-A.; Gregory, K. J.; White, P. J.; Sexton, P. M.; Christopoulos, A.; May, L. T. Quantification of adenosine A(1) receptor biased agonism: Implications for drug discovery. *Biochemical pharmacology* **2016**, *99*, 101–112. DOI: 10.1016/j.bcp.2015.11.013. Published Online: Nov. 12, 2015.

(58) Noor, N.; Patel, C. B.; Rockman, H. A. B-arrestin: a signaling molecule and potential therapeutic target for heart failure. *Journal of molecular and cellular cardiology* **2011**, *51* (4), 534–541. DOI: 10.1016/j.yjmcc.2010.11.005. Published Online: Nov. 11, 2010.

(59) Langemeijer, E. V.; Verzijl, D.; Dekker, S. J.; Ijzerman, A. P. Functional selectivity of adenosine A1 receptor ligands? *Purinergic signalling* **2013**, *9* (1), 91–100. DOI: 10.1007/s11302-012-9334-3. Published Online: Sep. 28, 2012.

(60) Schulte, G.; Fredholm, B. B. Signalling from adenosine receptors to mitogen-activated protein kinases. *Cellular signalling* **2003**, *15* (9), 813–827. DOI: 10.1016/S0898-6568(03)00058-5.

(61) Saecker, L.; Häberlein, H.; Franken, S. Investigation of adenosine A1 receptor-mediated β-arrestin 2 recruitment using a split-luciferase assay. *Frontiers in pharmacology* **2023**, *14*, 1172551. DOI: 10.3389/fphar.2023.1172551. Published Online: May. 30, 2023.

(62) Kim, Y.; Kim, H.; Lee, J.; Lee, J. K.; Min, S.-J.; Seong, J.; Rhim, H.; Tae, J.; Lee, H. J.; Choo, H. Discovery of β-Arrestin Biased Ligands of 5-HT7R. *Journal of medicinal chemistry* **2018**, *61* (16), 7218–7233. DOI: 10.1021/acs.jmedchem.8b00642. Published Online: Aug. 1, 2018.

(63) Dalrymple, M. B.; Jaeger, W. C.; Eidne, K. A.; Pfleger, K. D. G. Temporal profiling of orexin receptor-arrestin-ubiquitin complexes reveals differences between receptor subtypes. *The Journal of biological chemistry* **2011**, *286* (19), 16726–16733. DOI: 10.1074/jbc.M111.223537. Published Online: Mar. 4, 2011.

(64) Leathwood, P. D.; Chauffard, F.; Heck, E.; Munoz-Box, R. Aqueous extract of valerian root (Valeriana officinalis L.) improves sleep quality in man. *Pharmacology, biochemistry, and behavior* **1982**, *17* (1), 65–71. DOI: 10.1016/0091-3057(82)90264-7.

(65) Lanje, C. N.; Patil, S. R.; Wankhade, A. Medicinal Natural Drug of Valerian (Valerina Officinalis): An- Over Review. *American Journal of PharmTech Research* **2020**, *10* (1), 148–172. DOI: 10.46624/ajptr.2020.v10.i1.013.

(66) Nandhini, S.; Narayanan, K. B.; Ilango, K. VALERIANA OFFICINALIS: A REVIEW OF ITS TRADITIONAL USES, PHYTOCHEMISTRY AND PHARMACOLOGY. *Asian Journal of Pharmaceutical and Clinical Research* **2018**, *11* (1), 36. DOI: 10.22159/ajpcr.2018.v11i1.22588.

(67) Stevinson, C.; Ernst, E. Valerian for insomnia: a systematic review of randomized clinical trials. *Sleep medicine* **2000**, *1* (2), 91–99. DOI: 10.1016/s1389-9457(99)00015-5.

(68) Malva, J. O.; Santos, S.; Macedo, T. Neuroprotective properties of Valeriana officinalis extracts. *Neurotoxicity research* **2004**, *6* (2), 131–140. DOI: 10.1007/BF03033215.

(69) Diaper, A.; Hindmarch, I. A double-blind, placebo-controlled investigation of the effects of two doses of a valerian preparation on the sleep, cognitive and psychomotor function of sleep-disturbed older adults. *Phytotherapy research : PTR* **2004**, *18* (10), 831–836. DOI: 10.1002/ptr.1574.

(70) Sendker, J.; Lechtenberg, M.; Hensel, A. An Unsuccessful Attempt to Confirm the Occurrence of 4'-O-β- d-Glucosyl-9-O-(6″-deoxysaccharosyl)olivil in Valerian Root. *Planta medica* **2020**, *86* (15), 1133–1139. DOI: 10.1055/a-1078-5195. Published Online: Jan. 3, 2020.

(71) Hendriks, H.; Bos, R.; Allersma, D. P.; Malingré, T. M.; Koster, A. S. Pharmacological screening of valerenal and some other components of essential oil of Valeriana officinalis. *Planta medica* **1981**, *42* (1), 62–68. DOI: 10.1055/s-2007-971547.

(72) Wang, P.-C.; Ran, X.-H.; Chen, R.; Luo, H.-R.; Liu, Y.-Q.; Zhou, J.; Zhao, Y.-X. Germacrane-type sesquiterpenoids from the roots of Valeriana officinalis var. latifolia. *Journal of natural products* **2010**, *73* (9), 1563–1567. DOI: 10.1021/np100452a.

(73) Chavadej, S.; Becker, H.; Weberling, F. Further investigations of valepotriates in the Valerianaceae. *Pharmaceutisch weekblad. Scientific edition* **1985**, *7* (4), 167–168. DOI: 10.1007/BF02097255.

(74) Goppel, M.; Franz, G. Stability control of valerian ground material and extracts: a new HPLC-method for the routine quantification of valerenic acids and lignans. *Die Pharmazie* **2004**, *59* (6), 446–452.

(75) Patočka, J.; Jakl, J. Biomedically relevant chemical constituents of Valeriana officinalis. *Journal of Applied Biomedicine* **2010**, *8* (1), 11–18. DOI: 10.2478/v10136-009-0002-z.

(76) Torssell, K.; Wahlberg, K. Isolation, structure and synthesis of alkaloids from Valeriana officinalis L. *Acta chemica Scandinavica* **1967**, *21* (1), 53–62. DOI: 10.3891/acta.chem.scand.21-0053.

(77) Franck, B.; Petersen, U.; Hüper, F. Valerianie, a tertiary monoterpene alkaloid from valerian (1). *Angewandte Chemie (International ed. in English)* **1970**, *9* (11), 891. DOI: 10.1002/anie.197008911.

(78) Vissiennon, Z.; Sichardt, K.; Koetter, U.; Brattström, A.; Nieber, K. Valerian extract Ze 911 inhibits postsynaptic potentials by activation of adenosine A1 receptors in rat cortical neurons. *Planta medica* **2006**, *72* (7), 579–583. DOI: 10.1055/s-2006-931561. Published Online: Apr. 28, 2006.

(79) Schröder, R.; Schmidt, J.; Blättermann, S.; Peters, L.; Janssen, N.; Grundmann, M.; Seemann, W.; Kaufel, D.; Merten, N.; Drewke, C.; Gomeza, J.; Milligan, G.; Mohr, K.; Kostenis, E. Applying label-free dynamic mass redistribution technology to frame signaling of G protein-coupled receptors noninvasively in living cells. *Nature protocols* **2011**, *6* (11), 1748–1760. DOI: 10.1038/nprot.2011.386. Published Online: Oct. 20, 2011.

(80) Wouters, E.; Vasudevan, L.; Ciruela, F.; Saini, D. K.; Stove, C.; van Craenenbroeck, K. Assessing GPCR Dimerization in Living Cells: Comparison of the NanoBiT Assay with Related Bioluminescence- and Fluorescence-Based Approaches. In *Receptor-Receptor Interactions in the Central Nervous System*; FUXE, K., Borroto-Escuela, D. O., Eds.; Neuromethods; Springer New York, 2018; pp 239–250. DOI: 10.1007/978-1-4939-8576-0_15.

(81) Hoare, S. R. J.; Tewson, P. H.; Quinn, A. M.; Hughes, T. E. A kinetic method for measuring agonist efficacy and ligand bias using high resolution biosensors and a kinetic data analysis framework. *Scientific reports* **2020**, *10* (1), 1766. DOI: 10.1038/s41598-020-58421-9. Published Online: Feb. 4, 2020.

(82) Hoare, S. R. J.; Tewson, P. H.; Quinn, A. M.; Hughes, T. E.; Bridge, L. J. Analyzing kinetic signaling data for G-protein-coupled receptors. *Scientific reports* **2020**, *10* (1), 12263. DOI: 10.1038/s41598-020-67844-3. Published Online: Jul. 23, 2020.

(83) Shen, H.; Tauzin, L. J.; Baiyasi, R.; Wang, W.; Moringo, N.; Shuang, B.; Landes, C. F. Single Particle Tracking: From Theory to Biophysical Applications. *Chemical reviews* **2017**, *117* (11), 7331–7376. DOI: 10.1021/acs.chemrev.6b00815. Published Online: May. 18, 2017.

(84) Franken, S.; Bussmann, H.; Häberlein, H.; Bonke, E.; End, C. Single-particle tracking von GPCRs. *Biospektrum* **2020**, *26* (4), 414–415. DOI: 10.1007/s12268-020-1400-8.

(85) Jaqaman, K.; Loerke, D.; Mettlen, M.; Kuwata, H.; Grinstein, S.; Schmid, S. L.; Danuser, G. Robust single-particle tracking in live-cell time-lapse sequences. *Nature methods* **2008**, *5* (8), 695–702. DOI: 10.1038/nmeth.1237. Published Online: Jul. 20, 2008.

(86) Persson, F.; Lindén, M.; Unoson, C.; Elf, J. Extracting intracellular diffusive states and transition rates from single-molecule tracking data. *Nature methods* **2013**, *10* (3), 265–269. DOI: 10.1038/nmeth.2367. Published Online: Feb. 10, 2013.

(87) Bussmann, H.; Häberlein, H.; Boonen, G.; Drewe, J.; Butterweck, V.; Franken, S. Effect of St. John's wort extract Ze 117 on the lateral mobility of β1-adrenergic receptors in C6 cells. *Biomedicine & Pharmacotherapy* **2023**, *157*, 114006. DOI: 10.1016/j.biopha.2022.114006.

(88) Buck, L. T. Adenosine as a signal for ion channel arrest in anoxia-tolerant organisms. *Comparative Biochemistry and Physiology Part B: Biochemistry and Molecular Biology* **2004**, *139* (3), 401–414. DOI: 10.1016/j.cbpc.2004.04.002.

(89) Dolezelova, E.; Zurovec, M.; Dolezal, T.; Simek, P.; Bryant, P. J. The emerging role of adenosine deaminases in insects. *Insect biochemistry and molecular biology* **2005**, *35* (5), 381–389. DOI: 10.1016/j.ibmb.2004.12.009.

(90) Pall, M. L. Adenosine 3',5'-phosphate in fungi. *Microbiological reviews* **1981**, *45* (3), 462–480. DOI: 10.1128/mr.45.3.462-480.1981.

(91) Cristalli, G.; Costanzi, S.; Lambertucci, C.; Lupidi, G.; Vittori, S.; Volpini, R.; Camaioni, E. Adenosine deaminase: Functional implications and different classes of inhibitors. *Medicinal Research Reviews* **2001**, *21* (2), 105–128. DOI: 10.1002/1098-1128(200103)21:2<105:AID-MED1002>3.0.CO;2-U.

(92) Kim, C.-K.; Ahn, J.; Yu, J.; Le, D.; Han, S.; Lee, M. Analysis of Antioxidant Constituents from Ilex rotunda and Evaluation of Their Blood-Brain Barrier Permeability. *Antioxidants (Basel, Switzerland)* **2022**, *11* (10). DOI: 10.3390/antiox11101989. Published Online: Oct. 6, 2022.

(93) Ochiai, R.; Tomonobu, K.; Ikushima, I. Effect of chlorogenic acids on fatigue and sleep in healthy males: A randomized, double-blind, placebo-controlled, crossover study. *Food science & nutrition* **2018**, *6* (8), 2530–2536. DOI: 10.1002/fsn3.861. Published Online: Oct. 19, 2018.

(94) Wang, Y.; Minami, Y.; Ode, K. L.; Ueda, H. R. The role of calcium and CaMKII in sleep. *Frontiers in systems neuroscience* **2022**, *16*, 1059421. DOI: 10.3389/fnsys.2022.1059421. Published Online: Dec. 22, 2022.

(95) Blum, I. D.; Keleş, M. F.; Baz, E.-S.; Han, E.; Park, K.; Luu, S.; Issa, H.; Brown, M.; Ho, M. C. W.; Tabuchi, M.; Liu, S.; Wu, M. N. Astroglial Calcium Signaling Encodes Sleep Need in Drosophila. *Current biology : CB* **2021**, *31* (1), 150-162.e7. DOI: 10.1016/j.cub.2020.10.012. Published Online: Nov. 12, 2020.

(96) Carbone, E. A.; Menculini, G.; Filippis, R. de; D'Angelo, M.; Fazio, P. de; Tortorella, A.; Steardo, L. Sleep Disturbances in Generalized Anxiety Disorder: The Role of Calcium Homeostasis Imbalance. *International journal of environmental research and public health* **2023**, *20* (5). DOI: 10.3390/ijerph20054431. Published Online: Mar. 1, 2023.

(97) Atwood, B. K.; Lopez, J.; Wager-Miller, J.; Mackie, K.; Straiker, A. Expression of G protein-coupled receptors and related proteins in HEK293, AtT20, BV2, and N18 cell lines as revealed by microarray analysis. *BMC genomics* **2011**, *12*, 14. DOI: 10.1186/1471-2164-12-14. Published Online: Jan. 7, 2011.

(98) Navarro, G.; Gonzalez, A.; Campanacci, S.; Rivas-Santisteban, R.; Reyes-Resina, I.; Casajuana-Martin, N.; Cordomí, A.; Pardo, L.; Franco, R. Experimental and computational analysis of biased agonism on full-length and a C-terminally truncated adenosine A2A receptor. *Computational and structural biotechnology journal* **2020**, *18*, 2723–2732. DOI: 10.1016/j.csbj.2020.09.028. Published Online: Sep. 24, 2020.

(99) Jean-Charles, P.-Y.; Kaur, S.; Shenoy, S. K. G Protein-Coupled Receptor Signaling Through β-Arrestin-Dependent Mechanisms. *Journal of cardiovascular pharmacology* **2017**, *70* (3), 142–158. DOI: 10.1097/FJC.0000000000000482.

(100) Milasta, S.; Evans, N. A.; Ormiston, L.; Wilson, S.; Lefkowitz, R. J.; Milligan, G. The sustainability of interactions between the orexin-1 receptor and beta-arrestin-2 is defined by a single C-terminal cluster of hydroxy amino acids and modulates the kinetics of ERK MAPK regulation. *The Biochemical journal* **2005**, *387* (Pt 3), 573–584. DOI: 10.1042/BJ20041745.

(101) Fredholm, B. B.; Irenius, E.; Kull, B.; Schulte, G. Comparison of the potency of adenosine as an agonist at human adenosine receptors expressed in Chinese hamster ovary cells. *Biochemical pharmacology* **2001**, *61* (4), 443–448. DOI: 10.1016/s0006-2952(00)00570-0.

(102) Cordeaux, Y.; Briddon, S. J.; Megson, A. E.; McDonnell, J.; Dickenson, J. M.; Hill, S. J. Influence of receptor number on functional responses elicited by agonists acting at the human adenosine A(1) receptor: evidence for signaling pathway-dependent changes in agonist potency and relative intrinsic activity. *Molecular pharmacology* **2000**, *58* (5), 1075–1084. DOI: 10.1124/mol.58.5.1075.

(103) Calzetta, L.; Spina, D.; Cazzola, M.; Page, C. P.; Facciolo, F.; Rendina, E. A.; Matera, M. G. Pharmacological characterization of adenosine receptors on isolated human bronchi. *American journal of respiratory cell and molecular biology* **2011**, *45* (6), 1222–1231. DOI: 10.1165/rcmb.2011-0056OC. Published Online: Jun. 23, 2011.

(104) Kim, J.; Grotegut, C. A.; Wisler, J. W.; Mao, L.; Rosenberg, P. B.; Rockman, H. A.; Lefkowitz, R. J. The β-arrestin-biased β-adrenergic receptor blocker carvedilol enhances skeletal muscle contractility. *Proceedings of the National Academy of Sciences of the United States of America* **2020**, *117* (22), 12435–12443. DOI: 10.1073/pnas.1920310117. Published Online: May. 15, 2020.

(105) Ibrahim, I. A. A. E.-H.; Kurose, H. β-arrestin-mediated signaling improves the efficacy of therapeutics. *Journal of pharmacological sciences* **2012**, *118* (4), 408–412. DOI: 10.1254/jphs.11R10CP. Published Online: Mar. 23, 2012.

(106) Valant, C.; May, L. T.; Aurelio, L.; Chuo, C. H.; White, P. J.; Baltos, J.-A.; Sexton, P. M.; Scammells, P. J.; Christopoulos, A. Separation of on-target efficacy from adverse effects through rational design of a bitopic adenosine receptor agonist. *Proceedings of the National Academy of Sciences of the United States of America* **2014**, *111* (12), 4614–4619. DOI: 10.1073/pnas.1320962111. Published Online: Mar. 11, 2014.

(107) Wall, M. J.; Hill, E.; Huckstepp, R.; Barkan, K.; Deganutti, G.; Leuenberger, M.; Preti, B.; Winfield, I.; Carvalho, S.; Suchankova, A.; Wei, H.; Safitri, D.; Huang, X.; Imlach, W.; La Mache, C.; Dean, E.; Hume, C.; Hayward, S.; Oliver, J.; Zhao, F.-Y.; Spanswick, D.; Reynolds, C. A.; Lochner, M.; Ladds, G.; Frenguelli, B. G. Selective activation of Gαob by an adenosine A1 receptor agonist elicits analgesia without cardiorespiratory depression. *Nature communications* **2022**, *13* (1), 4150. DOI: 10.1038/s41467-022-31652-2. Published Online: Jul. 18, 2022.

(108) Albrecht-Küpper, B. E.; Leineweber, K.; Nell, P. G. Partial adenosine A1 receptor agonists for cardiovascular therapies. *Purinergic signalling* **2012**, *8* (Suppl 1), 91–99. DOI: 10.1007/s11302-011-9274-3. Published Online: Nov. 12, 2011.

(109) Brattström, A. Scientific evidence for a fixed extract combination (Ze 91019) from valerian and hops traditionally used as a sleep-inducing aid. *Wiener medizinische Wochenschrift (1946)* **2007**, *157* (13-14), 367–370. DOI: 10.1007/s10354-007-0442-6.

(110) Arts, I. C.; Coolen, E. J.; Bours, M. J.; Huyghebaert, N.; Stuart, M. A. C.; Bast, A.; Dagnelie, P. C. Adenosine 5'-triphosphate (ATP) supplements are not orally bioavailable: a randomized, placebo-controlled cross-over trial in healthy humans. *Journal of the International Society of Sports Nutrition* **2012**, *9* (1), 16. DOI: 10.1186/1550-2783-9-16. Published Online: Apr. 17, 2012.

(111) Nguyen, A. T. N.; Vecchio, E. A.; Thomas, T.; Nguyen, T. D.; Aurelio, L.; Scammells, P. J.; White, P. J.; Sexton, P. M.; Gregory, K. J.; May, L. T.; Christopoulos, A. Role of the Second Extracellular Loop of the Adenosine A1 Receptor on Allosteric Modulator Binding, Signaling, and Cooperativity. *Molecular pharmacology* **2016**, *90* (6), 715–725. DOI: 10.1124/mol.116.105015. Published Online: Sep. 28, 2016.

(112) Storme, J.; Cannaert, A.; van Craenenbroeck, K.; Stove, C. P. Molecular dissection of the human A3 adenosine receptor coupling with β-arrestin2. *Biochemical pharmacology* **2018**, *148*, 298–307. DOI: 10.1016/j.bcp.2018.01.008. Published Online: Jan. 5, 2018.

(113) Soave, M.; Kellam, B.; Woolard, J.; Briddon, S. J.; Hill, S. J. NanoBiT Complementation to Monitor Agonist-Induced Adenosine A1 Receptor Internalization. *SLAS discovery : advancing life sciences R & D* **2020**, *25* (2), 186–194. DOI: 10.1177/2472555219880475. Published Online: Oct. 4, 2019.

(114) White, C. W.; Johnstone, E. K. M.; See, H. B.; Pfleger, K. D. G. NanoBRET ligand binding at a GPCR under endogenous promotion facilitated by CRISPR/Cas9 genome editing. *Cellular signalling* **2019**, *54*, 27–34. DOI: 10.1016/j.cellsig.2018.11.018. Published Online: Nov. 22, 2018.

(115) DiRaddo, J. O.; Miller, E. J.; Hathaway, H. A.; Grajkowska, E.; Wroblewska, B.; Wolfe, B. B.; Liotta, D. C.; Wroblewski, J. T. A real-time method for measuring cAMP production modulated by Gαi/o-coupled metabotropic glutamate receptors. *The Journal of pharmacology and experimental therapeutics* **2014**, *349* (3), 373–382. DOI: 10.1124/jpet.113.211532. Published Online: Mar. 21, 2014.

(116) Kumar, B. A.; Kumari, P.; Sona, C.; Yadav, P. N. GloSensor assay for discovery of GPCR-selective ligands. *Methods in cell biology* **2017**, *142*, 27–50. DOI: 10.1016/bs.mcb.2017.07.012. Published Online: Sep. 11, 2017.

(117) Goulding, J.; May, L. T.; Hill, S. J. Characterisation of endogenous A2A and A2B receptor-mediated cyclic AMP responses in HEK 293 cells using the GloSensor™ biosensor: Evidence for an allosteric mechanism of action for the A2B-selective antagonist PSB 603. *Biochemical pharmacology* **2018**, *147*, 55–66. DOI: 10.1016/j.bcp.2017.10.013. Published Online: Oct. 26, 2017.

(118) Trinh, P. N. H.; Baltos, J.-A.; Hellyer, S. D.; May, L. T.; Gregory, K. J. Adenosine receptor signalling in Alzheimer's disease. *Purinergic signalling* **2022**, *18* (3), 359–381. DOI: 10.1007/s11302-022-09883-1. Published Online: Jul. 23, 2022.

(119) Lungato, L.; Gazarini, M. L.; Paredes-Gamero, E. J.; Tersariol, I. L. S.; Tufik, S.; D'Almeida, V. Sleep deprivation impairs calcium signaling in mouse splenocytes and leads to a decreased immune response. *Biochimica et biophysica acta* **2012**, *1820* (12), 1997–2006. DOI: 10.1016/j.bbagen.2012.09.010. Published Online: Sep. 20, 2012.

(120) Dickenson, J. M.; Hill, S. J. Adenosine A1-receptor stimulated increases in intracellular calcium in the smooth muscle cell line, DDT1MF-2. *British journal of pharmacology* **1993**, *108* (1), 85–92. DOI: 10.1111/j.1476-5381.1993.tb13444.x.

(121) Do, K. H.; Choi, Y. W.; Kim, E. K.; Yun, S. J.; Kim, M. S.; Lee, S. Y.; Ha, J. M.; Kim, J. H.; Kim, C. D.; Son, B. G.; Kang, J. S.; Khan, I. A.; Bae, S. S. Pinoresinol-4,4'-di-O-beta-D-glucoside from Valeriana officinalis root stimulates calcium mobilization and chemotactic migration of mouse embryo fibroblasts. *Phytomedicine : international journal of phytotherapy and phytopharmacology* **2009**, *16* (6-7), 530–537. DOI: 10.1016/j.phymed.2008.12.002. Published Online: Feb. 4, 2009.

(122) Ethier, M. F.; Madison, J. M. Adenosine A1 receptors mediate mobilization of calcium in human bronchial smooth muscle cells. *American journal of respiratory cell and molecular biology* **2006**, *35* (4), 496–502. DOI: 10.1165/rcmb.2005-0290OC. Published Online: May. 18, 2006.

(123) McDonald, R. L.; Roberts, D. J.; Palmer, A. C.; Ball, S. G.; Vaughan, P. F.; Peers, C. Regulation of [Ca++]i in human neuroblastoma (SH-SY5Y) cells expressing recombinant rat angiotensin1A receptors by angiotensin II and carbachol. *The Journal of pharmacology and experimental therapeutics* **1997**, *281* (3), 1257–1263.

(124) Daumas, F.; Destainville, N.; Millot, C.; Lopez, A.; Dean, D.; Salomé, L. Confined diffusion without fences of a g-protein-coupled receptor as revealed by single particle tracking. *Biophysical journal* **2003**, *84* (1), 356–366. DOI: 10.1016/S0006-3495(03)74856-5.

(125) Thurner, P.; Gsandtner, I.; Kudlacek, O.; Choquet, D.; Nanoff, C.; Freissmuth, M.; Zezula, J. A two-state model for the diffusion of the A2A adenosine receptor in hippocampal neurons: agonist-induced switch to slow mobility is modified by synapse-associated protein 102 (SAP102). *The Journal of biological chemistry* **2014**, *289* (13), 9263–9274. DOI: 10.1074/jbc.M113.505685. Published Online: Feb. 7, 2014.

(126) Snaar-Jagalska, B. E.; Cambi, A.; Schmidt, T.; Keijzer, S. de. Single-molecule imaging technique to study the dynamic regulation of GPCR function at the plasma membrane. *Methods in enzymology* **2013**, *521*, 47–67. DOI: 10.1016/B978-0-12-391862-8.00003-X.

(127) Jacobs, S.; Cuatrecasas, P. The mobile receptor hypothesis for cell membrane receptor action. *Trends in Biochemical Sciences* **1977**, *2* (12), 280–282. DOI: 10.1016/0968-0004(77)90281-X.

(128) Kusumi, A.; Sako, Y. Cell surface organization by the membrane skeleton. *Current opinion in cell biology* **1996**, *8* (4), 566–574. DOI: 10.1016/S0955-0674(96)80036-6.

(129) Fujiwara, T.; Ritchie, K.; Murakoshi, H.; Jacobson, K.; Kusumi, A. Phospholipids undergo hop diffusion in compartmentalized cell membrane. *The Journal of cell biology* **2002**, *157* (6), 1071–1081. DOI: 10.1083/jcb.200202050. Published Online: Jun. 10, 2002.

(130) Ohno-Iwashita, Y.; Shimada, Y.; Hayashi, M.; Inomata, M. Plasma membrane microdomains in aging and disease. *Geriatrics & gerontology international* **2010**, *10 Suppl 1*, S41-52. DOI: 10.1111/j.1447-0594.2010.00600.x.

(131) Laude, A. J.; Prior, I. A. Plasma membrane microdomains: organization, function and trafficking. *Molecular membrane biology* **2004**, *21* (3), 193–205. DOI: 10.1080/09687680410001700517.

(132) Sungkaworn, T.; Jobin, M.-L.; Burnecki, K.; Weron, A.; Lohse, M. J.; Calebiro, D. Single-molecule imaging reveals receptor-G protein interactions at cell surface hot spots. *Nature* **2017**, *550* (7677), 543–547. DOI: 10.1038/nature24264. Published Online: Oct. 18, 2017.

(133) Suzuki, K.; Ritchie, K.; Kajikawa, E.; Fujiwara, T.; Kusumi, A. Rapid hop diffusion of a G-protein-coupled receptor in the plasma membrane as revealed by single-molecule techniques. *Biophysical journal* **2005**, *88* (5), 3659–3680. DOI: 10.1529/biophysj.104.048538. Published Online: Jan. 28, 2005.

(134) England, C. G.; Luo, H.; Cai, W. HaloTag technology: a versatile platform for biomedical applications. *Bioconjugate chemistry* **2015**, *26* (6), 975–986. DOI: 10.1021/acs.bioconjchem.5b00191. Published Online: May. 22, 2015.

(135) Lillo, A.; Martínez-Pinilla, E.; Reyes-Resina, I.; Navarro, G.; Franco, R. Adenosine A2A and A3 Receptors Are Able to Interact with Each Other. A Further Piece in the Puzzle of Adenosine Receptor-Mediated Signaling. *International journal of molecular sciences* **2020**, *21* (14). DOI: 10.3390/ijms21145070. Published Online: Jul. 17, 2020.

(136) Aatz, S.; Franken, S.; Kolb, C.; Häberlein, H. St. John's wort extract STW3-VI affects the binding behaviour, signal transduction and lateral mobility of 5-HT2A receptors observed by single molecule detection and the use of a novel fluorescence-labeled ligand. *Phytomedicine Plus* **2022**, *2* (3), 100320. DOI: 10.1016/j.phyplu.2022.100320.

(137) Bussmann, H. W. *Influence of the St. John's Wort Extract Ze117 on the Lipidome of PBMC and on the Lateral Diffusion of ß1-Adrenergic Receptors in C6 Cells*, 2021.

(138) Schwenzer, N.; Bussmann, H.; Franken, S.; Häberlein, H. *Live-cell single-molecule analysis of β 2 -adrenergic receptor diffusion dynamics and confinement*, 2018. DOI: 10.1101/406488.

(139) Li, Y.; Wang, M.; Gao, N.; Li, D.; Lin, J. The effect of dimerization on the activation and conformational dynamics of adenosine A1 receptor. *Physical chemistry chemical physics : PCCP* **2019**, *21* (41), 22763–22773. DOI: 10.1039/c9cp04060a.

(140) Gracia, E.; Moreno, E.; Cortés, A.; Lluís, C.; Mallol, J.; McCormick, P. J.; Canela, E. I.; Casadó, V. Homodimerization of adenosine A_1 receptors in brain cortex explains the biphasic effects of caffeine. *Neuropharmacology* **2013**, *71*, 56–69. DOI: 10.1016/j.neuropharm.2013.03.005. Published Online: Mar. 22, 2013.

(141) Canals, M.; Burgueño, J.; Marcellino, D.; Cabello, N.; Canela, E. I.; Mallol, J.; Agnati, L.; Ferré, S.; Bouvier, M.; FUXE, K.; Ciruela, F.; Lluis, C.; Franco, R. Homodimerization of adenosine A2A receptors: qualitative and quantitative assessment by fluorescence and bioluminescence energy transfer. *Journal of neurochemistry* **2004**, *88* (3), 726–734. DOI: 10.1046/j.1471-4159.2003.02200.x.

(142) Butterweck, V.; Winterhoff, H.; Herkenham, M. St John's wort, hypericin, and imipramine: a comparative analysis of mRNA levels in brain areas involved in HPA axis control following short-term and long-term administration in normal and stressed rats. *Molecular psychiatry* **2001**, *6* (5), 547–564. DOI: 10.1038/sj.mp.4000937.

(143) Brattström, A. Long-term effects of St. John's wort (Hypericum perforatum) treatment: a 1-year safety study in mild to moderate depression. *Phytomedicine : international journal of phytotherapy and phytopharmacology* **2009**, *16* (4), 277–283. DOI: 10.1016/j.phymed.2008.12.023. Published Online: Mar. 18, 2009.

(144) Romero-Fernandez, W.; Borroto-Escuela, D. O.; Tarakanov, A. O.; Mudó, G.; Narvaez, M.; Pérez-Alea, M.; Agnati, L. F.; Ciruela, F.; Belluardo, N.; FUXE, K. Agonist-induced formation of FGFR1 homodimers and signaling differ among members of the FGF family. *Biochemical and biophysical research communications* **2011**, *409* (4), 764–768. DOI: 10.1016/j.bbrc.2011.05.085. Published Online: May. 20, 2011.

(145) Choi, R. C. Y.; Simon, J.; Tsim, K. W. K.; Barnard, E. A. Constitutive and agonist-induced dimerizations of the P2Y1 receptor: relationship to internalization and scaffolding. *The Journal of biological chemistry* **2008**, *283* (16), 11050–11063. DOI: 10.1074/jbc.M709266200. Published Online: Feb. 12, 2008.

(146) Small, K. M.; Schwarb, M. R.; Glinka, C.; Theiss, C. T.; Brown, K. M.; Seman, C. A.; Liggett, S. B. Alpha2A- and alpha2C-adrenergic receptors form homo- and heterodimers: the heterodimeric state impairs agonist-promoted GRK phosphorylation and beta-arrestin recruitment. *Biochemistry* **2006**, *45* (15), 4760–4767. DOI: 10.1021/bi052074z.

8 Supplementary Material and Data

8.1 Plasmids

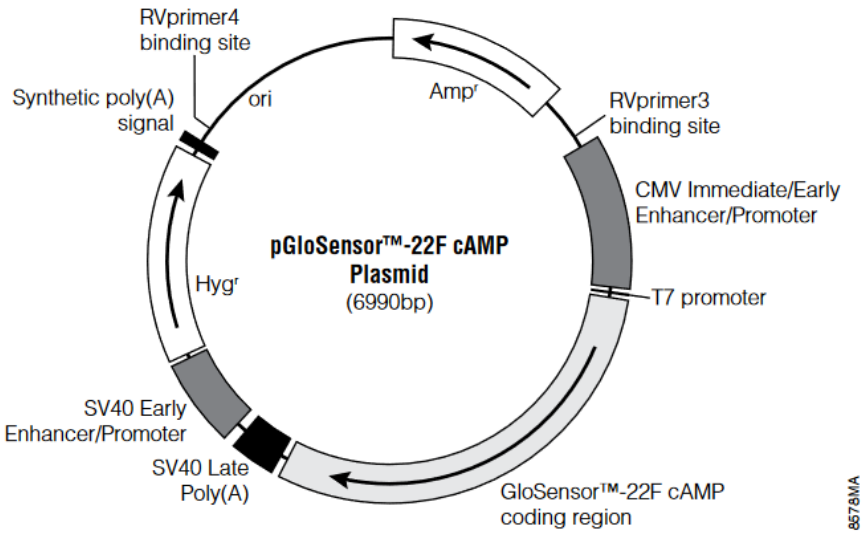

Figure 41. pGloSensor™-22F cAMP Plasmid. Detailed information: https://www.promega.de/products/cell-signaling/gpcr-signaling/glosensor-camp-cgmp-protease-biosensors/?tabset0=0&catNum=E1290

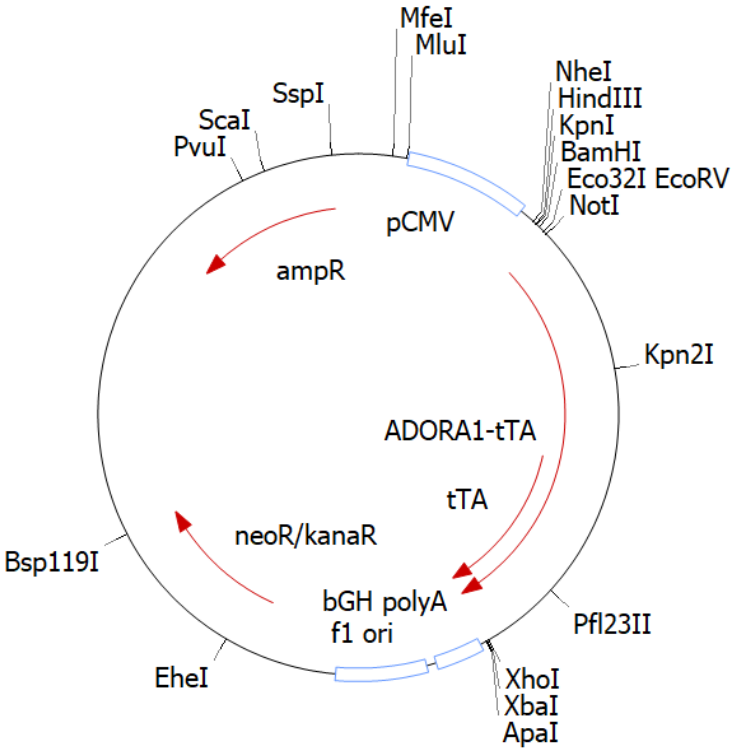

Figure 42. Plasmid ADORA1-Tango. Plasmid was a gift from Bryan Roth (Addgene plasmid # 66209; http://n2t.net/addgene:66209; PRID:Addgene_66209).

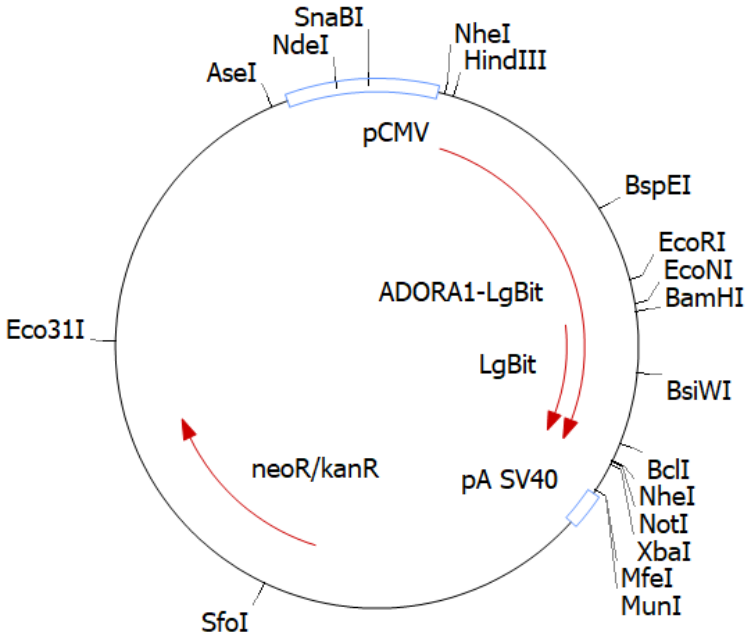

Figure 43. Plasmid pCMV_ADORA1-LgBiT. Plasmid to express human adenosine A1 receptor with Large-BiT fused to C-terminus in mammalian cells.

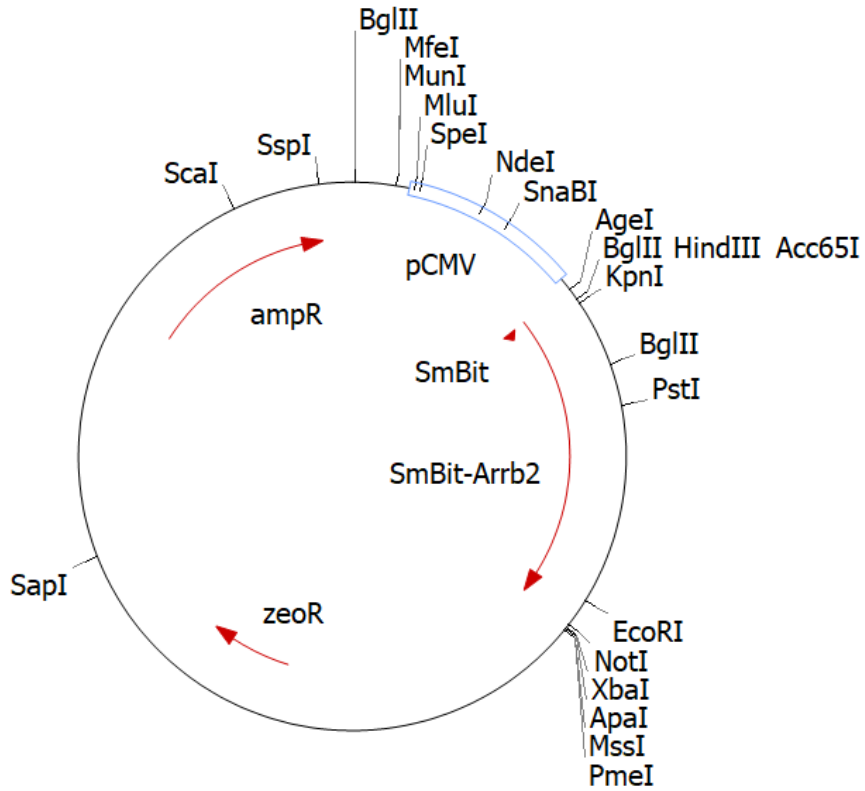

Figure 44. pCDNA3.1Zeo_SmBiT-ARRB2. Plasmid to express rat β-arrestin 2 with Small-BiT fused to N-terminus in mammalian cells.

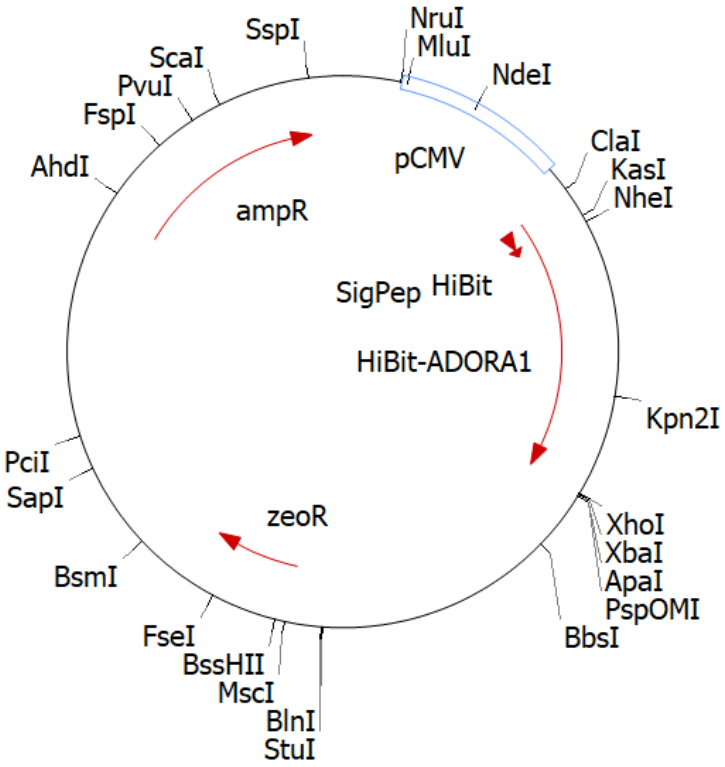

Figure 45. pCDNA3.1Zeo_HiBiT-ADORA1. Plasmid to express human adenosine A1 receptor with HiBiT fused to N-terminus in mammalian cells.

8.2 Identification of dicaffeoylquinic acids (DQAs) and adenosine by high-resolution liquid chromatography-mass spectrometry

Liquid chromatography tandem-mass spectrometry (LC-MS/MS) was used to analyse valerian extract Ze 911 and derivatives for the existence of dicaffeoylquinic acids (DQAs) and adenosine.

For analyses, 10 µg of either adenosine or Ze 911 were evaporated in 100 µl water containing 0.1 % DMSO using Thermo Scientific™ Savant™ SpeedVac™. Substances were re-dissolved in solvent A (0.1% formic acid (FA)) to yield a 1 g/L solution and separated on a Dionex Ultimate 3000 RSLC nano HPLC system (Dionex GmBH, Idstein, Germany). One µl of each substance solution was injected onto a C18 analytical column (self-packed 400 mm length, 75 µm inner diameter, ReproSil-Pur 120 C18-AQ, 1.9 µm, Dr. Maisch). A linear gradient from 1% to 55% solvent B (90% acetonitrile, 0.1% FA) at 300 nL/min during 70 min followed by 32 min at 98 % solvent B was used to separate the extract and adenosine. Orbitrap Fusion Lumos mass spectrometer (ThermoFisher Scientific, Bremen, Germany) was coupled online to nano-HPLC.

Ions between 100 and 2000 m/z were scanned in the Orbitrap detector every 3 s with a resolution of 60,000 (maximum fill time 50 ms, AGC target 300,000, normalized AGC target 75 %). For internal calibration (typical mass error ≤1.5 ppm) polysiloxane (445.12002 Da) was used. Top 10 precursor ions were chosen for synchronous precursor selection and fragmented with higher energy CID (HCD: 20, 30, 50 % collision energy) for detection of reporter ions in the Orbitrap analyser (resolution 15,000, maximum injection time 20 ms, AGC target 25,000, normalized AGC target 50 %). Fragmented ions were excluded from repeated analysis for 15 s.

Data was analysed using FreeStyle software (version 1.8; Thermo). Briefly, spectra were screened for precursor masses of positively charged DQAs (517.1346) or adenosine (268.1046). For verification, masses of the corresponding MS2 fragment spectra were compared to fragments recorded in the PubChem database (NIH; NCBI)

A

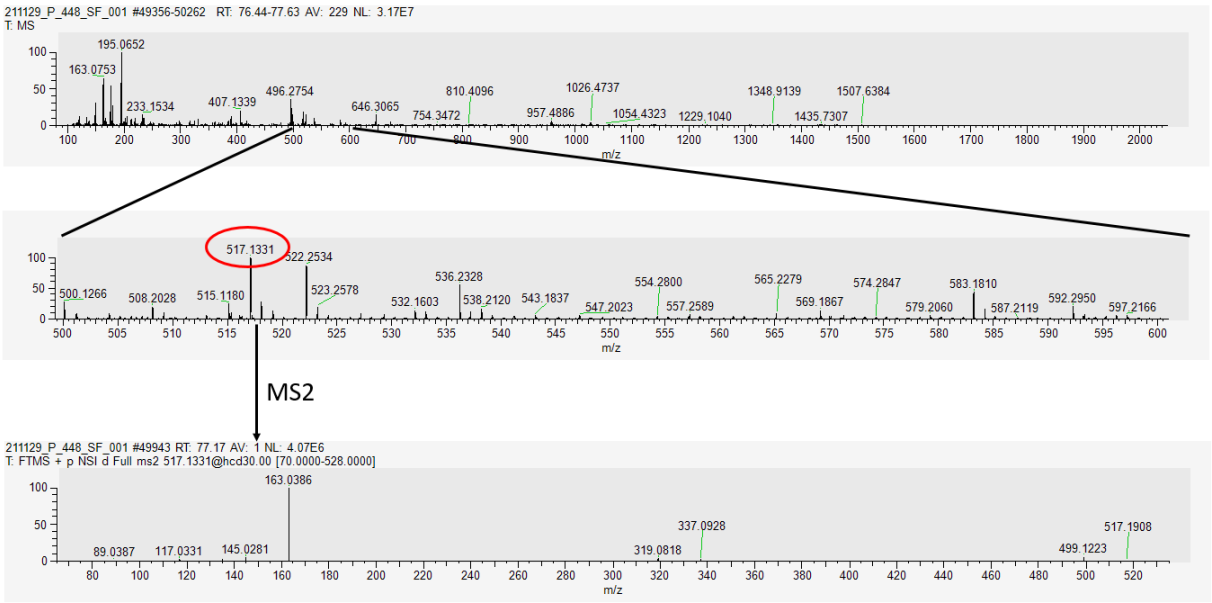

B

Top 5 Peaks	163.041885 100 319.086609 5.56 499.128113 5.56 145.028839 2.47 230.649307 1.85
SPLASH	splash10-03di-0900000000-7b6d7228827b3f8dd2ff
Thumbnail	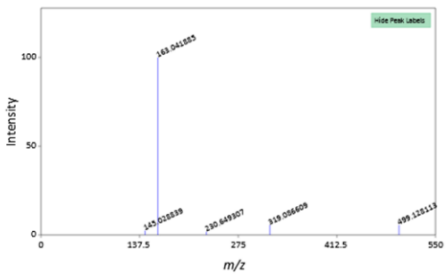

C

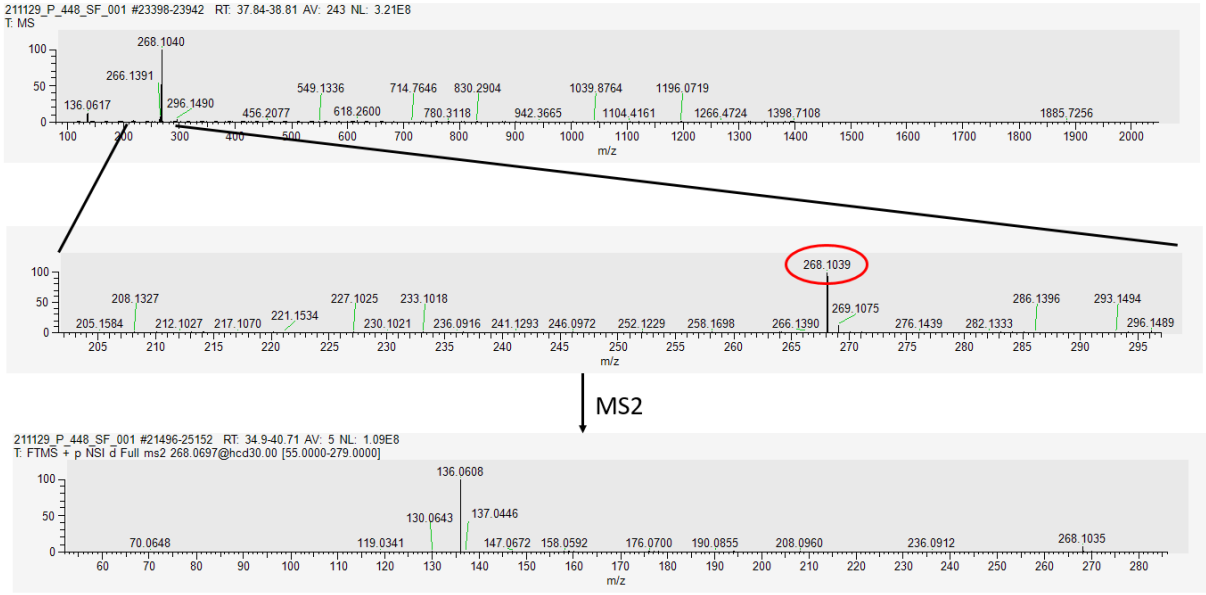

D

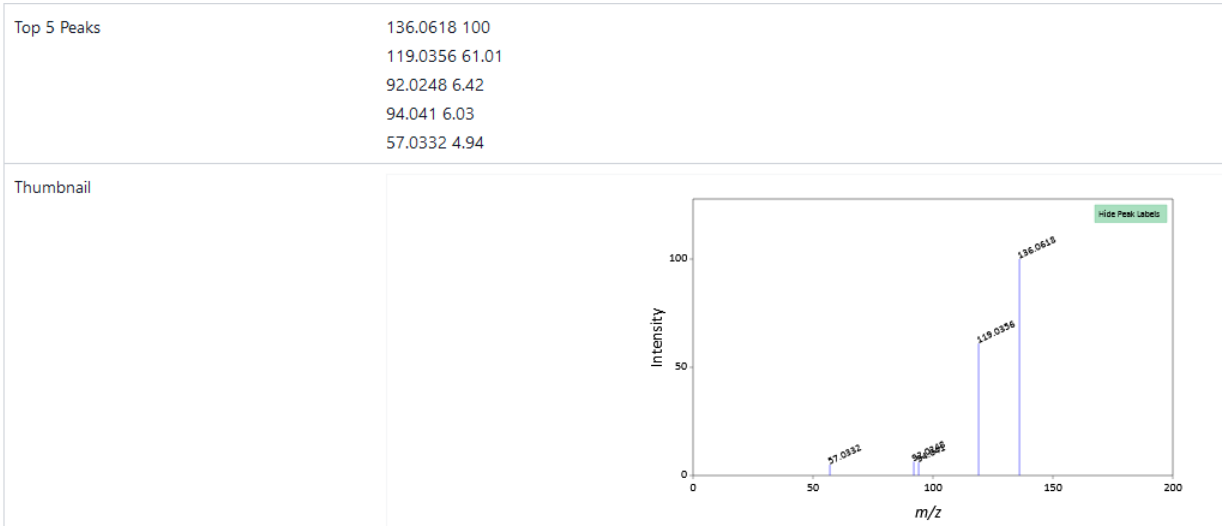

Figure 46. Mass spectrum of DQAs (A) and mass spectrum of adenosine (C). Corresponding PubChem results are shown in (B) for DQAs and (D) for adenosine. Zoomed in parts show fragmented masses+1.

9 Danksagung

Auf das Verfassen der Danksagung habe ich mich sehr gefreut. Eines steht nämlich fest: ohne die tatkräftige Unterstützung einiger toller Menschen wäre die Anfertigung dieser Arbeit nicht möglich gewesen.

Zuallererst möchte ich mich bei dir, lieber Hanns (Prof. Dr. Hanns Häberlein) bedanken. Du bist mir mit Rat und Tat zur Seite gestanden – in erfolgreichen und frustrierenden Zeiten. Egal ob ich Hilfe in experimentellen, organisatorischen oder privaten Angelegenheiten brauchte, ich konnte stets auf dich zählen. Ich werde die Jahre in der AG/Familie Häberlein sehr gut in Erinnerung behalten.

Ohne dich, Sebastian (Dr. Sebastian Franken) wären meine Experimente nicht halb so gut geglückt und ich würde vermutlich heute noch an dem einen oder anderen Projekt feilen müssen. Vielen Dank, dass du dein unschlagbares biologisches Wissen mit mir geteilt und stets an neuen Ideen für meine Dissertation mitgearbeitet hast. Neben der Arbeit im Labor, habe ich viele lustige, aber auch sehr tiefgründige Gespräche mit dir geführt und diese immer sehr geschätzt.

Nicht zu vergessen sind natürlich meine „für immer“-Lieblingskolleg*innen Eva, Fabio und Swen. Ich kann mir gar nicht vorstellen, wie die vergangenen Jahre ohne euch gewesen wären. Tausend Dank für einfach alles, insbesondere eure Freundschaft, euren Rat und euer offenes Ohr.

Zudem möchte ich mich herzlich bei dem Industriepartner meiner Dissertation, Max Zeller Söhne AG Switzerland, bedanken - ganz besonders bei Veronika (Prof. Dr. Veronika Butterweck) und Hendrik (Dr. Hendrik Bussmann). Die Zusammenarbeit war immer sehr angenehm – der regelmäßige Austausch und Input eurerseits haben einen großen Teil zum Erfolg meiner Arbeit beigetragen.

Vielen Dank auch an Frau Prof. Dr. Evi Kostenis, die nicht nur meine Zweitbetreuung übernommen hat, sondern mir auch die Gerätschaften aus Ihrem Labor (DMR) zur Verfügung gestellt hat.

Der letzte Absatz ist für meine wunderbare Familie. Mama und Papa, danke für eure bedingungslose Unterstützung, seit ich denken kann. Ich konnte immer bestärkt und ohne Sorgen genau meinen Weg gehen. Das ist ein echtes Privileg und dafür bin ich von Herzen dankbar.

Mein für immer Lieblingsmensch, Lebenspartner und bester Freund Fabi – danke, dass du es schon so lange mit mir aushältst. Deine entspannte Art viele Dinge zu sehen und dein liebevoller Umgang mit mir und allen anderen Menschen um dich herum schätze ich jeden Tag. Meine kleine Alma, du stellst alles anderer in den Schatten. Deine Ankunft bei uns hat mir gezeigt, worauf es im Leben wirklich ankommt. Dank dir habe ich es geschafft, Dinge aus einer anderen Perspektive zu sehen, den Fokus richtig zu setzen und alles etwas gelassener zu sehen. Danke, dass ich deine Mama sein darf.

10 Publikationen und Poster

Publikationen

Saecker, L.; Häberlein, H.; Franken, S. Investigation of adenosine A1 receptor-mediated β-arrestin 2 recruitment using a split-luciferase assay. *Frontiers in pharmacology* **2023**, *14*, 1172551. DOI: 10.3389/fphar.2023.1172551. Published Online: May. 30, 2023.

Poster

Knödler, L.; Roth, I.; Wos-Maganga, M.; Weickhardt, S.; Vogel, M.; Haas, B. Cardiac hERG channel blockers sensitize human glioblastoma cells towards the genotoxic effects of temozolomide.
German Pharm-Tox Summit (DGPT) 2022

11 Eidesstattliche Erklärung

Hiermit versichere ich, Luisa Katharina Säcker, dass ich die vorliegende Arbeit selbstständig angefertigt und keine anderen als die angegebenen Hilfsmittel und Quellen benutzt habe. Alle wörtlich oder inhaltlich übernommenen Stellen habe ich als solche gekennzeichnet. Ferner erkläre ich, die vorliegende Arbeit an keiner anderen Hochschule als Dissertation eingereicht zu haben. Ich habe noch keinen Promotionsversuch unternommen. Die von mir eingereichte Dissertation habe ich unter Beachtung der Grundsätze zur Sicherung guter wissenschaftlicher Praxis erstellt. Meine Angaben entsprechen der Wahrheit und ich habe diese nach bestem Wissen und Gewissen gemacht.

Bonn, den 14. Februar 2025